# The virus-receptor interaction in the pathogenesis of feline immunodeficiency virus infection

Inaugural-Dissertation

to obtain the academic degree

Doctor rerum naturalium (Dr. rer. nat.)

submitted to the Department of Biology, Chemistry and Pharmacy

of the Freie Universität Berlin

by

**Martin Kraase**

from Stralsund

Berlin, 2013

This dissertation was prepared at the MRC-Centre for Virus Research of the University of Glasgow under supervision of Prof. Dr. Brian J. Willett from September 2007 to October 2013.

1. Referee: Prof. Dr. Brian J. Willett
2. Referee: Prof. Dr. Rupert Mutzel

Date of thesis defense: 13.02.2014

# Acknowledgements

I am deeply indebted to my supervisors Prof. Brian Willett and Prof. Margaret Hosie. It was for their expertise, guidance and support that this thesis was possible. I am extremely thankful for the exceptional freedom I was offered and the trust in my work and in my person.

I am grateful to Prof. Mutzel for his interest in my work and his willingness to examine this thesis. Also I would like to thank the Free University of Berlin for the possibility to turn this project into a dissertation.

I wish to thank all the members of the retrovirus research lab for their support during this project and for sharing good times in and outside the lab. In particular Pawel Bęczkowski and Isabelle Dietrich for the honest talks and their advice during writing. I am also grateful to Hazel Stewart for her helpful comments on my thesis. I owe particular thanks to Nicola Logan and Linda McMonagle for their assistance in the lab and all the great laughs, may the LUCIFERASE always be with you. I would like to thank Will McEwan for many interesting discussions and for hosting me and Ayman Samman, Lesley Nicholson, Chi Chan for interesting cultural insights and sometimes very strange talks.

I thank Richard Sloan for supervising me during the first months of this work and handing over his project to me.

I am grateful to Roman Biek for helping me with the phylogenetic analysis and to my students Andrea Achleitner and Ismeta Curkic who assisted with the work on PBMC and tissue-derived virus.

I would like to acknowledge the Biotechnology and Biological Sciences Research Council for funding most of this project.

I thank Annett Quiel for the kick in the ass when needed.

I am extremely grateful to my family and friends who supported me during this thesis. Most of all I would like to thank Lucie for her love, the shared good and bad times, the sometimes needed pushiness and not to forget her expertise when it came to formatting this thesis.

# Table of Contents

# List of Figures

# List of Tables

# List of Abbreviations

| Abbreviation | Meaning |
|---|---|
| 7D6 | Monoclonal antibody against CD134 receptor |
| A3 | APOBEC3 |
| Ab | Antibody |
| AIDS | Acquired immunodeficiency syndrome |
| APOBEC3 | Apolipoprotein B mRNA editing enzyme catalytic polypeptide-like 3 |
| BEAST | Bayesian evolutionary analysis sampling trees |
| BIV | Bovine immunodeficiency virus |
| bp | Base pair |
| BSA | Bovine serum albumin |
| CA | Capsid |
| CD | Cluster of differentiation |
| CD134L | Ligand to the CD134 receptor |
| cDNA | Complementary deoxyribonucleic acid |
| CRD | Cysteine rich domain |
| CTL | Cytotoxic T lymphocyte |
| DMEM | Dulbecco's modified Eagle's medium |
| DMSO | Dimethyl sulfoxide |
| DNA | Deoxyribonucleic acid |
| dNTP | 2’-deoxynucleoside-5’-triphosphate |
| dUTPase | Deoxyuracil triposphatase |
| dN/dS | non-synonomous/synonomous mutation ratio |
| EDTA | Ethylenediaminetetraacetic acid |
| ELISA | Enzyme-linked immunosorbent assay |
| ELISpot | Enzyme-linked immunosorbent spot assay |
| Env | Envelope |
| Fc-TNC-CD134L | Trimeric form of the CD134 ligand |
| feA3C | Feline APOBEC3 C |
| feA3CH | Feline APOBEC3 CH |
| feA3H | Feline APOBEC3 H |
| FEL | Fixed Effects Likelihood |
| FFV | Feline foamy virus |
| FIV | Feline immunodeficiency virus |
| FIV-B2542 | B2542 strain of FIV |
| FIV-CPG | FIV subtype C, isolate PGammer |
| FIV-GL8 | Glasgow 8 strain of FIV |
| FIV-NCSU | NCSU (North Carolina State University) strain of FIV |
| FIV-PET | Petaluma strain of FIV |
| FIV-PPR | PPR strain of FIV |
| G | gamma distributed rate variation among sites |
| GL8-ABSN | FIV-GL8 mutant with ApaI, BssHII, SalI, NheI restriction sites |
| HEPES | 4-(2-hydroxyethyl)-1-piperazineethanesulfonic acid |
| HIV | Human immunodeficiency virus |

| | |
|---|---|
| HKY | Hasegawa-Kishino-Yano substitution model |
| HPD | Highest posterior density |
| HRP | Horseradish peroxidase |
| I | Proportion of invariable sites |
| IgG | Immunoglobulin G |
| IL-2 | Interleukin 2 |
| IN | Integrase |
| INF-γ | Interferon gamma |
| LB | Luria Bertani |
| LD-PCR | Limiting dilution PCR |
| LTR | Long terminal repeat |
| luc | Firefly luciferase |
| MA | Matrix |
| MCMC | Markov Chain Monte Carlo |
| MHC | Major histocompatibility complex |
| ML | Maximum likelihood |
| MLV | Murine leukaemia virus |
| MMTV | Mouse mammary tumour virus |
| NAb | Neutralising antibody |
| NJ | Neighbour joining |
| nt | nucleotide |
| ORF | Open reading frame |
| PBMC | Peripheral blood mononuclear cell |
| PBS | Phosphate buffered saline |
| PCR | Polymerase chain reaction |
| PR | Protease |
| qPCR | Quantitative real-time PCR |
| R5 | Strain of HIV utilizing CCR5 co-receptor |
| R5X4 | Strain of HIV utilizing both CCR5 and CXCR4 co-receptors |
| RNA | Ribonucleic acid |
| rpm | Revolutions per minute |
| RPMI | Roswell Park Memorial Institute medium |
| RRE | Rev response element |
| RT | Reverse transcriptase |
| sFcCD134 | Soluble CD134 receptor |
| SFU | Spot-forming unit |
| SGA | Single genome amplification |
| SIV | Simian immunodeficiency virus |
| SLAC | Single likelihood ancestor counting |
| SOC | Super optimal broth |
| SPF | Specific pathogen free |
| SU | Surface unit of Env |
| TCID50 | 50% tissue culture infectious dose |
| TM | Transmembrane protein of Env |
| Tris | Hydroxymethyl aminomethane |
| TVM | Transversion model |
| Tween 20 | Poloxyethylene-sobitanmonolaurate |

| | |
|---|---|
| UV | Ultra-violet |
| V | Volt |
| V loop | Variable loop |
| vif | Viral infectivity factor |
| VNA | Virus neutralisation assay |
| X4 | Strain of HIV utilizing CXCR4 co-receptor |

**Amino acids**

| | |
|---|---|
| A | Alanine |
| C | Cysteine |
| D | Aspartic acid |
| E | Glutamic acid |
| F | Phenylalanine |
| G | Glycine |
| H | Histidine |
| I | Isoleucine |
| K | Lysine |
| L | Leucine |
| M | Methionine |
| N | Asparagine |
| P | Proline |
| Q | Glutamine |
| R | Arginine |
| S | Serine |
| T | Threonine |
| V | Valine |
| W | Tryptophan |
| Y | Tyrosine |

# 1. Introduction

## 1.1. Feline immunodeficiency virus

### 1.1.1. Introduction to FIV

Understanding the evolution of retroviruses in their hosts is crucial for the development of therapies and vaccines. The evolutionary pattern of retroviral infection is shaped by viral factors, such as their mechanism of replication, and by host factors, mainly the immune system. In the long term, the co-evolution of virus and host may lead to a non-pathogenic co-existence, as it is seen with endogenous retroviruses or simian immunodeficiency virus (SIV) in its original host. However, upon recent transmission of pathogens into new host species, so-called zoonoses, infections may be fatal for the naïve host. The infections of domestic cats with the feline immunodeficiency virus, FIV, and humans with the human immunodeficiency virus, HIV, are such recent zoonosis events. The transmission of FIV from wild felids to domestic cats probably took place after their domestication, estimated at 10,000 years ago (Driscoll et al., 2007; Pecon-Slattery et al., 2008; Vigne et al., 2004), while the transmission events giving rise to HIV are believed to have occurred within the last 150 years (Damond et al., 2004; Gao et al., 1999; Keele et al., 2006). Infection of domestic cats with FIV was first described in 1987 (Pedersen et al., 1987), only shortly after the discovery of its human homologue (Barre-Sinoussi et al., 1983; Gallo et al., 1984). In the course of FIV infection animals may develop symptoms similar to that of HIV-infected patients with acquired immunodeficiency syndrome (AIDS) (Callanan et al., 1992; Pedersen et al., 1987; Yamamoto et al., 1989). This feature is unique for non-primate lentiviral infection and underlines the importance of FIV not only as a pathogen of veterinary significance but also as a valuable model for HIV infection and possible vaccine design.

### 1.1.2. FIV epidemiology

FIV is a pathogen in various members of the Felidae family, including lions and pumas, as well as the domestic cat (Biek et al., 2003; Troyer et al., 2008; VandeWoude and Apetrei, 2006). However, FIV is highly host specific to felids and there is no evidence

for transmission to humans (Pedersen et al., 1987). The worldwide prevalence of FIV infection in domestic cats is estimated at 11% (Courchamp and Pontier, 1994). In the United Kingdom approximately 5% of healthy and 47% of sick cats are infected with FIV (Hosie and Beatty, 2007). The virus is mainly transmitted by biting during territorial fights of male cats. Accordingly, FIV is highly prevalent in free roaming male cats (Courchamp and Pontier, 1994). Infection of female cats occurs by biting during mating. Furthermore, vaginal and rectal infections of cats as well as *in utero* transmission and infection via milk could be demonstrated experimentally (Bishop et al., 1996; Burkhard and Dean, 2003; O'Neil et al., 1995). However, the occurrence of such trans-mucosal infections and vertical transmissions in nature is considered low as the number of infected female cats and kittens in the field is limited (Yamamoto et al., 1989).

Based on the nucleotide sequence, FIV can be classified into five subtypes (A-E). In the UK, South Africa and Australia subtype A is prevalent almost exclusively, while subtypes A and B are present in continental Europe. In North America and Japan subtypes A-D are prevalent, subtype E, however, has only been detected in South America. Additionally inter-subtype recombinations have been described and may further complicate classification of the virus (Bachmann et al., 1997; Reggeti and Bienzle, 2004).

### 1.1.3. FIV pathogenesis

The pathogenic potential of FIV has been shown in epidemiological and clinical studies as well as in experimental infections (Hosie et al., 1989; Ishida et al., 1992; Yamamoto et al., 1988). However, the scope and severity of an infection with FIV is difficult to predict and depends on several factors, including age and health status of the cat as well as virus strain and infectious dose (Diehl et al., 1995).

Typically, FIV infections are associated with lymphadenopathy and gingivitis-stomatitis and disease progresses at a time-scale similar to HIV infection (Fig. 1-1) (Elder et al., 2010). Following transmission FIV quickly establishes high plasma virus loads (Callanan et al., 1992). This acute viremic phase is accompanied by a rapid depletion of CD4+ T helper cells and symptoms like fewer, diarrhoea, conjunctivitis and lymphadenopathy (Callanan et al., 1992). FIV induces both the humoral and cellular immune response (Beatty et al., 1996). Following seroconversion viral titers decrease and infected cats enter an asymptomatic stage usually lasting several years. Throughout the

asymptomatic phase the numbers of CD4+ helper T cells decline slowly (Barlough et al., 1991). At the same time numbers of CD8+ T cells increase in response to infection resulting in an inversion of the CD4:CD8 ratio. The ongoing depletion of CD4+ helper T cells may eventually lead to an immunodeficiency, the last stage of FIV infection. Immunodeficient cats display high viral loads and suffer from opportunistic infections and AIDS-like symptoms including gingivitis-stomatitis, wasting, cachexia and neuropathologic deficits (Diehl et al., 1995; Sparger et al., 1989). Furthermore, terminally ill cats were reported to show a higher incidence of lymphosarcoma development (Callanan et al., 1996; Gabor et al., 2001; Hutson et al., 1991).

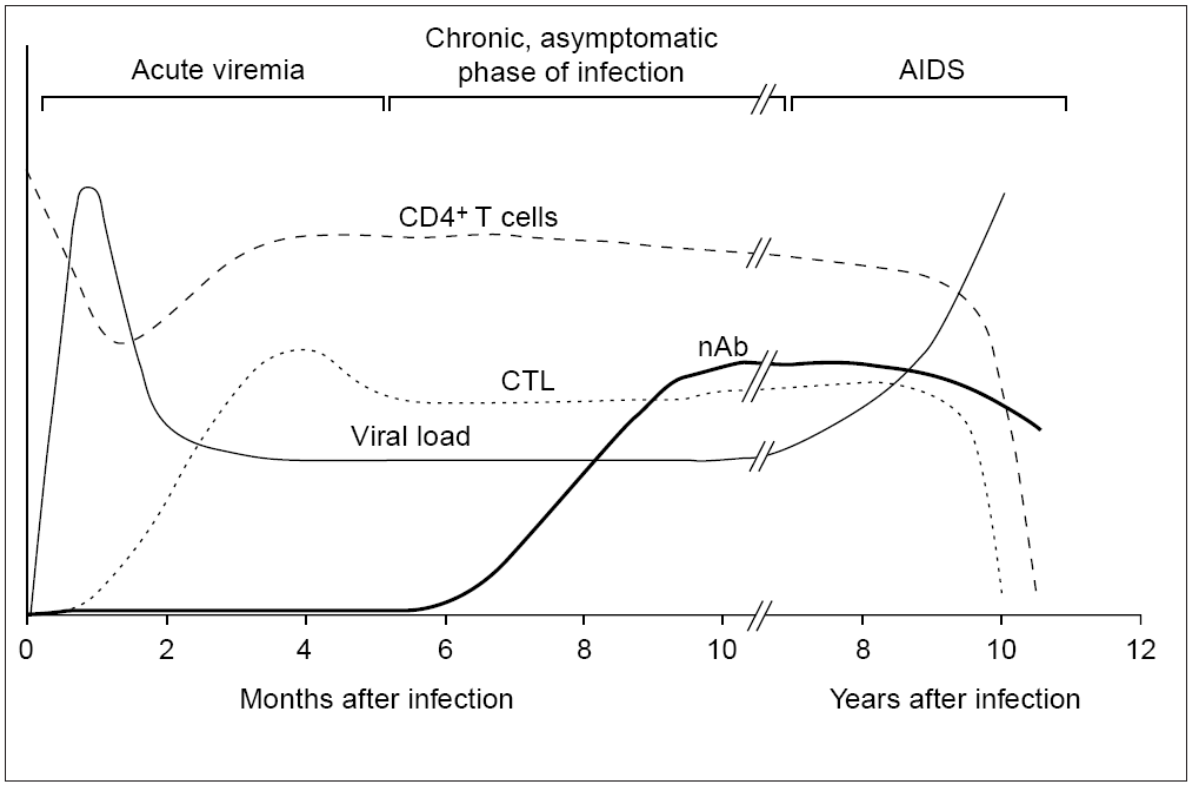


**Figure 1-1. Disease progression following HIV infection.**
Changes in viral loads, numbers of CD4+ cells, humoral (nAb) and cellular (CTL) immune response during acute, asymptomatic and AIDS phase of infection. A similar course of disease progression is followed by FIV (Elder et al., 2010). Adapted from (Ferrantelli and Ruprecht, 2002).

The main target cells for early FIV infection are CD4+ helper T cells, dendritic cells (DCs) and macrophages, while in later stages of infection the tropism expands to CD8+ T cells and B cells (reviewed in (Willett and Hosie, 2008)). Additionally, FIV has been reported to infect microglia cells and bone marrow stromal cells (English et al., 1993; Tanabe and Yamamoto, 2001). This broad tropism allows the establishment of viral reservoirs in

several tissues including lymphatic tissue, spleen, thymus, brain, bone marrow and tonsils (Callanan et al., 1992; Dow et al., 1992; Rideout et al., 1992). Furthermore, FIV infects the salivary gland from where it is shed into the saliva allowing subsequent transmission by biting.

## 1.2. Human immunodeficiency virus

### 1.2.1. HIV epidemiology

The human immunodeficiency virus is a global health threat. According to the world health organisation (WHO) a total of 34 million individuals are infected with HIV (Global summary of the HIV/AIDS epidemic Dec 2011). The number of new infections per year is estimated at 2.5 million. Untreated infections result in a high mortality, with approximately 1.7 million AIDS related deaths in 2011 (http://www.who.int/hiv/data/en/). The main routes of HIV transmission are heterosexual and homosexual intercourse. Sex workers and partners of infected individuals are at a high risk of becoming infected. Another high-risk group are intravenous drug users (IDUs) who might become infected by the re-use of contaminated needles. Furthermore, HIV can be transmitted vertically from mother to child during birth or via milk.

HIV was introduced to humans through zoonotic transmission of simian immunodeficiency virus, SIV, from non-human primates. At least three separate transmission events of SIV from chimpanzees (SIVcpz) gave rise to the HIV-1 subgroups M (major), O (outlier) and N (non-M, non-O) (Gao et al., 1999; Keele et al., 2006). Cross-species transmission of SIV from sooty mangabeys (SIVsm) on eight separate occasions is thought be to the source of HIV-2 subgroups A to H (Damond et al., 2004).

HIV-1 subgroup M is the major cause for the global AIDS pandemic while HIV-1 subgroups O and N, and HIV-2 are largely confined to central and western Africa, respectively.

### 1.2.2. HIV pathogenesis

In contrast to FIV, the development of disease during an untreated HIV infection is almost inevitable. However, pathogenesis of both viruses essentially follows the same pattern (Fig 1-1). Similar to FIV, the early HIV infection is marked by a rapid burst in viral replication. The acute phase is followed by an asymptomatic stage once the immune response suppresses viral replication. The asymptomatic phase can last several years and can be prolonged by antiretroviral therapy. If the infection remains untreated or if drug resistant viral variants emerge, infected individuals will eventually progress towards AIDS which is defined by a drop of CD4+ T helper cells numbers below 200 cells per µl or the occurrence of specific symptoms. These include a severe immunodeficiency, lymphosarcoma, pneumonia, wasting and opportunistic infections (Cheung et al., 2005; Holmes et al., 2003). Most patients eventually die of opportunistic infections.

## 1.3. Virus biology

### 1.3.1. Lentiviral genome organisation and proteins

Lentiviral particles are typically 105 to 125 nm in diameter and carry two copies of a single stranded positive sense RNA genome (Fig. 1-2). The approx. 9.5 kb long RNA genome is bound to nucleocapsid proteins (NC) and contained within the capsid (CA, p24), thus forming the so-called core particle. The core is surrounded by the matrix (MA) protein which carries a phospholipid bilayer derived from the host cell. This viral membrane is spiked with envelope proteins (Env) which shield the particle and facilitate entry into host cells.

HIV and FIV share a similar genome organisation (Fig. 1-3). Three major genes encode for the group specific antigens (*gag*), enzymes (*pol*) and envelope (*env*). The *gag* gene encodes the structural proteins (NC, CA and MA) which form the virus particle. The viral enzymes that are encoded on the *pol* gene are necessary for viral replication. The reverse transcriptase (RT) transcribes the viral RNA genome into DNA while the integrase (IN) inserts the viral DNA into the genome of host cells and the protease (PR) cleaves immature viral polyproteins to functional proteins. In addition, FIV encodes dUTPase, a protein, absent in HIV, which is necessary for the infection of non-dividing cells such as

macrophages which contain high levels of dUTP. The dUTPase prevents the mis-incorporation of uracil into viral DNA by decreasing the levels of dUTP through conversion to dUMP (Lerner et al., 1995; Steagall et al., 1995). The *env* gene encodes the surface unit (SU, gp120) and transmembrane protein (TM, gp41), which form the envelope of the particle.

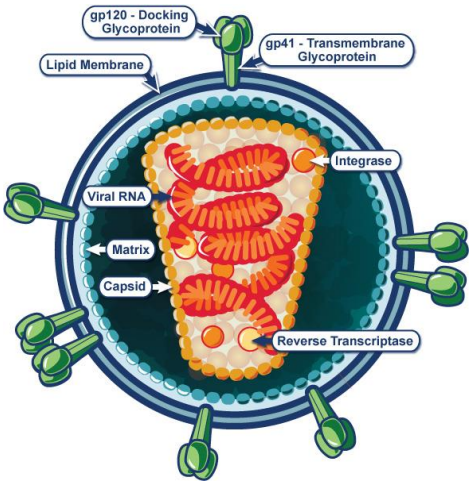


**Figure 1-2. Schematic structure of a lentiviral particle.**
The viral enzymes and the viral genomic RNA are contained within the core particle which is composed of capsid proteins. The core particle is surrounded by the matrix which carries the lipid membrane with the envelope proteins. (Source: National Institute of Allergy and Infectious Diseases; http://www.niaid.nih.gov/topics/HIVAIDS/Understanding/Biology/Pages/hivVirionLargeImage.aspx)

Additionally, the accessory genes *vif*, *Orf-A* and *rev* are contained within the FIV genome. The proteins encoded by these genes possess diverse functions. Vif counteracts the cellular restriction factor APOBEC3 (see 1.6 Evolution of Env), the ORF-A protein has multiple functions in the transactivation of transcription, control of splicing and release of virus particles (de Parseval and Elder, 1999; Gemeniano et al., 2003; Sundstrom et al., 2008) and Rev supports the export of viral RNA from the cell's nucleus (Phillips et al., 1992). In addition, HIV encodes the accessory genes *nef*, *vpr, tat* and *vpu*, which are absent in FIV (Miyazawa et al., 1994).

The genome is flanked by the long terminal repeats (LTRs), which are non-coding regions containing promoter and enhancer elements that increase the transcription of viral RNA. Additionally, these regions are indispensable for the reverse transcription as they complementarily bind to each other and function as primers for viral DNA elongation.

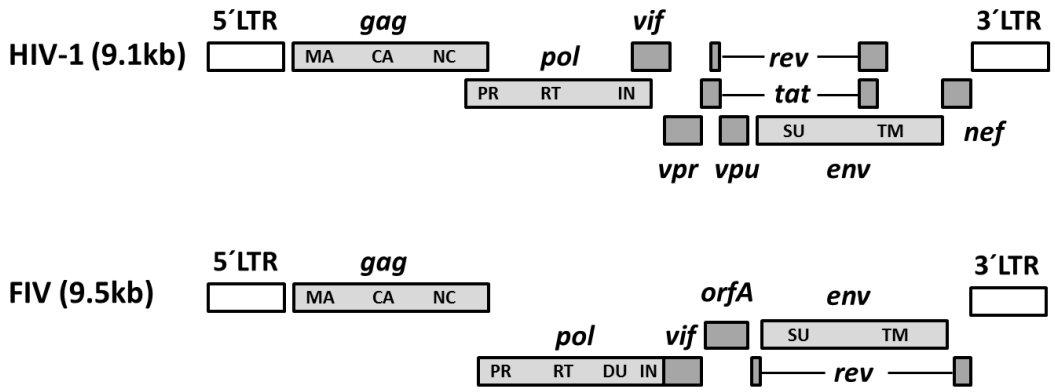


**Figure 1-3. Genome organisation of FIV and HIV-1.**

The three major genes *gag*, *pol* and *env* are flanked by the 5' and 3' long terminal repeat (LTR). The Gag proteins are produced as a polyprotein and cleaved into matrix (MA), capsid (CA) and nucleocapsid (NC). The polyprotein generated from the *gag-pol* open reading frame is cleaved into the structural proteins and protease (PR), reverse transcriptase (RT), dUTPase (DU) and integrase (IN). The *env* gene encodes the surface unit (SU) and the transmembrane protein (TM). Additionally, the accessory genes *vif, vpr, rev, tat, nef* and *orfA* are encoded on the genome.

## 1.3.2. Viral life cycle

Lentiviruses are obligate parasites depending on cellular factors to enable their replication. The infection commences with the recognition of the main receptor on the membrane of a susceptible cell by the surface unit of the envelope protein. Subsequent conformational changes within the SU expose the co-receptor binding site (Jones et al., 1998). The interaction with the co-receptor triggers the dissociation of the SU from the TM which then commences the fusion with the cell membrane (Gallo et al., 2001). Subsequently, the viral core particles are released into the cytoplasm. They interact with the cellular microtubule (McDonald et al., 2002) and cortical actin network (Bukrinskaya et al., 1998) and are transported to the nuclear membrane where they bind to nuclear pore complexes (Schaller et al., 2011). While trafficking to the nuclear membrane the reverse transcription of the viral RNA genome into double stranded DNA occurs within the core particle and is catalysed by the error-prone RT (Temin and Mizutani, 1970). Following the loss of viral capsid or so-called uncoating, the complex of nascent viral DNA and IN is shuttled into the nucleus where the IN facilitates the insertion of the viral DNA into the host cell genome (Arhel, 2010; Brown, 1997). The integrated viral DNA, or so-called provirus, can now be transcribed into mRNA which either serves as a template for translation into amino acids and formation of viral proteins or it functions as a genome

for new virus particles. Gag, Pol and Env are produced as immature polyproteins. The Gag and Gag-Pol polyprotein precursors are enriched at the cell membrane while the Env polyprotein is shuttled through the Golgi apparatus where it is cleaved to its functional proteins gp41 and gp120 by the cellular enzyme furin (Hallenberger et al., 1992). Gp41 and gp120 stay in close proximity via a non-covalent bond and are transported to the cell surface where they associate with viral Gag through a putative interaction of the cytoplasmatic tail of gp41 and the MA domain of the Gag polyprotein (Murakami and Freed, 2000). The NC domain of the Gag polyprotein binds the viral RNA genome and mediates its trafficking into the assembling particle (Kemler et al., 2002). At the cell membrane new viral particles are formed by Gag and Gag-Pol polyproteins, enclosing the viral RNA (Luttge and Freed, 2010). Upon budding from the cell surface components of the cellular lipid bilayer and the Env proteins present within remain with the viral particle and form its membrane and envelope. Finally, maturation of the viral particle occurs as the protease cleaves the Gag and Gag-Pol polyprotein precursors into their respective proteins (Kohl et al., 1988).

### 1.3.3. Viral Env

The majority of structural analyses of Env proteins have been performed on HIV and SIV. However, recent studies on FIV suggest that mechanism of attachment and fusion is very similar for both FIV and HIV (Elder et al., 2008; Willett and Hosie, 2008). Although, highly diverse on the amino acid (AA) sequence level (only 20% AA identity), Env proteins of HIV and FIV are thought to share a similar loop structure as defined by cysteine bonds (Pancino et al., 1993) (Fig. 1-4). The envelope proteins are produced as 160 kDa polyproteins that are cleaved into the surface unit, SU, and the transmembrane protein, TM. The SU is a trimeric 120 kDa glycoprotein (gp120), consisting of several variable loops (V1-V5) interspersed with conserved regions (C1-C5) (Leonard et al., 1990; Starcich et al., 1986). The SU enables the attachment of the virus to the host cell. Accordingly, several motifs on gp120 have been identified to influence the properties of binding to the main and co-receptor. For instance, mutations in the V1/V2 loop and V3 loop of HIV were found to modulate the co-receptor usage as well as altering the binding to the main receptor (Nabatov et al., 2004). Similarly, the V1/V2 homologue of FIV gp120 was shown to alter the interaction with the attachment receptor (Willett et al., 2008) and certain

residues on the V3 homologue were found to determine main receptor independent infection (de Parseval and Elder, 2001; Hosie et al., 2002; Verschoor et al., 1995). Gp120 is non-covalently bound to the trimeric transmembrane protein gp41, which consists of an extracellular region, a transmembrane region and a cytoplasmic tail. The major function of gp41 is to facilitate host cell entry. For this purpose the hydrophobic N-terminus of the extracellular region, the so-called fusion peptide, is inserted into the target cell's membrane following the binding of main and co-receptor by gp120 (Sodroski, 1999). Subsequent, conformational rearrangements in gp41 lead to a shortening of the distance between viral and cellular membrane, eventually allowing membrane fusion (Gallo et al., 2001; Weissenhorn et al., 1997). This highly complex function does not tolerate extensive alterations in the protein's structure. Accordingly, gp41 is highly conserved among different FIV and HIV strains. In contrast, the sequence of gp120 is highly variable between virus strains as the variable loops allow significant sequence variation while preserving receptor binding function.

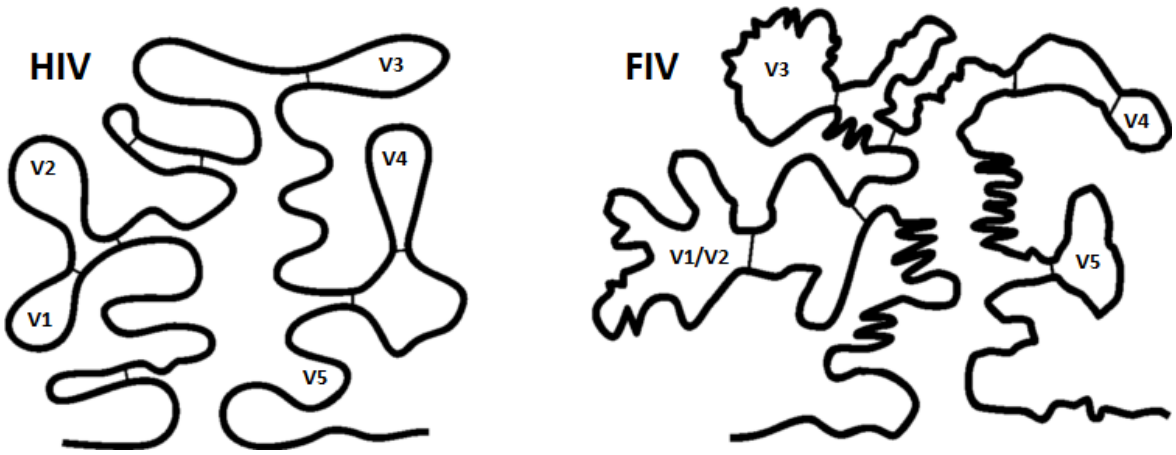


**Figure 1-4. Schematic structure of HIV-1 and FIV gp120.**
Regions with high variability are labelled with V1-V5. Loop structures are created by cysteine disulphide bonds (thin black lines). Adapted from (Leonard et al., 1990; Pancino et al., 1993).

## 1.4. Lentiviral entry receptors

Specific interactions of lentiviral Env proteins with the main entry receptor and co-receptor are necessary for successful infection of cells. These Env-receptor interactions primarily determine the cell tropism and are a critical parameter in the pathogenesis of disease.

Both HIV and FIV share a similar cell tropism preferentially targeting T helper cells and cells of the monocyte/macrophage lineage. Indeed, the co-receptor CXCR4 is utilised by both viruses, however, their main entry receptor differs significantly.

### 1.4.1. HIV receptors

The cellular expression of CD4, the main attachment receptor for HIV, correlates well with the viral cell tropism. CD4 is a glycoprotein of the immunoglobulin superfamily that is expressed on T helper cells, monocytes, macrophages and dendritic cells. CD4 functions *in vivo* as an assisting protein that increases the activation of T helper cells by amplifying the intracellular signal generated upon activation of the T cell receptor (TCR) (Delon and Germain, 2000). CD4 facilitates attachment of HIV by binding to gp120. However, for efficient infection the primary attachment to CD4 must be followed by a secondary interaction of the Env protein with a co-receptor. These co-receptors, typically the chemokine receptors CXCR4 and CCR5, belong to the 7 transmembrane domain (7TM) molecule super-family (Alkhatib et al., 1996; Dragic et al., 1996; Feng et al., 1996). CCR5 is widely expressed on T cells, macrophages, dendritic cells (DC) and microglia. On human T helper cells CCR5 expression is restricted to the subpopulation of memory T cells (CD45RA+). In contrast, CXCR4 is highly expressed on naïve T helper cells (CD45RO+) (Bleul et al., 1997) explaining the broad T cell tropism of X4 tropic strains (Barre-Sinoussi et al., 1983). Furthermore, a number of other 7TM molecules have been described that facilitate infection with certain HIV strains, albeit with a lower efficiency. Of these CCR3 and the chemokine receptor D6 were found to be utilised by some primary isolates of HIV-1 (Aasa-Chapman et al., 2006). Expression of D6 was described on astrocytes, therefore, this receptor may contribute to the dissemination of HIV into the central nervous system (Neil et al., 2005). Classically HIV strains were defined by their tropisms into either “T cell-tropic” or “macrophage-tropic” isolates (Collman et al., 1989; Gendelman et al., 1988). Although this allocation correlates to some extent with the usage of either CXCR4 (T cells) or CCR5 (macrophages), this observation does not hold true in all cases as there have been reports of X4 tropic virus infecting macrophages and R5 strains that poorly infect macrophages (Peters et al., 2006; Simmons et al., 1998). In these cases the major determinant for macrophage tropism seems to be the ability to efficiently utilise low levels of surface expressed CD4 (Gray et al., 2005; Tokunaga et al.,

2001). Moreover certain isolates of HIV-2 have even been shown to infect cells in the absence of CD4 via a direct interaction with CXCR4 (Endres et al., 1996; Reeves et al., 1999).

### 1.4.2. FIV primary receptor

Similar to HIV, FIV is able to infect T cells, monocytes and macrophages. However, in cats CD4 expression is restricted to T helper cells and is absent from cells of the monocyte/macrophage lineage. This inconsistency was solved only recently when CD134 (OX40) was identified as the main attachment receptor of FIV (Shimojima et al., 2004). Expression of CD134 on feline cells follows the pattern of CD4 expression in humans explaining the similar target cell types for FIV and HIV. It is expressed primarily on activated CD4+ T cells, at lower levels on macrophages, DCs and B cells, and a small sub-population of activated CD8+ T cells (de Parseval et al., 2004; Reggeti et al., 2008; Shimojima et al., 2004; Willett et al., 2007).

CD134 is a member of the tumour necrosis factor receptor (TNFR) super-family (Latza et al., 1994)) and functions as a co-stimulatory molecule on T cells. The signals generated through the interaction of CD134 with its ligand (CD134L), which is expressed on antigen presenting cells, lead to the full activation of the T cells that have recognised antigen (Gramaglia et al., 1998; Kopf et al., 1999; Pippig et al., 1999).

Both human and feline CD134 share a similar structure and display a high degree of homology, however, human CD134 does not facilitate entry of FIV (Shimojima et al., 2004). This fact allowed the mapping of binding sites of FIV Env on CD134 by employing feline x human chimeric CD134 molecules (de Parseval et al., 2005; Willett et al., 2006a; Willett et al., 2006b). The ectodomain of CD134 contains three cysteine-rich domains, CRDs, which were exchanged between feline and human CD134. CRD1, the proportion of CD134 that was predicted to be most membrane distal, was found sufficient for successful infection by certain laboratory FIV strains, like FIV-PPR and FIV-B2542. However, several primary strains like FIV-GL8 depend on the expression of certain residues of CRD2 in addition to CRD1 to efficiently infect target cells (Willett et al., 2006a; Willett et al., 2006b). This discrepancy in the receptor interactions between virus strains is further underlined by differences in the inhibitory effects of soluble proteins. Both CD134 ligand and receptor exist as membrane bound and soluble proteins *in vivo*. Therefore, an

interaction of the soluble forms with FIV seems possible. Indeed, *in vitro* experiments showed an inhibitory activity of trimeric CD134L to infection with FIV (Willett et al., 2009). However, primary strains like FIV-GL8 were less sensitive to inhibition than laboratory adapted strains like FIV-PPR and FIV-B2542. Similarly, differences in the interaction with soluble CD134 receptor have been described. Incubation of a soluble N-terminal immunoglobulin Fc region-CD134 fusion protein (sFc-CD134) with FIV-PPR led to conformational changes in Env that allowed the infection of CD134 negative target cells by a direct interaction with CXCR4 (de Parseval et al., 2005; de Parseval et al., 2006). In contrast, sFc-CD134 has been shown to block the infection of CD134 positive target cells by several primary strains of FIV including FIV-GL8 (Willett et al., 2009). These examples clearly demonstrate differences in the utilisation of CD134. Furthermore, certain cell culture-adapted FIV strains, e.g. FIV-PET and FIV-34TF10 (Olmsted et al., 1989; Talbott et al., 1989), are CD134-independent and infect cells by direct utilisation of CXCR4 (Shimojima et al., 2004), a mechanism that is similar to the CD4-independent infection by certain HIV-2 isolates (Endres et al., 1996).

### 1.4.3. FIV co-receptor

Following attachment to the main receptor by HIV and FIV an interaction with a second receptor is necessary for successful infection (Poeschla and Looney, 1998; Willett et al., 1997a; Willett et al., 1997b). FIV solely depends on CXCR4 for this purpose. Other receptors utilised by HIV like CCR5 or CCR3 do not support FIV entry. Expression of CXCR4 in cats occurs on similar cells as in primates. Furthermore, canine and human CXCR4 supports infection in the presence of feline CD134 (Willett et al., 2008; Willett et al., 2006b). The interaction of FIV and HIV with feline and human CXCR4 respectively can be inhibited by the natural ligand for CXCR4, SDF-1, however, the affinity of the ligand is low (Bleul et al., 1996; Hosie et al., 1998a; Oberlin et al., 1996). A bicyclic compound named AMD3100 displays a high affinity to human and feline CXCR4 and has been shown to inhibit infection by HIV and FIV efficiently (Egberink et al., 1999; Richardson et al., 1999).

# 1.5. Immune response to lentiviral infection

## 1.5.1. Humoral and cellular immune responses

Following the burst of viral replication during the acute phase of infection a cytotoxic T lymphocyte (CTL) mediated immune response is induced by HIV and FIV. The population of cytotoxic CD8+ lymphocytes expands rapidly and is thought to reduce viral loads significantly (Borrow et al., 1994; Koup et al., 1994; Willett et al., 1993). CD8+ T cells specific to HIV-1 have been detected in infected individuals prior to virus specific antibodies (Ab) (Pantaleo et al., 1994; Wilson et al., 2000). In FIV infected cats a non-cytolytic T cell response may be detected as early as one week post-infection by an increase in chemokines, which suppress viral replication (Choi et al., 2000; Flynn et al., 2002). In addition to CD8+ T cells responses, CD4+ T cells show an increased secretion of interferon gamma (IFN-γ) (Liang et al., 2000), an immunostimulatory cytokine that enhances the activation and maturation of immune cells but also induces innate antiviral immune factors like APOBEC3 and tetherin (Dietrich et al., 2011; Peng et al., 2006).

Both HIV and FIV induce a strong humoral immune response during infection. The generation of neutralising antibodies (NAb) is thought to be vital for controlling the infection (Spenlehauer et al., 2001). The development of anti-FIV Ab has been described as early as six weeks post-infection (Hosie et al., 1998b), but the maturation of NAb usually requires more time (Moog et al., 1997). For instance, an efficient NAb response to HIV-1 may take eight months to develop (Richman et al., 2003). Similarly, the humoral immune response to FIV matures over several months to years (Hosie et al., 2011). For efficient neutralisation, Abs need to block the interaction of Env and its receptors. Accordingly, Abs have been described in HIV infected individuals that bind CD4 (Chams et al., 1988; Corre et al., 1991) or that block FIV infection by binding to CD134 (Grant et al., 2009). However, receptor specific NAb only represent a small fraction of the NAb which are generated, as the main NAb response is directed against Env. Antibodies are generated against both gp120 and gp41, however gp41 is largely hidden below gp120, making gp120 the more easily accessible target for NAb. The structure of gp120 is highly variable and it appears this protein is providing largely irrelevant Ab binding surfaces, while preserving regions necessary for the cell entry (Karlsson Hedestam et al., 2008). Changes in the amino acid (AA) sequence of gp120, especially the exchange of charged

AA, can strongly influence the surface structure and could impede binding of NAb (Naganawa et al., 2008). Furthermore, carbohydrate structures on the envelope are major surface determinants for the binding of NAb (Dacheux et al., 2004; Wyatt and Sodroski, 1998). The majority of these sugar molecules are bound via N-glycosylation sites which require an amino acid motif in which an asparagine is followed by any AA, except proline, and a serine or threonine at third position (NXS/T) (Marshall, 1974). The exchange of a single nucleotide in the viral DNA may lead to an altered first or third AA in the NXS/T motif which could delete or create a potential N-glycosylation site. This mechanism allows rapid alterations in the surface structure and is thought to largely increase the viruses' ability to evade the humoral immune response (Wei et al., 2003). Gp41 does not contain a vast amount of N-glycosylation sites and its AA sequence is more conserved as its function in membrane fusion does not tolerate significant changes. However, the induction of gp41 specific antibodies is difficult as its exposure to the immune system is very limited.

The immune system may contribute to the emergence of viral variants with distinct receptor interactions. These escape mutants may display impaired infection capabilities due to adaption of gp120. Conversely, changes in the Env-receptor interaction usually appear upon significant damage to the immune system. For example, the switch from CCR5 to CXCR4 co-receptor usage, which is accompanied by an increased virulence, often occurs at late stages of HIV infection when the immune response is weakened (Connor et al., 1997). These X4 variants may be more sensitive to neutralisation in comparison with their progenitors as a result of alterations in gp120 that lead to the exposure of certain epitopes. Similarly, mutations of CXCR4 binding epitopes may arise that allow the direct interaction with the co-receptor in the absence of CD134 (de Parseval and Elder, 2001; Hosie et al., 2002; Verschoor et al., 1995) however, the exposure of the V3 loop makes these variants more readily neutralisable (Osborne et al., 1994) which is why these mutations usually manifest during later stages of FIV infection.

### 1.5.2. APOBEC3

Apolipoprotein B mRNA editing enzyme catalytic polypeptide-like 3 (APOBEC3) is an anti-viral host restriction factor which is part of the innate immune response (Fig. 1-5). In HIV or FIV infected cells APOBEC3 proteins interact with the viral nucleocapsid and are

encapsulated into newly formed virions (Malim and Bieniasz, 2012; Munk et al., 2008). During reverse transcription in the subsequent target cell APOBEC3s specifically deaminate cytidine (C) to uracil (U) on nascent viral (-) strand DNA resulting in guanidine (G) to adenosine (A) hypermutated (+) strand proviral DNA (Harris et al., 2003; Mangeat et al., 2003; Munk et al., 2008; Sheehy et al., 2002; Zhang et al., 2003). These G-to-A hypermutations may result in preliminary stop codons, nonsense mutations or alternative splicing of viral transcripts leaving the virus with a defective genome (Zheng and Peterlin, 2005). Additionally, a deamination-independent APOBEC3-mediated inhibition has been described that functions via a direct block of reverse transcription, however the relative contribution of this effect to viral restriction is not fully clear (Bishop et al., 2008; Holmes et al., 2007; Newman et al., 2005).

In many species the family of APOBEC3 proteins consists of several members which differ in their expression, anti-viral activity and target sequence specificity. The cat genome contains four APOBEC3 genes; *feA3Ca*, *feA3Cb* and *feA3Cc* which show high nucleotide identity of approximately 98% and the more distantly related *feA3H* (Munk et al., 2008). However, a fifth APOBEC3 transcript, feA3CH, is generated by read-trough alternative splicing utilising exons from *feA3C* and *feA3H* (Munk et al., 2008). The anti-viral activity of feline APOBEC3 proteins is virus-specific. FeA3H and feA3CH are highly active against FIV but are relative inefficient in restricting feline foamy virus (FFV), a retrovirus of the spumavirus genus (Hooks and Gibbs, 1975; Munk et al., 2008). In contrast, the three forms of feA3C exhibit high activity against FFV but fail to restrict FIV (Munk et al., 2008; Zielonka et al., 2010a). APOBEC3 proteins differ in their target sequence preference. The two best characterised human APOBEC3 proteins, hA3G and hA3F, preferentially deaminate C<u>C</u> and T<u>C</u> dinucleotides resulting in <u>G</u>G-to-<u>A</u>G and <u>G</u>A-to-<u>A</u>A mutations on the (+) plus strand DNA (Liddament et al., 2004; Yu et al., 2004). Feline APOBEC3 proteins do not show such clear preference. The activity of feA3H and feA3CH results in mutations of <u>G</u>G, <u>G</u>C and <u>G</u>A residues, while <u>G</u>T-to-<u>A</u>T mutations are rare. Conversely, feA3C proteins preferentially edit A<u>C</u> residues resulting in <u>G</u>T-to-<u>A</u>T mutations (Munk et al., 2008).

Lentiviruses are not defenceless against APOBEC3 proteins; both HIV and FIV express the accessory protein Vif, which induces polyubiquitination and proteosomal degradation of APOBEC3 in the virus producing cell (Munk et al., 2008; Wang et al., 2011).

Additionally, binding of Vif to APOBEC3 reduces packaging of APOBEC3 into viral particles (Kao et al., 2007; Opi et al., 2007). Thus *in vitro* FIV resists the detrimental effects of APOBEC3 in the presence of Vif but is efficiently restricted in the absence of Vif. (Munk et al., 2008; Zielonka et al., 2010a).

The *in vivo* consequences of the action of APOBEC3 on lentiviral infection are not fully understood. Clinical isolates of HIV display a bias towards G-to-A mutations (Fitzgibbon et al., 1993; Janini et al., 2001) and an inverse correlation of proviral load and APOBEC3 expression has been reported (Kourteva et al., 2012). However, these findings are not supported by other studies (Amoedo et al., 2011). Furthermore, it has been speculated that contrary to its anti-viral activity the action of both APOBEC3 and Vif may lead to an equilibrium in which a sub-lethal degree of hypermutations induced by minor amounts of APOBEC3 might increase virus diversity allowing faster adaption to the host's immune system (Munk et al., 2012). Accordingly, it has been shown that limited packaging of APOBEC3 into HIV-1 particles resulted in quicker resistance to anti-retroviral drugs *in vitro* (Fourati et al., 2010; Kim et al., 2010; Mulder et al., 2008).

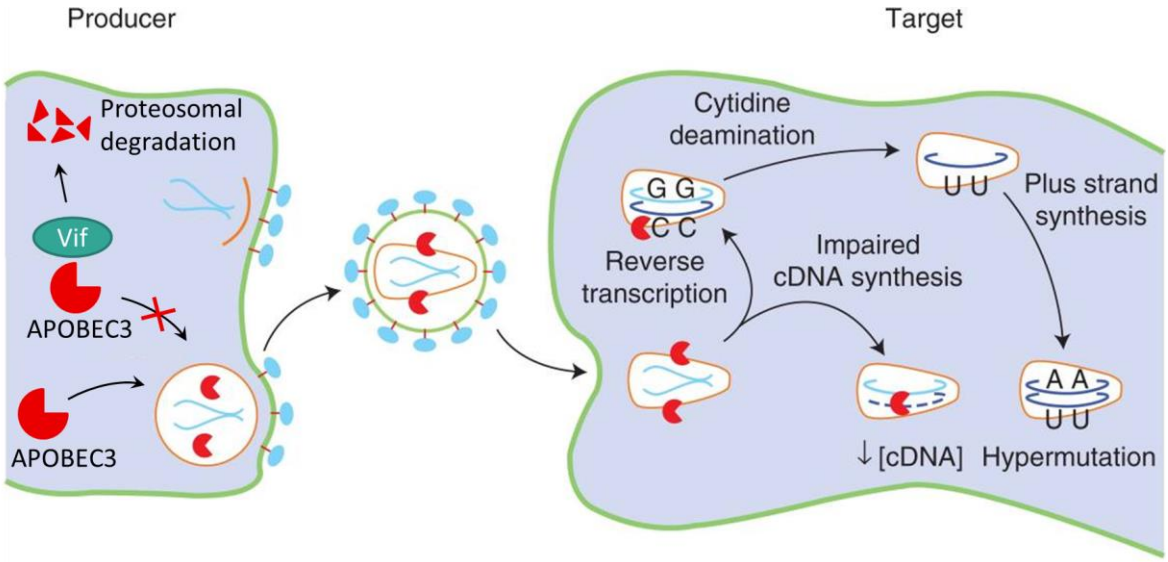


**Figure 1-5. Mechanism of viral restriction by APOBEC3 proteins.**
The restriction factor APOBEC3 is produced by the host cells. Lentiviral Vif targets APOBEC3 to proteasomal degradation thereby reducing levels of free APOBEC3 molecules in the cytoplasm. In the absence of Vif APOBEC3 is encapsulated in budding virus and transferred to the new target cell. During reverse transcription APOBEC3 deaminates cytidine to uracil on nascent viral single-stranded minus-strand DNA. During subsequent DNA plus strand synthesis adenosines are incorporated instead of guanines resulting in G-to-A mutations. Additionally, APOBEC3 also functions via a deaminase-independent direct inhibition of reverse transcription. APOBEC3 is marked in red. Viral RNA is shown in light blue, viral DNA in dark blue. Modified from (Malim and Bieniasz, 2012).

## 1.6. Vaccines against FIV and HIV

An ideal vaccine should elicit a sterilising protection through the action of both the humoral and cellular immune response. In spite of considerable global research, the development of an efficient vaccine against HIV has remained elusive. Several vaccine candidates that seemed promising in studies on primates failed to elicit broadly neutralising Ab against HIV when tested in human cohorts. A recent major vaccine trail by Merck (phase-IIb STEP trial) aimed to elicit CTL activity against HIV. However, the vaccine group showed signs of vaccine mediated enhancement of HIV infection, therefore the trial had to be terminated before completion (Barouch and Korber, 2010). A more promising phase-III trial was performed with a vaccine named RV144 and was meant to induce a humoral as well as a cell mediated immune response. This vaccine displayed an overall efficacy of 31%, yet, only led to a weak protection (3%) of the high risk group (Rerks-Ngarm et al., 2009). Thus, an efficient HIV vaccine remains a distant target. In this respect FIV has attracted considerable attention as a model for lentiviral infection and the development of an HIV vaccine. A commercial vaccine against FIV, Fel-O-Vax®, has been available since 2002. It consists of inactivated cells infected with FIV-Petaluma (clade A) and FIV-Shizuoka (clade D). The vaccine proved protective against clade A and B challenge viruses (Huang et al., 2004). However, the percentage of protected cats ranged from 0 to 100% depending on the dosage and challenge virus. For instance, in two trials vaccination lead to 0% or 40% protected cats when challenged with the primary isolate FIV-GL8 (Dunham et al., 2006a; Dunham et al., 2006b). Due to the variability in protection rates and the fact that vaccinated cats cannot be differentiated from infected cats by ELISA against capsid protein p24, the use of Fel-O-Vax has not been recommended to practitioners. Nevertheless, due to the similarities of FIV and HIV, future vaccine trials against FIV may contribute to the development of an effective HIV vaccine.

## 1.7. Evolution of Env

The example of zoonotic transmission of HIV type 1 and 2 to humans demonstrates how viruses that are apathogenic in their original host can lead to fatal disease in their new host species. The high genetic variability of lentiviruses enables such quick adaption

to the new host. Lentiviruses are unique from other viruses in their high mutation rate, which for HIV-1 is approximately 3 substitutions per $10^{-5}$ nucleotides per replication cycle (Mansky and Temin, 1995). This is due mainly to the dependence on reverse transcriptase to copy the RNA genome into DNA. During the process of reverse transcription lentiviruses accumulate errors of base substitution, insertion and deletion due to the low fidelity of RT and its lack of proof reading activity (Roberts et al., 1988). Besides the RT, cellular enzymes involved in the transcription of viral DNA to RNA, in particular the RNA Polymerase II, may induce additional substitutions (Thomas et al., 1998). Moreover, recombination events might increase the complexity of a virus population within an infected individual (Hayward and Rodrigo, 2008). Following the infection of a host cell by more than one virus particle, viral genomes from different origins may be packaged during the formation of new particles. Upon infection of a subsequent target cell, reverse transcription may result in recombinant viral DNA as the RT is able to jump between RNA strands (Neher and Leitner, 2010; Zhuang et al., 2002). Additional variability may arise through the action APOBEC3. Conversely to its anti-viral effect limited packaging of APOBEC3 into Vif competent viruses may result in sub-lethal mutations that accumulate over time and increase viral diversity (Mulder et al., 2008; Munk et al., 2012).

The influence of the factors described above on viral replication results in the evolution of the virus from the infecting strain to an emerging population of closely related mutant genomes. The complexity of such a virus population, or so-called “quasispecies” (Eigen, 1971), is shaped by the activity of the adaptive immune system. Accordingly, viral variants carrying non-synonymous mutations that allow immune evasion without impeding replication are retained selectively in the viral population that emerges during infection (Domingo and Holland, 1997; McGrath et al., 2001). Sequence evolution is not distributed equally over the viral genome, but is highest in the *env* gene. In HIV infected patients the quasispecies present within an individual may display variation of up to 10% in its *env* sequences (Delwart et al., 1997). Furthermore, the detection of a highly diverse virus population during acute infection is linked with both a higher viral burden and a faster decline in numbers of CD4+ cells (Sagar et al., 2003). These findings suggest that a highly heterogenic viral quasipecies may impair the immune control of infection and is more likely to cause disease.

However, the degree of heterogeneity of a virus population can be limited by several factors. For example, following HIV-1 infection with body fluids containing both R5 and X4 tropic variants, R5 tropic isolates seem to be transmitted preferentially and dominate early in infection, whereas X4 variants emerge at later stages of infection (Zhu et al., 1993). Until recently it was unclear whether both R5 and X4 tropic viruses were transmitted and replication of X4 variants was impaired during early infection or if solely R5 variants were transmitted and the X4 variants evolved from their corresponding R5 ancestor. Yet, sequence analysis performed early after transmission revealed that the X4 variants that appear late in infection are indeed not transmitted and evolve *de novo* from R5 tropic variants (Salazar-Gonzalez et al., 2009). The results fuelled speculation about a "gatekeeper" that prevents transmission of X4 tropic virus selectively (Margolis and Shattock, 2006). Furthermore, it appears that in most cases, transmission is limited to a single variant of R5 tropic virus indicating that the gatekeeper might even act on the R5 tropic strain. Such gatekeeping mechanisms have mainly been observed during mucosal (vaginal and rectal) transmission of HIV. It appears that some components of mucus are restrictive for X4 viruses (Seidel et al., 2010). Additionally, high epithelial expression of SDF-1, the natural ligand of CXCR4 may inhibit infection of X4 variants by down-modulation of CXCR4 from target cell surfaces (Agace et al., 2000). However, there is also evidence for additional post-mucosal barriers of X4 tropic virus. Upon direct, intravenous infection with HIV (via contaminated needles) R5 variants are selectively transmitted and dominate during infection (Spijkerman et al., 1995). One possible explanation could be an unequal cytotoxic T lymphocyte (CTL) response targeting infected cells. Macrophages, which become mainly infected by R5 tropic virus, are relatively resistant to a CTL response. In contrast, T cells which are the target of X4 variants are susceptible for CTL mediated killing. The transmission of R5 tropic virus may be favoured further by viral cell-to-cell spread through viral synapses, which are virally induced extensions of the cell membrane that almost exclusively allow dissemination of R5 strains (David et al., 2001). A more detailed review on these mechanisms is given in (Grivel et al., 2011). Together these reports show the high potential for adaption by HIV but also that certain mechanisms pose a bottleneck to the evolution of HIV.

Little is known about the evolution of FIV *in vivo*. Sampling of virus early after natural infection is complicated as symptoms of acute infection are difficult to diagnose in

cats. Furthermore, the identification of founder viruses requires knowledge of the source of infection. Therefore, most reports on FIV quasispecies concentrate on analysis of inter-host diversity and assignment of variants to clades or subtypes (Carpenter et al., 1998; Pistello et al., 1997; Sodora et al., 1994). However, there are a few experimental infections comparing single virus infections of different FIV strains. These studies covered periods of more than two years (Huisman et al., 2008; Motokawa et al., 2005) up to 9 years (Ikeda et al., 2004). Although these reports describe the emergence of variants with sequence changes in V3, V5 and gp41, the actual number of mutations were relatively low.

In the course of infection, HIV-1 may acquire mutations in the *env* gene that increase virulence, e.g. the switch from R5 to X4 tropism. Similarly, the virulence of FIV can increase during long-term infection. For example, infection of cats with Petaluma-F14, a relatively avirulent strain of FIV, led to the emergence of viral variants with increased virulence as shown by higher proviral load and activation of a certain population of CD8 positive T cells (Hosie et al., 2002). Mutations causing this increase in virulence were mapped to the V3 loop of gp120 and are thought to have altered the interaction with CXCR4.

Unlike HIV, FIV depends solely on CXCR4 as a co-receptor for infection. In the absence of an alternative co-receptor viral adaption might be achieved through alterations in the usage of CD134. Accordingly, well-studied laboratory strains like FIV-Pet or FIV-PPR which were isolated during chronic infection and are relatively avirulent, display a reduced dependency for CD134. Indeed, these isolates may even accomplish cell entry in the absence of CD134. Other strains, including FIV-GL8 and FIV-CPG, isolated during early infection are virulent and show a high dependency on CD134. A model of FIV evolution has been proposed which links molecular mechanisms of virus-receptor interaction and disease progression (Willett and Hosie, 2008). During the early stage of infection, FIV infects a limited spectrum of cells via a high affinity attachment to CD134. The rather complex Env-receptor interaction is characterised by the dependence on both CRD1 and CRD2 on CD134. Subsequently, the infection occurs as a two-step process in which the CXCR4 binding site is only exposed following attachment to CD134. Upon disease progression and immune suppression new variants emerge that display a reduced requirement for protecting their CXCR4 binding site, allowing a more efficient interaction

with CXCR4. In return the need to retain a high affinity interaction with CD134 is reduced and variants only require CRD1 for successful infection. This more relaxed interaction allows the utilisation of low surface CD134 resulting in a broader cell tropism (including B cells and CD8+ T cells) and the dissemination of virus into new tissues. The outcome of transmitting such a quasispecies is unknown. Two scenarios seem possible: either the wider variety of variants leads to an increased virulence with high proviral loads and the infection of a broad spectrum of cells; or isolates from later stages of infection will be filtered out by a specific bottleneck and isolates from early stage infection will remain.

## 1.8. Aims of this thesis

The evolution of retroviruses during infection is shaped by viral factors, such as their mechanism of replication, and by host factors, mainly the immune system. The goal of this project was to shed light into the *in vivo* evolution of the FIV. We aimed to elucidate how immune pressure impacts on the virus, in particular the interaction of the viral envelope protein (Env) and the viral entry receptors.

First, we intended to characterise viral populations, quasispecies, in cats infected with a molecular clone of FIV-GL8 for a period of up to six years. We planned to illustrate the relationship of viral *env* sequences isolated from PBMCs and lymphoid and non-lymphoid tissues by phylogenetic trees and analysis of divergence, diversity and rate of evolution.

Subsequently, we aimed to investigate whether the Env-receptor interaction of virus variants isolated 322 weeks post-infection had evolved *in vivo.* In particular we were interested in the determinants important for receptor recognition, sensitivities to entry inhibitors and the impact of neutralising antibodies on viral Env.

Finally, we wished to compare the *in vivo* replication kinetics during infection of cats with either a clonal preparation of FIV-GL8 or a defined mixture comprising FIV-GL8 progeny. Such an artificial quasispecies should closely resemble the situation in the field where chronically infected cats transmit a viral population rather than a single virus. We aimed to compare proviral loads and humoral and cellular immune responses to investigate the impact of viral diversity on pathogenicity and to determine which variants of the mixed inoculum would display improved replication kinetics and which would fail to thrive following transmission. Such findings may allow the identification of future targets for FIV vaccines.

# 2. Material and methods

## 2.1. Animal studies

### 2.1.1. Study one: long term infection versus short term infection

In the first animal study, infections of cats were performed to investigate differences of viral evolution during short-term and long-term infection. Challenge virus was prepared by transfection of a molecular clone of FIV-GL8 into the murine fibroblast cell line 3T3. Subsequently, virus containing supernatant was filtered through Minisart® 0.45µm-pore-size filters (Sartorius, Epsom, UK) and used for infection of the IL-2 dependent feline T-cell line Q201 (Willett et al., 1991). Infection was monitored visually for cytopathic effects and by p24 ELISA (PetCheck FIV antigen ELISA, IDEXX Corp., Portland, Maine, USA). Virus stocks were harvested at peak p24 levels, filtered at 0.45µm and stored at -80°C.

Two groups of age-matched specific-pathogen-free kittens were inoculated intraperitoneally with 10 CID50 (50% cat infectious doses) of homogenous FIV-GL8 (Hosie et al., 2002). Each group consisted of three animals and infection proceeded for either 12 weeks (cats A773, A774 and A775) or 322 weeks (cats A611, A612 and A613), when the cats were sacrificed. Samples of whole blood were taken at regular intervals. Peripheral blood mononuclear cells (PBMC) were isolated from EDTA anti-coagulated blood and processed for flow cytometry or were stored at -80°C. Plasma samples were cryo-preserved at -80°C for subsequent neutralisation assays. Tissue samples were collected post mortem and stored at -80°C until required for DNA extraction.

Viral *env* gene sequences were derived from PBMCs and tissues as described in 2.2.2-2.2.3 and phylogenetic analysis (2.2.4) performed. Subsequently, a set of *env* sequences from animal A613 was cloned (2.2.6-2.2.9) and their biological properties analysed (2.3.2-2.3.6). Finally, six variants (B14, B19, B28, B30, B31 and B32) of this phenotype analysis were chosen to be used in the second *in vivo* study (2.1.2).

### 2.1.2. Study two: homogenous versus heterogeneous virus

The aim of the second study was to distinguish differences in the biological phenotypes of parental virus FIV-GL8 (B32) and an artificial quasispecies comprising FIV-GL8 (B32) and viral variants (B14, B19, B28, B30 and B31) derived from animal A613 after more than six years of infection with FIV-GL8. The molecular clones needed for the preparation of virus were generated by cloning the variants *env* genes into the FIV-GL8mya plasmid (2.2.6). Thus all clones shared a common FIV-GL8-derived *gagpol* sequence. The *env* sequence of B32 is identical to that of FIV-GL8 but it had been isolated from cat A613 and underwent all subsequent cloning steps and therefore was used (instead of FIV-GL8) to compensate for any cloning related errors. Challenge viruses were prepared by transfection of HEK293T cells with molecular clones of each of the six variants. Subsequently, virus was recovered on Mya-1 cells, which express CXCR4, CD134 and CD4 at levels similar to mitogen-stimulated feline helper T cells. Mya-1 cells support the growth of all FIV isolates tested to date, but do not apply a selective pressure on the virus such that the *env* gene sequence remains unchanged post-culture. Virus stocks were filtered at 0.45 µm and stored at -80°C. Virus titre of each variant was determined by serial dilution of virus stocks on naïve Mya-1 cells and subsequent detection of productive infection by visual inspection for cytopathic effects and by p24 ELISA (IDEXX). Each titration was performed in duplicate and repeated, the virus titre was then calculated using the Kärber formula wherein $\log_{10}$ TCID50= ($X_0$- 0.5d + dΣp) with $X_0$=$\log_{10}$ of highest dilution giving 100% of wells p24 positive, d=$\log_{10}$ of dilution interval, p=proportion of p24 positive tests at any given dilution, Σp=sum of values of p for X0 and all higher dilutions. Additionally, reverse transcriptase activity in each virus stock was assayed by Lenti-RT non-isotopic RT assay (Cavidi AB, Uppsala, Sweden) as per manufacturer's instruction. Each of the individual virus stocks contributed approx. $3 \times 10^9$ viral genomes (range $1.3\text{-}6.0 \times 10^9$) to the inoculum. Specifically, variant B14 accounted for $2.2 \times 10^9$ genomes, while B32 contributed $1.3 \times 10^9$ genomes.

Previous studies have suggested that four animals per group would be sufficient to discern differences in CD4/CD8 ratios and proviral load (Hosie et al., 2002). Hence, two groups of four age-matched specific-pathogen-free kittens were infected intraperitoneally with 10,000 tissue culture infectious doses (TCID50) of either the parent molecular clone

of B32 (animals 821, 822, 823 and 824) or an artificial quasispecies containing equal TCID50 of six variants bearing the *env* genes of B14, B19, B28, B30, B31 and B32 to a final combined challenge dose of 10,000 TCID50 (animals 825, 826, 827 and 828). Thus, Group 1 received 10,000 TCID50 of clonal virus, while Group 2 received 10,000 TCID50 of a pool of variants.

EDTA-anti-coagulated blood samples were collected at three-weekly intervals and processed for flow cytometry, while plasma was stored for neutralisation assays and immunoblotting. PBMCs were prepared using whole blood lysis and stored at -80◦C for subsequent analysis of proviral loads. Lymphoid tissues were collected and processed at post-mortem, 21 weeks post-infection. The separated cells were cryo-preserved and frozen at -80°C for subsequent ELISpot analyses.

Virus stocks were generated and titrated by Prof. Brian Willett, University of Glasgow.

### 2.1.3. Ethical statement

Animal studies were approved by the University of Glasgow Institutional Animal Care and Use Committee. Studies were conducted under licence from the UK Government Home Office under the Animals (Scientific Procedure) Act 1986. Usage of recombinant retroviruses was approved by the Health and Safety Executive under the Genetically Modified Organism (Contained Use) Regulations 2000.

## 2.2. Molecular cloning

### 2.2.1. DNA extraction from peripheral blood mononuclear cells (PBMCs) and tissue

DNA was extracted from $1x10^6$ PBMCs resuspended in 200 µl Phosphate Buffered Saline (PBS) using QIAamp DNA blood mini kit (QIAgen Ltd., Crawley, UK) according to the manufacturer's instructions. DNA was eluted in 200µl AE buffer and either used immediately for PCR or stored at -20°C. For DNA extraction from tissue an approximately pea-sized piece was freed from fatty tissue using a scalpel, snap frozen with liquid nitrogen and disrupted using mortar and pestle. The tissue was then resuspended in 200 µl PBS and DNA extracted using the QIAamp DNA blood mini kit as described above.

## 2.2.2. Primers and probes

All primers and probes were synthesised by Eurofins MWG (Ebersberg, Germany), shipped in lyophilised form and resuspended in DNase/RNase-free water (Promega). Primers and probes were diluted to stock concentrations of 100 pmol/µl, used at working concentrations of 10 pmol/µl and were stored at -20°C. Sequences of all primers and probes are displayed in the Appendix.

## 2.2.3. Limiting dilution PCR

Amplification of viral sequences directly from genomic DNA using conventional PCR presents a number of technical challenges. In a DNA sample containing a mixture of virus variants an abundant isolate may conceal scarce variants. Moreover, there is the possibility of PCR-induced recombination of viral genes as the polymerase is able to jump between strands (Cronn et al., 2002). To overcome these hurdles we amplified *env* sequences from single viral copies. We utilised a previously established limiting dilution PCR (LD-PCR) which had been shown to amplify the FIV *env* gene from a single copy of the plasmid $pGL8_{MYA}$ (encoding one full length FIV-GL8 genome) in a background of 5 µg per reaction of feline genomic DNA. The nested PCR protocol utilised high-fidelity proofreading polymerase and consisted of two rounds of "touchdown" PCR.

The first round amplification (nt position 5888–9127 of FIV-GL8) comprised primers 1F4 and 1R4 at 0.5 µM, 0.2 µl sample, 4 µl High-Fidelity (HF) Buffer (New England Biolabs, NEB, Hitchi, UK), 0.2 mM 2'-deoxynucleoside-5'-triphosphates (dNTPs) (Invitrogen Life Technologies Ltd. Paisley, UK), 4% DMSO (NEB), 1U Phusion™ Polymerase (NEB) and nuclease free water (Promega UK Ltd., Southampton, UK) to 20 µl. Amplifications were performed with the following temperature parameters: initial denaturation at 98°C for 3 min, followed by 14 cycles of 98°C for 10 s, 69°C* for 30 s (*decreasing by 0.5 °C/cycle), 72°C for 2 min, then a further 21 cycles of 98°C for 10 s, 62°C for 30 s, 72°C for 2 min, followed by 72°C for 10 min and a final hold at 4°C. The second-round amplification (nt position 6218–8892 of FIV-GL8) was performed using 0.8 µl of the first round PCR product and the primers XF2B and XR2 at 0.5 µM, in a reaction mixture containing 4 µl HF Buffer, 0.2 mM dNTPs, 3% (v/v) DMSO, 1U Phusion™ Polymerase and nuclease-free water to 20 µl. Second-round PCRs were performed using a protocol consisting of the following

parameters: initial denaturation at 98°C for 3 min, followed by 14 cycles of 98°C for 10 s, 70°C* for 30 s (*decreasing by 0.5°C/cycle), 72°C for 1 min 30 s, then 21 cycles of 98°C for 10 s, 63°C for 30 s, 72°C for 1 min 30 s, followed by 72°C for 10 min and a final hold at 4°C. Initially, the dilution of genomic DNA containing a single virus copy had to be determined. Therefore, an endpoint dilution of four replicates of genomic DNA from infected PBMCs was performed through a five-fold dilution series until three consecutive dilutions were found PCR negative for all four replicates. The template dilution containing a single viral copy was then calculated by counting the number of positive reactions at higher dilutions and using "QUALITY" (http://ubik.microbiol.washington.edu/computing/quality/jquality.htm; (Rodrigo et al., 1997)) a calculation tool for limiting dilution assays, based on the minimum $c^2$ (MC) method (Taswell, 1981). Once the dilution containing a single virus copy had been determined, the LD-PCR was scaled up and performed with 20 or more replicates of the original PBMC DNA extracts at that dilution. If more than 1/3 of replicates were PCR positive the reactions were discarded and the PCR was repeated at a higher dilution to ensure amplification from a single *env* gene. Subsequently, amplicons were purified from solution using the GFX PCR purification kit (Pharmacia GEHealthcare Life Sciences, Little Chalfont, UK). DNA was eluted in 50 µl nuclease-free water (Promega) and either used immediately for sequencing and cloning or stored at -20$^{o}$C.

## 2.2.4. Sequencing

Sequencing reactions were set up in-house using the Big Dye Terminator V1.1 kit (Applied Biosystems, Warrington, UK) as per manufacturer's instruction. For the sequencing of the entire FIV *env* coding region the following primers were used: XF2B, MluSeqF, V3R, XV5R, XV6R, XV6F, AYSeqR and XR2. Purification of sequencing reactions was performed using the DyeEx 2.0 96 dye-terminator removal kit (Qiagen). Purified products were resuspended in HiDi (Applied Biosystems) and sequenced utilising the ABI 3700 automated capillary array sequencer (Applied Biosystems). Analysis of raw chromatograph data was performed using either 'Contig Express' sequence analysis software within the Vector NTI suite of programs (Invitrogen) or DNA Dynamo (Blue Tractor Software, UK). Chromatogram traces that appeared to contain multiple peaks,

indicative of mixed virus populations, were discarded and concluded to be from samples amplified above true limiting dilution.

## 2.2.5. Phylogenetic analysis

Multiple alignments of nucleotide sequences coding for the SU and TM domain of FIV *env* (from nt 6819 to nt 8849) were made using the Clustal W algorithm (Thompson et al., 1994) within the BioEdit software package (http://www.mbio.ncsu.edu/bioedit/bioedit.html). Alignments were edited manually to maximise similarities. Unless stated otherwise, repeats of identical sequences were included in analyses only once. Sequences identical to FIV-GL8 were excluded. An exception to this was the calculation of evolutionary rates where all sequences were included.

A Maxium Likelihood (ML) tree was estimated under the topological constrain of having six virus clades corresponding to the PBMC derived virus populations from animals A773-775 and A611-A613. The ML tree was calculated with PAUP (Wilgenbusch and Swofford, 2003) using a substitution model (TVM + G + I) selected based on Akaike's Information Criterion (AIC) in MODELTEST (Posada and Crandall, 1998). For further phylogenetic analysis the estimated ML tree together with the alignment was submitted to the web version of the HyPhy suite (www.datamonkey.org; (Pond and Frost, 2005a)). Global non-synonomous/synonomous ratio (dN/dS) was calculated using SLAC (single likelihood ancestor counting) analysis, while site specific selection was estimated utilising the FEL (Fixed Effects Likelihood) algorithm (Pond and Frost, 2005b). Both calculations were performed under the REV (General Reversible Model) nucleotide substitution model.

The occurrence or disappearance of N-linked glycosylation sites on the amino acid sequence was predicted using the NetNGlyc 1.0 Server (R.Gupta, Technical University of Denmark). Pairwise distances of nucleotide sequences (including identical sequences) were calculated using the TVM+G+I model in PAUP (Kimura, 1980). Nucleotide diversity was calculated as the mean distance of all sequences within each cat, while nucleotide divergence was calculated as the mean distance to the parental strain FIV-GL8. We estimated the rate of evolution for each cat using the BEAST program suite (Drummond and Rambaut, 2007) under a strict molecular clock and a constant population size prior.

The SRD06 model of substitution was selected (Shapiro et al., 2006), otherwise, estimation was based on default options. Following the MCMC runs, mean rates for the long-term and short-term infected cohort were calculated by averaging across the three posterior distributions corresponding to the three cats in each cohort.

Maximum likelihood trees for tissue derived quasispecies were estimated in MEGA5 (Tamura et al., 2011) using the HKY+G+I substitution model (Hasegawa et al., 1985) and were rooted on the parental strain FIV-GL8.

Phylogenetic analysis was performed with the help of Dr. Roman Biek, University of Glasgow.

## 2.2.6. Hypermutation analysis

G-to-A mutation rates and dinucleotide context of mutations were analysed using the calculation tool Hypermut ((Rose and Korber, 2000); http://www.hiv.lanl.gov/content/sequence/HYPERMUT/hypermut.html).

## 2.2.7. Cloning of *env* sequences into pGL8$_{MYA}$ and VR1012

In order to produce full length molecular clones of FIV carrying *env* genes from different viral variants, *env* sequences had to be cloned into the FIV-GL8 expression vector pGL8$_{MYA}$. This vector is based on the low-copy-number plasmid pBR328. Low expression was necessary as primary *env* genes are instable in bacteria upon expression on high-copy plasmids. FIV *env* genes that had been sequenced after second-round LD-PCR amplification were reamplified using primers GL8MluI F and GL8NdeI R which incorporated a MluI digestion site into the 5' L-SU (leader-surface unit) cleavage site and an NdeI digestion site into the Rev responsive element at the 3'end of *env*. PCR was performed using each primer at 0.5 µM, 2 µl of second-round PCR product, 10 µl HF Buffer (NEB), 0.2 mM dNTPs (Invitrogen), 4% DMSO (NEB), 1U Phusion$^{TM}$ Polymerase (NEB) and nuclease free water (Promega) to 50 µl. The following amplification conditions were performed in a GeneAmp® PCR System (Applied Biosystems): initial denaturation at 98°C for 3 min, followed by 25 cycles of 98 °C for 10 s, 55°C for 30 s and 72°C for 1 min 30 s, followed by a final extension step of 72° C for 10 min and a final hold at 4°C. Subsequently PCR products were separated by agarose gel electrophoresis, excised from

gel and gel purified using QIAquick Gel Extraction Kit (Qiagen). Purified PCR products were then digested using MluI and NdeI and ligated into the $pGL8_{MYA}$ plasmid that had been cut with these enzymes prior to ligation.

In order to allow pseudotyping of HIV(Luciferase) virus-like particles, the *env* genes were cloned into the eukaryotic expression plasmid VR1012 (Vical Inc., San Diego, CA; (Hartikka et al., 1996)). Env sequences were PCR amplified using primers GL8SalI F and GL8NotI R at 0.5 µM, 2 µl of second-round PCR product or $pGL8_{MYA}$ constructs, 10 µl HF Buffer (NEB), 0.2 mM dNTPs (Invitrogen), 4% DMSO (NEB), 1U Phusion™ Polymerase (NEB) and nuclease free water (Promega) to 50 µl. Cycling conditions were as follows: initial denaturation at 98°C for 3 min, followed by 25 cycles of 98 °C for 10 s, 58°C for 30 s and 72°C for 1 min 30 s, followed by a final extension step of 72 ° C for 10 min and a final hold at 4°C. PCR products were run on an agarose gel, excised from gel and gel purified using QIAquick Gel Extraction Kit (Qiagen). Purified PCR products were digested using SalI and NotI and ligated into VR1012 that had been cut with these enzymes prior to ligation. Sequences of all primers are displayed in the Appendix.

## 2.2.8. Enzymatic digest and ligation of DNA

Purified PCR fragments or plasmids were usually digested using 5U of restriction endonucleases (NEB and Invitrogen) per 1 µg of DNA. Digests were performed at 37°C for 1-2h in buffers as per manufacturer's instruction. Subsequently digests of plasmids were gel purified, while digested PCR products were purified directly using QIAquick Gel Extraction Kit (Qiagen). Ligations were performed using T4 DNA ligase (Promega) at 1 U/µl at 15 °C overnight. Typically 100 ng of digested vector was ligated with digested PCR products in a 1:3 vector to insert ratio.

## 2.2.9. Transformation

Transformation of chemocompetent DH5α high efficiency *Escherichia coli* (Invitrogen) was performed using the heat shock protocol as per manufacturer's instruction and bacteria plated onto LB-Agar plates containing ampicillin at 50 µg/ml or kanamycin at 30 µg/ml. Bacteria were grown for 24-48 hrs at 30°C due to instability of the primary *env* genes. Subsequently, colonies were picked and grown for 24 hrs at 30°C in 5

ml LB broth containing ampicillin or kanamycin at 50 or 30 µg/ml, respectively. Plasmid DNA was isolated using QIAprep Spin Miniprep kit (Qiagen) according to the manufacturer's instructions. Screening of positive clones was performed by restriction enzyme digests with MluI and NdeI (pGL8Mya) or NotI and SalI (VR1012). Digests using AflII were conducted to exclude purification of original vector plasmid. For preparation of large scale DNA, 200 ml of bacterial culture was incubated for 24 hrs at 30°C in an orbital shaker at 225 rpm. DNA was extracted using the PureLink HiPure Filter Plasmid Maxiprep Kit (Invitrogen) as per the manufacturer's instructions. Isolated plasmid DNA was resuspended in 200 µl of TE buffer and stored at 4°C. Concentration and purity of DNA was measured using a NanoDrop™ 2000 spectrophotometer (Thermo Scientific). For long term storage, bacterial cultures were mixed with sterile glycerol to a final concentration of 15% glycerol (v/v) and kept at -80°C.

## 2.2.10. Construction of chimaeric FIV-GL8 Env variants

In order to investigate which region of Env conferred resistance to neutralising antibodies we generated the Env vector FIV-GL8ABSN a mutant of the VR1012-FIV-GL8 construct which contained four digestion sites (**A**paI, **B**ssHII, **S**alI, **N**heI) in the *env* gene at nucleotide positions 1000, 1366, 1528 and 1848, respectively (while the amino acid sequence remained unchanged). To generate the FIV-GL8ABSN, five regions (corresponding to V1/V2, V3, V4, V5, V6/gp41) were amplified separately by PCR using mutagenesis primer pairs MluGL8F- ApaI7291R (55°C); ApaI7285F - BssHII7672R (57°C); BssHII7644F - Sal7802R (57°C); Sal7799F - NheI8123R (55°C); NheI8118F - NdeGL8R (65°C). The amplifications were performed using the VR1012-FIV-GL8 construct as a temple in reaction mixtures containing primers at 0.4 µM, 10 µl HF Buffer, 0.2 mM dNTPs, 3% (v/v) DMSO, 2.5U Phusion$^{TM}$ Polymerase and nuclease-free water to 50 µl. Cycling conditions were as follows: initial denaturation at 98°C for 1 min, followed by 30 cycles of 98 °C for 10 s, annealing for 10 s (temperatures are given in brackets behind each primer pair) and 72°C for 20 s, followed by a final extension step of 72 ° C for 10 min and a final hold at 4°. Following gel purification the five amplicons were mixed in ratios of 100:1:1:1:100 (from 3' to 5') and amplified in an overlap extension PCR using a reaction mixture as described above but without primers and cycling conditions as follows: initial denaturation at 98°C for 1 min, followed by 30 cycles of 98 °C for 10 s, 70°C for 10 s and

72°C for 1 min 10 s, followed by a final extension step of 72 ° C for 10 min and a final hold at 4°. The resulting FIV-GL8ABSN *env* gene was then cloned into the MluI/NdeI sites of the VR1012 vector. The exchange of regions encompassing variable loops V4/V5 of variants B14, B19 and B28 was facilitated by amplifying the according sequences from the viral variants using mutagenesis primers BssHII7644F and NheI8123R to introduce flanking BssHII and NdeI sites, respectively. The amplicons were then digested, purified and ligated into FIV-GL8ABSN that had been digested with BssHII and NdeI. Successful construction of the chimaeric *env* genes was confirmed by sequencing and plasmids were used for the generation of HIV(FIV) pseudotypes as described below. Sequences of all primers are displayed in the Appendix.

# 2.3. Cell culture

## 2.3.1. Maintenance of cells

All cell lines were maintained under standard conditions of 37°C and 5% CO2 in a humidified incubator. Adherent cells were grown in Dulbecco's modification of Eagle's medium (DMEM; Invitrogen), while suspension cells were maintained in RPMI 1640 (Invitrogen). Both media were supplemented with 10% foetal bovine serum, 2 mM glutamine, 0.11 mg/ml sodium pyruvate, 100 IU/ml penicillin, 100 µg/ml streptomycin. Additionally, medium for suspension cells was supplemented with 50 µM β-mercaptoethanol. For maintaining Mya-1 cells conditioned medium from a murine cell line (L2.3) transfected with a human interleukin-2 (IL-2) expression construct (kind gift of M. Hattori, University of Tokyo, Japan) was added to the medium at a concentration equivalent to 100U/ml human interleukin-2. Selection antibiotic G418 (400 µg/ml, Invitrogen) was supplemented to medium of HEK293T and to CLL, MCC expressing variants of the CD134 receptor. No G418 was used when performing infection assays or transfecting cells.

**Table 2-1. Cell lines used in this study.**

| Cell line | Origin | Adherent or Suspension | Specification | Reference |
|---|---|---|---|---|
| HEK293T | Human | A | embryonic kidney cells expressing SV40 large T-antigen | (Graham et al., 1977) |
| Mya-1 | Cat | S | primary T-cell line, IL-2 dependent | (Miyazawa et al., 1989) |
| CLL-CD134 | Dog | S | lymphocytic leukaemia cells, transduced to express feline CD134 | (Willett et al., 2006b) |
| MCC-CD134 | Cat | S | large granular lymphocyte, transduced to express feline CD134 | (Cheney et al., 1990) |

## 2.3.2. Preparation of replication competent virus

One day prior to transfection, HEK293T cells were seeded at 1.0 x $10^6$ cells onto Poly D-Lysine COSTAR® 6 Well plates (Corning Incorporated, Corning, USA). Cells were transfected with 2 µg of $pGL8_{MYA}$ plasmid (encoding the *gagpol* gene of FIV-GL8 and the *env* gene of FIV-GL8 or of other variants) using 10 µl SuperFect transfection reagent (Qiagen) as per manufacturer's instruction. Virus was harvested 72 hrs post-transfection, passed through Minisart® 0.45µm-pore-size filters (Sartorius, Epsom, UK) and either used for infection immediately or frozen at -80°C until required. Infection of Mya-1 cells was performed by applying virus containing supernatant directly onto the cells. Virus growth was monitored visually for the occurrence of cytopathic effects and confirmed by p24 ELISA (2.4.2.). At peak p24 values virus containing supernatant was harvested, filtered at 0.45 µm and stored at -80°C.

## 2.3.3. Preparation of HIV(FIV) pseudotypes

In order to assess the abilities of FIV Env variants to interact with their viral receptors and their sensitivities to entry inhibitors and neutralising antibodies, FIV Env

pseudotyped HIV particles restricted to single round infection were prepared. These "HIV(FIV)" denoted pseudotypes delivered a luciferase reporter gene to the target cell that allowed to assay the efficiency of transduction by quantification of luciferase induced luminescence. For the generation of HIV(FIV) pseudotypes, two plasmids were co-transfected into HEK293T cells that had been seeded at 1.0 x $10^6$ cells onto Poly D-Lysine COSTAR® 6 Well plates (Corning) 24 hrs prior to transfection. To transfect, 2 µg of FIV *env* expressing plasmid VR1012 and 3 µg of pNL-Luc-$E^-R^-$, encoding HIV-1 NL4-3 provirus with a luciferase gene inserted into the *nef* gene and lacking functional *env* and *vpr* genes (Connor et al., 1995), were mixed with 10 µl of SuperFect transfection reagent (Qiagen) in 100 µl of serum-free DMEM. Following incubation at room temperature for 15 min to allow DNA-complex formation, 600 µl of complete DMEM were added and the mixture added to the HEK293T cells at 37°C for 3 hrs. Subsequently, cells were washed with 2 ml of PBS and 2 ml of complete DMEM added. Culture supernatants were collected 72 hrs post-transfection, filtered at 0.45 µm and stored at -80°C until required. Target cell lines were seeded onto CulturePlate™-96 assay plates (PerkinElmer Life and Analytic Sciences, Shelton, USA) at densities of 5 x $10^4$ cells per well and infected with 50 µl of HIV(FIV) luciferase pseudotypes. After 72 hrs luciferase activity was quantified by addition of 100 µl Steadylite HTS™ (Perkin Elmer) luciferase substrate and measurement of single photons on a MicroBeta TriLux luminometer (PerkinElmer). Infections were performed in triplicates and results indicated in counts per minute (CPM).

## 2.3.4. Virus neutralisation assay

Heat inactivated (56°C, 30min) plasmas of the infected cats were serially diluted in Mya-1 culture medium. Subsequently, 25 µl of each plasma dilution or a medium control were added per well of a CulturePlate™-96 assay plates (PerkinElmer) and incubated with 25 µl of HIV(FIV) pseudotype for one hour at 37°C. 50 µl of target cells (5x$10^4$ of Mya-1 or CLL-CD134) were then added to each well and cultured for 72 hrs. Luciferase activity was quantified by the addition of 100 µl Steadylite HTS™ (Perkin Elmer) luciferase substrate and single photon counting on a MicroBeta TriLux luminometer (PerkinElmer). Infections were performed in triplicate and results presented in either counts per minute (CPM) or percent neutralisation.

Percent neutralisation was calculated as follows:

$$\%Neutralisation = \frac{\text{mean CPM no plasma control - mean CPM virus plus plasma}}{\text{mean CPM no plasma control}} * 100\%$$

## 2.3.5. Inhibition of viral entry

Four specific inhibitors of viral entry were available to investigate the interaction of Env variants and cellular receptors CD134 and CXCR4. The first, **sFcCD134**, is a soluble form of the entry receptor CD134 that has been generated by fusing an immunoglobulin Fc region to the N-terminus of CD134 (de Parseval et al., 2004). Infection of target cells expressing CD134 can be inhibited by the binding of sFcCD134 to FIV (Willett et al., 2009). However, sFcCD134 may also facilitate infection of CD134 negative, CXCR4 positive cells by inducing conformational changes in Env that expose gp41 and allow the direct binding to CXCR4 (de Parseval et al., 2004; de Parseval et al., 2006). The second inhibitor, the **monoclonal antibody 7D6**, is directed against an epitope on feline CD134. Pre-treating CD134 positive cells with 7D6 can leave CD134 inaccessible for FIV Env and therefore block infection (Willett et al., 2007). The third compound, the **bicyclam AMD3100**, is a selective antagonist of the CXCR4 receptor. Binding of AMD3100 inhibits HIV and FIV entry and membrane fusion via the CXCR4 receptor (Donzella et al., 1998; Egberink et al., 1999). The fourth inhibitory agent is the ligand to the CD134 receptor which naturally is expressed as a trimer on the surface of activated antigen presenting cells. The soluble monomeric form of this protein, CD134L, does not show binding affinity to CD134 (Willett et al., 2007). However, fusion of the CD134L to a subdomain of the tenascin-C (TNC) oligomerisation domain results in a soluble trimeric form of the ligand (**Fc-TNC-CD134L**) that efficiently blocks FIV infection (Willett et al., 2009).

In order to study the effects of the four inhibitors on different Env variants we used HIV(FIV) pseudotypes carrying Env proteins of the FIV variants obtained from cat A613. Prior to infection, $1x10^5$ target cells (Mya-1, MCC-134 or CLL-134) were seeded per well of a CulturePlate™-96 assay plate (PerkinElmer) and incubated with either sFcCD134, 7D6, AMD3100 or Fc-TNC-CD134L for 30 min at 37°C. Pseudotypes were then added to target cells and infection allowed to proceed for 72 hrs at 37°C. Then luciferase activity was quantified by adding 100 µl Steadylite HTS™ (Perkin Elmer) luciferase substrate and counting single photons on a MicroBeta TriLux luminometer (PerkinElmer).

In order to assess whether sFcCD134 could trigger conformational changes in gp120 that would allow CD134 independent infection, HIV(FIV) pseudotypes were pre-incubated with sFcCD134 for 30min at 37°C and then added to MCC cells ($CD134^-$, $CXCR4^+$). 72 hrs post-infection luciferase activity was measured as mentioned above. In all assays inhibitors were used in concentrations ranging from 0 µg/ml to 50 µg/ml and infection were performed in triplicates. Percent infection was calculated as follows:

$$\%Infection = \frac{\text{mean CPM infection with inhibitor}}{\text{mean CPM infection without inhibitor}} * 100\%$$

Assays for the inhibition of infection were performed by Mrs. Elizabeth McMonagle and Prof. Brian Willett, University of Glasgow.

## 2.3.6. Receptor usage assay

The CD134 receptor consists of three cysteine rich domains (CRDs) and utilisation of feline CRD1 and CRD2 for viral entry may differ depending on the strain of FIV, while human CD134 does not support FIV infection (Willett et al., 2006a; Willett et al., 2006b). In order to assess the dependence on feline CRD2 of different Env variants, HIV(FIV) pseudotypes were utilised to infect MCC cells stably transduced to express either feline CD134, human CD134 or a feline x human chimera containing feline CRD1 in the context of human CD134. 50 µl of target cells ($5x10^4$ cells per well) were seeded in triplicate in CulturePlate™-96 assay plates (PerkinElmer) and infected with 50 µl of HIV(FIV) luciferase pseudotypes bearing different A613 derived Env proteins. After 72 hrs luciferase activity was quantified by addition of 100 µl Steadylite HTS™ (PerkinElmer) luciferase substrate and measurement of single photons on a MicroBeta TriLux luminometer (PerkinElmer). As a means of quantifying dependence on the CRD2 of feline CD134 for successful infection, the ratio of luciferase counts on MCC expressing feline CD134 divided by counts on MCC expressing feline x human chimearic CD134 was calculated. High ratios indicate high dependence on feline CDR1 and CRD2, while ratios close to 1 suggest infection mainly via CRD1.

# 2.4. Quantitative and immunologic methods

## 2.4.1. Quantitative real-time PCR (qPCR)

### *2.4.1.1. Quantification of total proviral load by qPCR on gag*

Proviral loads in the two animal studies had been assessed by different qPCRs targeting sequences in the proviral *gag* gene that had been shown to be conserved among different FIV strains. The quantification of proviral loads in PBMCs of cats from our first animal study was performed by Dieter Klein, University of Veterinary Medicine, Vienna, as previously described (Hosie et al., 2002). Briefly, proviral loads in DNA extracts from PBMCs of infected animals were quantified using 300 nM of primers FIV0771F, FIV108R and 200 nM of dual-labeled fluorogenic TaqMan probe FIV1010p. Furthermore, realtime PCR reactions contained 50 mM KCl, 10 mM Tris (pH 8.3), 3 mM $MgCl_2$, 200 nM dCTP, dGTP and dATP, 400 nM dUTP and 2.5 U of Taq DNA polymerase. The PCR was performed on a Sequence Detector System ABI 7700 (Applied Biosystems) with the following cycling conditions: initial denaturation at 95°C for 2 min followed by 45 cycles at 95°C for 15 s and 60°C for 60 s. The DNA content per qPCR was estimated using a second PCR targeting the 18S ribosomal DNA genes as described below.

Total proviral load in PBMCs of infected cats in the second animal study were quantified using primers FIV1360F and FIV1437R at 500 nM and FAM-TAMRA labelled fluorogenic TaqMan probe FIV1416P at 250 nM (Ryan et al., 2003), 20 µl of 2xTaqman Universal mastermix (no AmpErase®UNG, Applied Biosystems), 400 ng of DNA extracted from PBMCs and nuclease-free water to a volume of 40 µl. The thermal cycling was performed on a 7500 Real-Time PCR cycler (Applied Biosystems) under the following cycling conditions: initial denaturation at 95°C for 10 min followed by 45 cycles at 95°C for 15 s and 60°C for 1 min. A standard curve to quantify infectivity was established by serial dilution of DNA from FIV-GL8 infected Mya-1 cells in a DNA extract from uninfected cells of the same cell type. Previously proviral loads of the standard had been determined using FIV-GL8 encoding plasmid serially diluted in gDNA of Mya-1 cells.

### *2.4.1.2. Quantification of single viral variants by V5-specific qPCR*

The variants used in the artificial quasispecies in group 2 of the second animal study differed mainly in their V5 region. Variants B31 and B32 displayed a V5 sequence identical

to that of FIV-GL8. In contrast, all other variants carried insertions (B14, B28, B30) or deletions (B19) in V5 (Fig. 2-1). Therefore qPCRs targeting V5 to discriminate between the different variants were designed. This approach proved challenging as the V5 insertions in part were duplications of the region to be amplified, leading to misamplification and false positive results. We tested several setups including change of primer/probe sets, primers containing mismatches and oligonucleotides containing spacer groups that would block misamplification (Vestheim and Jarman, 2008).

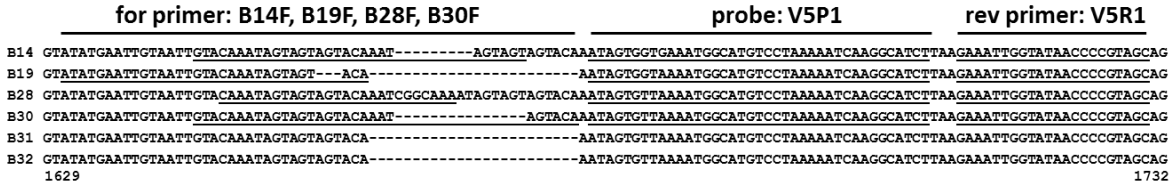


**Figure 2-1. Alignment of V5 sequences of viral variants B32, B31, B30, B28, B19 and B14.**
Positions of forward (for) primers B14F, B19F, B28F, B30F, FAM-TAMRA labelled TaqMan probe V5P1 and reverse (rev) primer V5R1 are underlined.

We established four qPCRs targeting V5 of B14, B19, B28 and B30. It was not possible to specifically quantify proviral loads of B31 and B32 as no primer/probe system tested could distinguish B31 and B32 from other variants. All variant-specific qPCRs utilised the same reverse primer V5R1 and the FAM-TAMRA labelled TaqMan probe V5P1 in conjunction with a forward primer specific for the respective variant B14F, B19F, B28F or B30F. Additionally, quantification of all variants via the V5 region was performed using a forward primer, G8V57829F, binding to a conserved region upstream of the variable region V5, together with reverse primer V5R1 and probe V5P1. This primer/probe set allowed the detection of all variants with equal efficiency.

V5 specific qPCRs were carried out using forward and reverse primer at 500 nM, probe at 250 nM, 2x Taqman Universal mastermix (no AmpErase®UNG, Applied Biosystems), 400 ng of DNA and water to a total of 40 µl. QPCRs were thermally cycled on a 7500 Real-Time PCR cycler (Applied Biosystems) under the following cycling conditions: initial denaturation at 95°C for 10 min followed by 45 cycles at 95°C for 15 s and 60°C for 1 min. Solely qPCR for B19 differed; the reverse primer was used at 250 nM and annealing was performed at 62°C.

Prior to quantification of proviral loads, we analysed the specificity and sensitivity of the V5 specific qPCRs. Sensitivity was determined on dilutions of homologous molecular clone in a background of genomic DNA from uninfected Mya-1 cells. Specificity was tested on dilutions of homologous molecular clone in a constant background of the five remaining molecular clones. In such a setup B28 could be amplified specifically in a 100,000 fold excess of the other five plasmids and 62 copies of B28 could be detected in cellular DNA, while B30 was exclusively detectable in a 1,000 fold excess of the other variants and could also be detected at 62 copies in cellular DNA. PCRs for B14 and B19 were less specific and allowed detection in a 100 and a 20 fold excess of background plasmids, respectively, while sensitivity of both PCRs in the background of genomic DNA was 62 copies and 620 copies of B14 and B19, respectively.

To confirm robustness of proviral quantification we used a bulk sequencing approach. V5 sequences from PBMCs harvested post-mortem from animals 825, 826, 827 and 828 were amplified using primers SalI7799F and G8NotI8030R flanking the V5 loop. Purified PCR products were digested using SalI and NotI and ligated into VR1012 that had been cut with these enzymes prior to ligation. Following transformation, approximately 50 clones from each cat were sequenced as described above. V5 sequences were aligned to FIV-GL8 and viral variants and occurrence of the respective sequences counted.

### *2.4.1.3. Quantification of cellular genomes by qPCR on 18S rDNA*

Concentrations of genomic DNA from PBMCs had been determined by spectrophotometry using NanoDrop™ 2000 (Thermo Scientific). Protein and RNA contamination within the sample might bias results of these measurements and thus influence directly the estimations of proviral loads. Therefore we quantified genomic DNA in the samples using a qPCR targeting 18S ribosomal DNA (rDNA) (Klein et al., 2000). PCRs utilised 10 µl of 2xTaqman Universal mastermix (no AmpErase®UNG, Applied Biosystems), 100 ng of sample, 10 pmol of forward (rDNA343F) and reverse (rDNA409R) primers and 5 pmol of FAM-TAMRA labelled probe rDNA370P and water to a total volume of 20 µl. Cycling conditions were as follows: initial denaturation at 95°C for 10 min followed by 45 cycles at 95°C for 15 s and 60°C for 1 min. All estimations of proviral load using *gag* or V5 specific PCR were adjusted for values obtained by qPCR on 18S rDNA.

## 2.4.2. ELISA on p24

For monitoring infections with replication competent FIV, an enzyme-linked immunosorbent assay (ELISA) against viral capsid protein p24 was performed 7 and 14 days post-infection using the PetCheck FIV antigen ELISA kit (IDEXX, Portland, USA) as per manufacturer's instructions. Virus containing cell culture fluid was clarified by centrifugation and 200 µl of cell-free culture supernatant were incubated with 20 µl of sample treatment solution on anti-p24 coated ELISA plates for 30 min at room temperature. After washing the ELISA plates as per manufacturer's instructions, p24 was detected by adding anti-FIV-HRP (horseradish peroxidase) conjugated antibody (IDEXX) and developed using HRP substrate (IDEXX). ELISA plates were read on a Thermo Labsystems Multiscan Ascent Photometric plate reader (MTX Lab Systems, Inc., Vienna, USA) at 450 nm.

## 2.4.3. Flow cytometry

Progressive FIV infection is usually accompanied by a decline of CD4+ T cells, while the number of CD8 positive cells may increase. In order to assess the effect of FIV infection on the proportion of CD4+ and CD8+ T cells, flow cytometric analysis was performed. PBMCs were separated from EDTA anti-coagulated blood by whole blood lysis and processed for flow cytometry (Willett et al., 1993). Cells were stained using either anti-feline CD4-FITC (vpg34), anti-feline CD8-PE (vpg9) or anti-human CD14-FITC (TÜK4) antibodies (AbD Serotec Ltd. Oxford, UK). Analysis was performed on a Beckman Coulter EPICS MCS-XL flow cytometer. 10,000 events were collected for each sample in LIST mode. Data was processed utilising the EXPO 32 ADC Analysis software (Advanced Cytometry systems). All flow cytometric analyses were performed by Prof. Brian Willett, University of Glasgow.

## 2.4.4. Western Blot

For analysis of serological responses to FIV infection, supernatant from FIV-GL8 infected Mya-1 cells was filtered at 0.4 µm and virus pelleted in a SW28 rotor (Beckman, UK) for 2 hrs at 28,000 rpm on a Beckman L8-70 ultracentrifuge. The virus pellet was resuspended in SDS loading buffer, boiled for 5 min and loaded on 4-15% polyacrylamide

gels (Invitrogen). Separated proteins were transferred to nitrocellulose membranes using rapid dry blotting system (iBlot™, Invitrogen) and antigens detected using either plasma samples from infected cats or pooled plasmas from uninfected cats (negative control) or FIV-GL8-infected cats (positive control). Bound primary antibodies were detected using biotinylated goat anti-cat IgG (Vector Laboratories Ltd., Peterborough, UK) followed by chromogenic development using Vectastain ABC kit (Avidin: Biotinylated enzyme Complex) and 5-bromo-4-chloro-3-indolyl phosphate/nitroblue tetrazolium substrate (Vector Laboratories Ltd.). Western Blot analysis was performed by Ms. Nicola Logan, University of Glasgow.

## 2.4.5. ELISpot

Lymph nodes were extracted *post mortem* and transferred to ice-cold cell culture medium. Following disruption of tissues using a crossed scalpel, cells were resuspended by pipetting and separated from debris by centrifugation and purified by centrifugation through Ficoll-Plaque™ (GE Healthcare UL Ltd, Little Chalfont, UK) separation medium. Lymphocytes were extracted from the interface layer, washed by centrifugation and resuspended in cryo-preservation medium (70% RPMI, 20% FCS and 10% DMSO) before being stored in the vapour phase of liquid nitrogen. For ELISpot analysis, cells were defrosted in a water bath at 37°C and washed in cell culture medium at 37°C. IFN-γ producing cells were quantified utilising commercial IFN-γ ELISpot kits (R&D Systems, Abingdon, Oxford, UK) as per manufacturer's instructions. 5 x $10^5$ cells were incubated with either 0.1, 1.0 or 10 µg of purified FIV-GL8 that had been inactivated with Aldrithiol™-2 (AT-2, Sigma, Poole, UK). For virus inactivation, 150 ml viral supernatant was clarified by centrifugation at 2000 rpm for 5 min and incubated with a final concentration of 300 µM AT-2 at 37°C for 1 h. Subsequently, virus was pelleted in a SW28 rotor (Beckman, UK) for 1.5 hrs at 28,000 rpm on a Beckman L8-70 ultracentrifuge, resuspended in 5 ml PBS and dialysed against PBS overnight. For controls, cells were incubated with cell culture medium alone or medium containing 5 µg/ml Concanavalin A (Con A). Spot-forming cells were counted using an AID ViruSpot Reader (CADAMA Medical Ltd., UK). In subsequent analyses lymphocytes were incubated with pools of FIV-GL8 Env derived peptides (15mers overlapping by 10 amino acids) spanning the whole leader, SU and TM. Peptides were synthesised by Alta Biosciences (Birmingham, UK) and were

dissolved initially in DMSO (HPLC-grade, Sigma-Aldrich) and were diluted in PBS (pH 7.4) prior to use. ELISpot analyses were performed by Mrs. Elizabeth McMonagle, Ms. Nicola Logan and Prof. Brian Willett, University of Glasgow.

# 3. Results

## 3.1. Overview

Like other lentiviruses, FIV is extremely variable. The high mutation rate induced by the error-prone reverse transcriptase coupled with pressure from adaptive and innate immune system results in diverse viral populations. The highest variability is located in the *env* gene and this has been studied most extensively (Kakinuma et al., 1995; Pecoraro et al., 1996; Sodora et al., 1994). However, the majority of FIV phylogenetic analyses have focused on the inter-host diversity following natural infection, thus being informative at the population level (Bachmann et al., 1997; Carpenter et al., 1998; Pistello et al., 1997; Sodora et al., 1994; Steinrigl and Klein, 2003). In contrast, knowledge about FIV evolution within cats is very limited. We therefore sought to assess viral evolution following experimental infection and its impact on viral phenotype *in vivo* and *in vitro*.

In a first animal study we intended to analyse evolutionary patterns of the FIV *env* gene in short-term and long-term infected cats (Fig 3-1). Use of a clonal virus preparation for the initial infection enabled direct sequence comparisons to the parental virus. We utilised phylogenetic methods to examine the genotype and relationship between *env* sequences isolated from PBMCs and tissues. Subsequently, we analysed the phenotype of several Env variants by investigating receptor interactions and susceptibility to neutralising antibodies *in vitro*.

In a second animal study we used viral variants derived from a single long-term infected cat (A613) to prepare a defined mixture of cloned viral variants. This reconstituted quasispecies was compared *in vivo* with a clonal preparation of the parental strain FIV-GL8. The comparison between the clonal population and the defined quasispecies allowed us to investigate the influence of the *in vitro* Env phenotype on viral fitness *in vivo*.

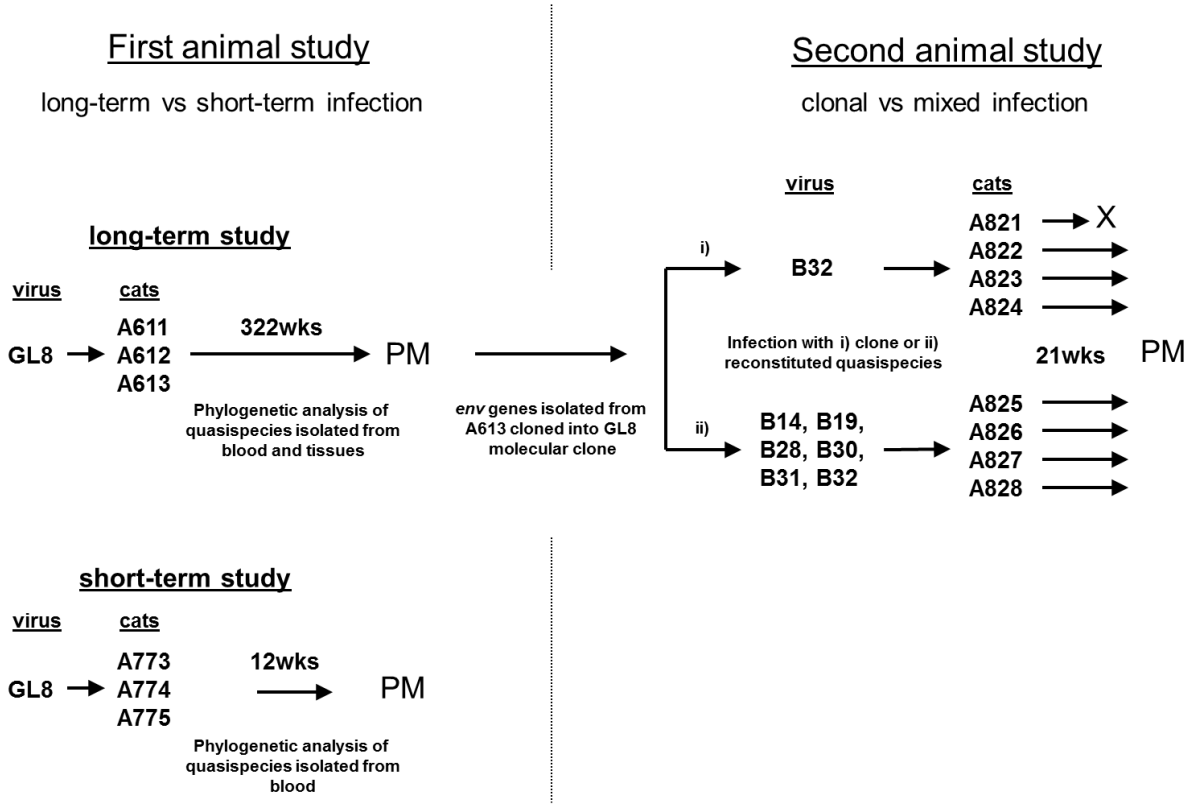


**Figure 3-1. Project overview.**
The first animal study was performed to analyse evolutionary changes in the *env* gene of FIV following infection of cats for 12 weeks (cats A773 – 775) or 322 weeks (cats A611 – A613) with FIV-GL8. The second animal study aimed to compare mixed infection with an artificial quasispecies (viral variants B14-B32; cats A825-A828) and clonal infection with parental virus GL8 (identical to viral variant B32) (cats A821 – A824). Abbreviations: PM= post mortem; GL8 = FIV strain Glasgow 8; B14-B32 Env variants derived from long term infected cat A613; B32 is identical to FIV-GL8 but was isolated from cat A613 and underwent all cloning steps. Cat A821 died mid-study as a result of a condition unrelated to FIV infection.

# 3.2. Phylogenetic properties of FIV *env* sequences from long-term and short-term infected cats

## 3.2.1. Infection of cats and clinical data

Two groups of cats, consisting of three animals each, were infected with a clonal preparation of the FIV strain GL8. Animals of group one (cats A773, A774, A775) were sacrificed after 12 weeks, while infection of animals in group two (cats A611, A612, A613) was terminated 322 weeks post-infection. Blood samples and tissues were collected post-mortem.

Following FIV infection, the proviral load peaks within a few weeks post-infection and subsequently decreases as the adaptive immune system of the infected animal starts

controlling the virus. However, progression towards the terminal AIDS-like phase of infection is accompanied by a second rise in proviral loads since the increasingly damaged immune system is no longer able to restrain the infection.

In our study, proviral loads in PBMCs were determined using qPCR on a sequence in the viral *gag* gene (Table 3-1). The animals infected for 12 weeks revealed high proviral loads ranging from 2,000 to almost 10,000 copies per $10^6$ PBMCs, which is consistent with the peak proviral loads of an early infection. The long-term infected animals of group 2 displayed lower proviral loads ranging from below 1 (cat A613) to 485 (cat A612) copies per $10^6$ PBMCs, indicating the stage of "asymptomatic" infection (lacking clinical signs).

During the course of infection of either humans with HIV or cats with FIV, CD4+ T cells are the main target of infection. The progression of HIV and FIV infections is accompanied by a decrease in CD4+ T cells while the number of CD8+ T cells increases. A declining ratio of CD4+ to CD8+ T cells is therefore an indicator of disease progression in HIV infected individuals and can also be used to monitor FIV infection. In our study the numbers of CD4+ and CD8+ T cells within the PBMCs of the FIV infected cats had been determined using flow cytometry (Table 3-1). Values for CD4:CD8 ratios in the short term infected group ranged from 1.23 to 1.98, whereas values in the long-term infected group generally were lower, ranging from 1.0 to 1.64.

**Table 3-1. Summary of infection data and *env* sequences recovered by LD-PCR.**
Adapted from (Kraase et al., 2010)).

| Animal | Weeks post-infection | Sequences obtained | Repeated sequences (identical to GL8) | Repeated sequences (not identical to GL8) | Proviral load (copies per $10^6$ PBMCs) | CD4:CD8 ratio |
|---|---|---|---|---|---|---|
| 773 | 12 | 12 | 0 | 9 | 5380 | 1.23 |
| 774 | 12 | 14 | 1 | 7 | 2110 | 1.4 |
| 775 | 12 | 13 | 5 | 2 | 9850 | 1.98 |
| 611 | 322 | 18 | 1 | 2 | 23 | 1.16 |
| 612 | 322 | 18 | 0 | 11; 3 | 485 | 1.0 |
| 613 | 322 | 17 | 4 | 0 | <1 | 1.64 |

## 3.2.2. Genotype of PBMC-derived FIV *env* sequences

### *3.2.2.1. Phylogenetic analyses*

Next, we sought to examine proviral *env* sequences present in the infected animals. We utilised a previously established limiting dilution PCR (LD-PCR) to amplify single copy *env* genes from genomic DNA of the infected PBMCs. Using this method we were able to recover 12 to 18 full length *env* sequences from PBMCs of each cat. Sequence analysis revealed several unique sequences, but also some sequences that were identical to the inoculum FIV-GL8 or repeats of other sequences isolated from that cat. A detailed overview of the number of amplified sequences can be found in table 3-1.

Subsequent phylogenetic analyses were performed using the part of the *env* gene (nt6819 – nt8849 of FIV-GL8) that corresponds to the membrane external proportion of the Env protein. In order to measure the degree of relation and diversity all sequences were aligned and trimmed to start and end at identical nucleotide positions. The 2030 nt long alignment was then used to calculate the diversity (pairwise distances) between all sequences within each cat and the divergence, which is the mean distance between each virus population and parental FIV-GL8 (Table 3-2). Virus populations in the 12 weeks infected cats were largely homogeneous with a mean diversity and divergence of 0.08 and 0.07%, respectively. In contrast, viruses in the long-term infected animals A611 and A613 were more heterogeneous with diversities of 0.67 and 0.61 %, however the viral population in cat A613 was clearly more closely related to the parental strain FIV-GL8 than viruses in A611 as demonstrated by a divergence of 0.32 compared to 0.52 %. In contrast, variants isolated from cat A612 only demonstrated a low degree of viral evolution, underlining the importance of the individual virus-host interaction in the creation of diversity. Interestingly, animal A612 had displayed the highest proviral load (485 per $10^6$) in group two. None of the long-term infected animals had developed signs of disease progression towards AIDS during the course of the study, yet the CD4:CD8 ratio of cat A612 was lowest among all long-term infected animals and might indicate first signs of immune dysfunction.

The analysis of the mean divergence per year suggested a 5 times faster evolution in the 12 weeks group (0.3) compared to the 322 weeks cohort (0.06). A more exact estimation of evolution over time can be obtained by calculating the evolutionary rate.

This was done using the BEAST program suite (Drummond and Rambaut, 2007). The short-term infected cats displayed an average rate of evolution of 6.72 x $10^{-3}$ substitutions per site per year (95% Highest Posterior Density [HPD] lower 1.73 x $10^{-3}$; upper 1.34 x $10^{-2}$), while evolution rate in long term infected cats was approx. 7 times lower (mean 9.15 x $10^{-4}$ substitutions per site per year (95% HPD lower 1.82 x $10^{-4}$; upper 1.52 x $10^{-3}$), indicating that viral evolution slows during the course of infection.

**Table 3-2. Summary of mean diversity and divergence for *env* sequences per cat and per cat cohort.** Adapted from (Kraase et al., 2010).

| Animal | % Mean diversity [a] | % Mean divergence [b] | Range [c] | % Mean divergence per year [d] |
|---|---|---|---|---|
| 773 | 0.04 | 0.07 | 0.05-0.20 | 0.30 |
| 774 | 0.11 | 0.08 | 0.05-0.20 | 0.37 |
| 775 | 0.10 | 0.05 | 0.05-0.05 | 0.22 |
| 12 weeks mean | 0.08 | 0.07 | | 0.30 |
| | | | | |
| 611 | 0.67 | 0.52 | 0.10-0.92 | 0.1 |
| 612 | 0.08 | 0.17 | 0.10-0.47 | 0.03 |
| 613 | 0.61 | 0.32 | 0.05-0.82 | 0.06 |
| 322 weeks mean | 0.45 | 0.34 | | 0.06 |

Pairwise distances were calculated using the TVM+G+I model in PAUP.

[a] Diversity (pairwise distances) amongst all sequences within each cat at post-mortem.

[b] Mean distances between virus population and parental virus FIV-GL8 at post-mortem.

[c] Range of divergence from parental virus at post-mortem.

[d] Divergence per year was calculated as: (divergence x 52)/weeks post-infection

Next, we used the sequence alignment to calculate a maximum likelihood (ML) tree utilising the TVM+G+I model of substitution in PAUP. As the cats were infected with a clonal preparation of FIV-GL8, the ML tree was rooted on GL8 and was under the topological constraint of having six virus clades which corresponded to the virus population of each cat. Similar to the diversity/divergence data the tree (Figure 3-2) showed that viral variants from cat A611 and A613 were heterogeneous and reached the greatest distance from the parental virus, FIV-GL8, while variants from cat A612 and short-term infected cats ranged in close relation to FIV-GL8 and were rather homogeneous.

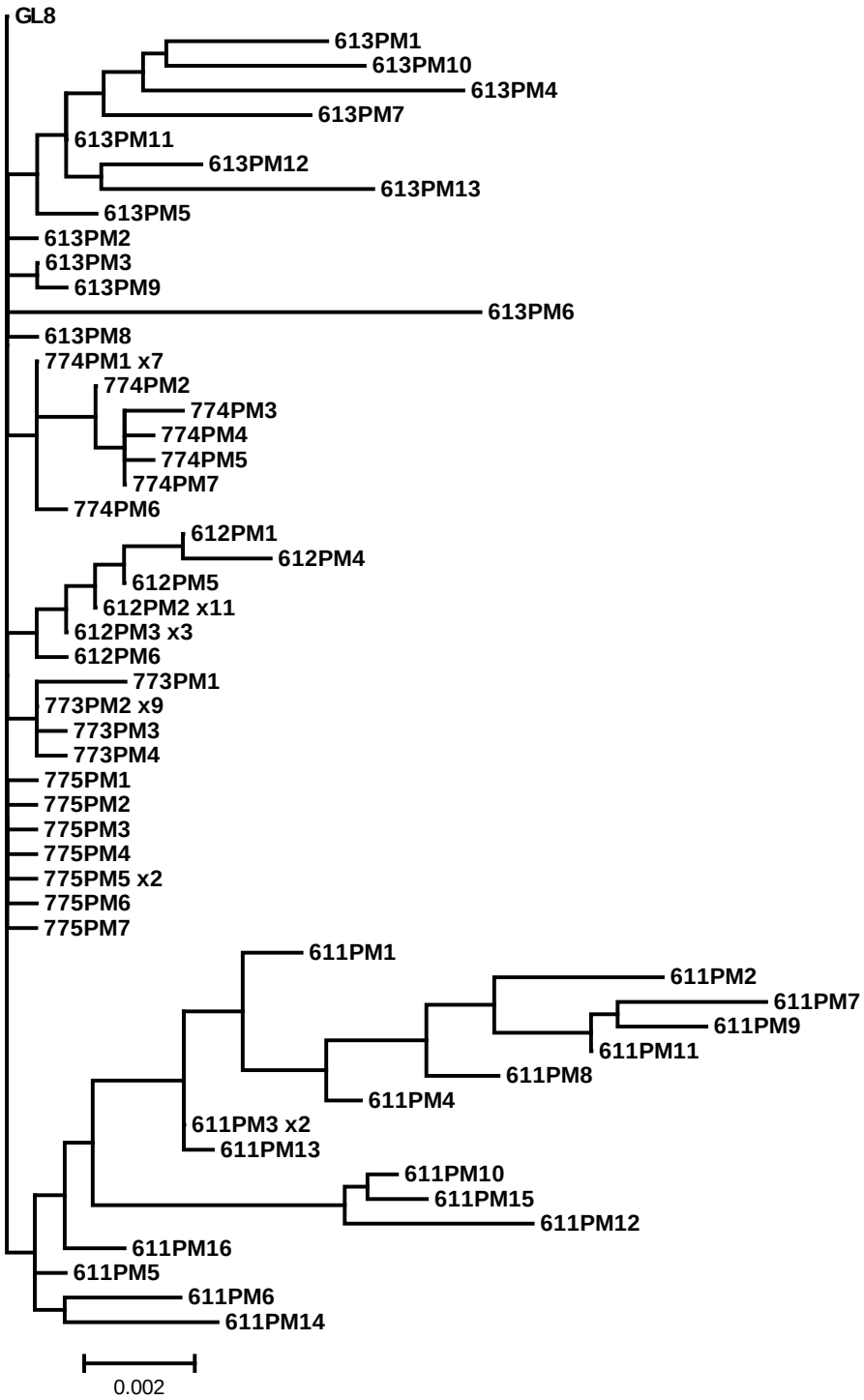


**Figure 3-2. Phylogenetic maximum likelihood tree of PBMC-derived *env* sequences.**
54 proviral *env* sequences were amplified from PBMCs of long-term (A611-613) and short-term (A773-775) FIV infected cats using LD-PCR. A 2030nt long sequence alignment was used to calculate a ML tree utilising the TVM+G+I model of substitution in PAUP. The tree was estimated under the topological constrain of treating all *env* sequences from one cat as a monophyletic group. The tree is rooted on the parental strain GL8. Repeated sequences were included once and were marked by an "x" followed by the number of repeats. Sequences identical to GL8 were excluded. Adapted from (Kraase et al., 2010).

Substitutions of nucleotides can either result in mutations of amino acids (non-synonymous) or might not affect the amino acid sequence (synonymous). The ratio of

non-synonymous (dN) to synonymous (dS) mutations, dN/dS, is an indicator for evolutionary selection processes. Provided a virus is already well-adapted to its host, the majority of novel non-synonymous mutations may be disadvantageous, therefore one would expect the number of synonymous mutations (dS) to exceed the number of non-synonymous mutations (dN) resulting in a mean dN/dS ratio <1, representing negative selection. Conversely, mean dN/dS ratios >1 indicate positive selection of quasispecies that acquired a higher proportion of mainly advantageous non-synonymous mutations, while neutral selection is represented by dN/dS=1.

We utilised the sequence alignment of variants of the long-term infected cats (A611-A613) to estimate the selection within each cat using the SLAC (single likelihood ancestor counting) algorithm in HyPhy (Pond and Frost, 2005a). Quasispecies isolated from cats A611 and A613 showed negative selection indicated by dN/dS ratios of 0.65 and 0.83 respectively. In contrast, the viral population in cat A612 displayed a dN/dS ratio of 2.05 suggesting positive selection. Of note, the HyPhy package only allows non-identical sequences for the calculation of selection. As shown in table 3-1 we recovered a total of 14 variants from cat A612 that were sequence repeats. These were included in the dN/dS analysis only once. However, if only the repeated sequences from cat 612 were compared to FIV-GL8 using HyPhy the mean dN/dS ratio was 0.54 indicating negative selection. Therefore, the overall selection pressure on viruses of animal 612 is probably negative with some variants being under positive selection. Thus, the majority of variants in all long-term infected cats were under negative selection suggesting that the parental virus FIV-GL8 may already have exhibited optimal replication characteristics *in vivo*.

Next, we analysed the selection pressure on each codon using the Fixed Effects Likelihood (FEL) method in HyPhy (Pond and Frost, 2005b). Again positive selection would indicate non-synonymous mutations at defined sites that are of replicative advantage, whereas negative selection would represent residues that are important for the virus to retain in their original state as changes my decrease fitness. The analysis of sequences from all six cats revealed three sites under positive selection and 25 negatively selected residues (Figure 3-3). The positively selected sites included only one major mutation (E/K) at position 225, leading to a switch from a negative to a positive charge. The other sites under positive selection contained a V373I and a V558G/D/I mutation which only represent a minor change in chemical properties of the substituted amino acids. Yet, care

must be taken when drawing conclusions from this analysis as again one limitation in the HyPhy package is the deletion of repeated sequences, which in the cat may represent the majority of virus variants but were included in the analysis only once. Therefore, we next looked at the amino acid changes in individual cats.

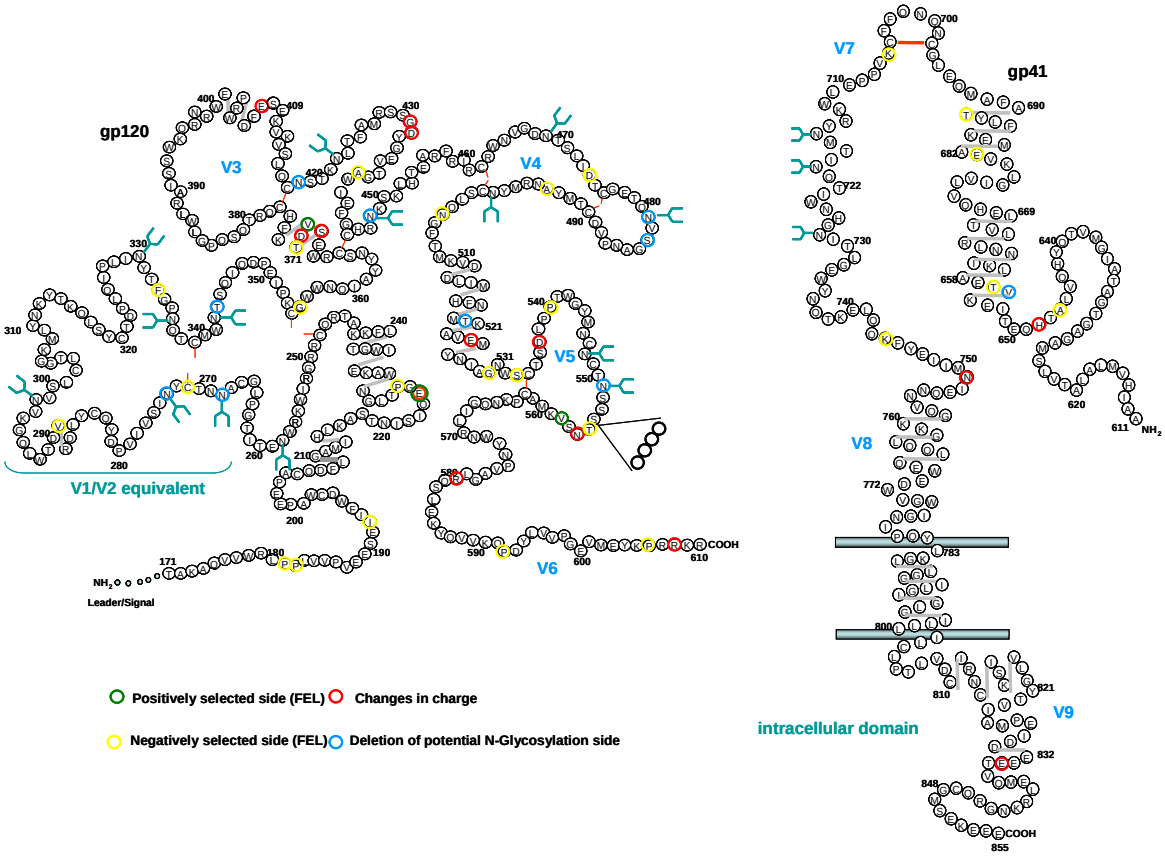


**Figure 3-3. Selection pressure on surface unit and transmembrane protein of FIV-GL8.**
Residues under positive (green) or negative (yellow) selection were estimated utilising the Fixed effects likelihood (FEL) algorithm in HyPhy. Substitutions that led to a change in charge (red) or deletion of potential N-linked glycosylation sites (blue) are shown. Adapted from (Kraase et al., 2010).

### *3.2.2.2. Sequence evolution within infected cats*

During the course of infection viral variants of the short-term infected cats had acquired only a few non-synonymous mutations (Table 3-3). All sequences isolated from animal A773 carried a L538M substitution in V5, however this mutation was confined to A773 only. Eight out of 14 variants isolated from cat A774 harboured a conservative change from valine to isoleucine at position 373 in the V3 loop. Interestingly, this mutation was also present in the majority of A611 and A612 derived sequences and occurred once in cat A613. Furthermore, four sequences from cat A774 displayed a S554G mutation in the V5 loop which was shared by four variants derived from animal A611.

Thus, these two substitutions may represent mutations that are acquired early in infection and are kept throughout the course of disease. In animal A775 the number of AA substitutions was very low with only two sequences harbouring a R583S mutation and one sequence carrying a V776A switch.

Viral variants in the long-term infected group had accumulated a number of non-synonymous mutations that disrupted predicted N-linked glycosylation sites (cat A611: N448K/S in 10/18, S483P/L in 11/18; cat A612:N274H in 1/18, T343P in 1/18; cat A613: N269D/G in 2/17, N418H in 1/17, N481K in 1/17). A few mutations occurred in several cats and/or at a high frequency and may indicate regions under selection by the immune system. In the V3 loop such residues included position 373, which was changed in variants from four animals (611-613 and 774) at high frequency and the L386S mutation which occurred in cats A611 (13/18 variants) and A613 (4/17 variants). Another target of common mutations was identified within gp41 where all long-term infected cats harboured substitutions in residues 648 and 651 at high frequency. Furthermore the valine at position 558 in V5 was exchanged in variants from cats A611 (15/18), A612 (2/18) and A613 (2/17) by three different mutations. Additionally the V5 loop contained length polymorphisms namely deletions (cat A611 and A613) and insertions of two or three amino acids (cat A613), which appear to have arisen through duplication of the preceding nucleic acid sequence. Such diversity may indicate selective immune pressure acting on this region.

**Table 3-3. Changes in amino acid sequence in Env in early and late viral populations.**
Adapted from (Kraase et al., 2010).

| Location[a] | Mutation[b] | Comment[c] | 12 weeks p.i. | | | 322 weeks p.i. | | |
|---|---|---|---|---|---|---|---|---|
| | | | 773 (12)[d] | 774 (14)[d] | 775 (13)[d] | 611 (18)[d] | 612 (18)[d] | 613 (17)[d] |
| C1 | E225K | charge 2+ | | | | 4 | | |
| V1/V2 | L265S | | | | | | | 1 |
| | N269D | del. N-x-S/T | | | | | | 1 |
| | N269G | del. N-x-S/T | | | | | | 1 |
| | N274H | del. N-x-S/T | | | | | 1 | |
| | V299I | | | | | 5 | | |
| | T343P | del. N-x-S/T by P insert. | | | | | 1 | |
| | Q347P | | 1 | | | | | |
| C3 | N364T | | 1 | | | | | |
| V3 | S370R | charge 1+ | | | | | 1 | |
| | D372N | charge 1+ | | | | 2 | | |
| | D372E | | | | | 1 | | |
| | V373I | | | 8 | | 10 | 18 | 1 |
| | L386S | | | | | 13 | | 4 |
| | F406L | | | | | | | 1 |
| | F406Y | | | | | | | 1 |
| | E407K | charge 2+ | | | | | | 2 |
| | S408V | | | | | | | 2 |
| | E409D | | | | | 1 | | |
| | L415V | | | | | | | 1 |
| | N418H | del. N-x-S/T | | | | | | 1 |
| | R428T | | | | | | | 1 |
| | S430L | | | | | | | 1 |
| | G431E | charge 1- | | | | 2 | 3 | |
| | D432N | charge 1+ | | 2 | | | | |
| C4 | N448K | del. N-x-S/T; charge 1+ | | | | 6 | | |
| | N448S | del. N-x-S/T | | | | 4 | | |
| | K451R | | | | | 3 | | |
| V4 | 4463K | | | 1 | | | | |
| | I473T | | | | | | | 1 |
| | T479I | | | | | | | 1 |
| | Q480P | | | | | | | 1 |
| | N481K | del. N-x-S/T; charge 1+ | | | | | | 1 |
| | S483P | del. N-x-S/T | | | | 8 | | |
| | S483L | del. N-x-S/T | | | | 3 | | |
| | D489E | | | | | | | 1 |
| C5 | L502F | | | | | | | 1 |
| | Q503L | | | | | | | 1 |
| | Q503P | | | | | | | 1 |
| | T520A | del. N-x-S/T | | | | | | 1 |
| | E524K | charge 2+ | | 1 | | | | |
| | I528N | | | | | | | 1 |
| V5 | D537A | charge 1+ | | | | | | 1 |
| | L538M | | 12 | | | | | |
| | N551S | del. N-x-S/T | | | | | | 1 |
| | S553N | N-Glyc moves 2 AA | | | | | | 1 |
| | S554G | | | 4 | | 4 | | |
| | 554 +SS | | | | | | | 1 |
| | 554 +TNS | insert. N-x-S/T | | | | | | 2 |
| | 554 +TNS | | | | | | | 1 |
| | T555A | | | | | | | 2 |
| | N556H | charge 1+ | | | | 4 | | |
| | 557 -S | | | | | 3 | | 1 |
| | V558G | | | | | 12 | | 1 |
| | V558D | charge 1- | | | | | 2 | |
| | V558I | | | | | 3 | | 1 |
| | N565S | | | | | 5 | | |
| | L579F | | | | | 1 | | 1 |
| | R580S | charge 1- | | | 2 | | | 1 |
| | Q581P | | | | | | | 1 |
| | Q587P | | | | | | | 1 |

**Table 3-3 (continued)**

| Location[a] | Mutation[b] | Comment[c] | 12 weeks p.i. | | | 322 weeks p.i. | | |
|---|---|---|---|---|---|---|---|---|
| | | | 773 (12)[d] | 774 (14)[d] | 775 (13)[d] | 611 (18)[d] | 612 (18)[d] | 613 (17)[d] |
| gp 41 | R608S | charge 1- | | | | 5 | | |
| | H648Q | charge 1- | | | | 8 | 3 | 3 |
| | T651A | | | | | 13 | 17 | 7 |
| | V655M | | | | | | | 2 |
| | Q700P | | | | | | | 1 |
| | P709L | | | | | 11 | | |
| | N751D | charge 1- | | | | | | 3 |
| | N755S | | | | | | | 1 |
| | K760R | | | | | | | 1 |
| | D771E | | | | | 1 | | |
| | V773A | | | | 1 | | | |
| | G794S | | | 1 | | | | |
| | S816N | | | | | | | 1 |
| | I829T | | | | | | | 1 |
| | E834V | charge 1+ | | | | 1 | | |
| | V836A | | | | | | | 1 |

Amino acids are numbered from the first methionine of the *env* ORF. The number of sequences per cat with a particular mutation is shown.

[a] Location in *env* gene equivalent to variable loop (V) and conserved region (C) of HIV *env*.

[b] Insertions and deletions are indicated with +/- followed by the amino acids.

[c] Major mutations that altered the charge of the protein or led to a deletion or insertion of potential N-glycosylation sites (N-x-S/T).

[d] Analysed cat. Brackets contain number of sequences obtained by LD-PCR.

### 3.2.3. Genotype of tissue derived FIV *env* sequences from animal A611

Certain tissues pose distinct growth conditions for viruses and may result in isolated viral evolution. Such compartmentalisation has been reported for HIV in the brain (Ohagen et al., 2003), lymphoid tissues (Thomas et al., 2007), gut tissue (van Marle et al., 2007), semen (Delwart et al., 1998) and female genital tract (Kemal et al., 2003; Philpott et al., 2005). These differences in viral populations are of importance for the transmission of the virus, as the transmitted isolates may not be identical to the most prominent variants in the blood stream and it also may have an influence on viral rebound from latent reservoirs.

Not much is known about the compartmentalisation of FIV in tissues other than the brain (Hein et al., 2003; Liu et al., 2006). This is due to unknown source of natural infection and/or low viral diversity after short infection periods, which does not allow differentiation between PBMC and tissue derived virus. To investigate the compartmentalisation of FIV, genomic DNA was extracted from tissues of FIV-GL8 infected cat A611 at 322 weeks post-infection. Using LD-PCR we recovered between two

and six full length *env* sequences from thymus, bone marrow, tonsil, large intestine and salivary gland. Sequence analysis revealed mainly non-identical sequences, besides two single sequence repeats in the thymus and bone marrow sample set (Table 3-4).

**Table 3-4. Summary of *env* sequences obtained from PBMCs and tissues of cat A611.**

| Tissue | Sequences obtained | Repeated sequences (identical to GL8) | Repeated sequences (not identical to GL8) |
|---|---|---|---|
| PBMC | 18 | 1 | 2 |
| Thymus | 6 | 0 | 1 |
| Tonsil | 5 | 0 | 0 |
| Bone marrow | 4 | 0 | 1 |
| Large intestine | 3 | 0 | 0 |
| Salivary gland | 2 | 0 | 0 |

We next aligned the tissue derived nucleotide sequences against variants isolated from PBMCs of cat A611 (see 3.1.2) and used the 2030 nt long alignment to calculate a maximum likelihood tree in MEGA5 using the HKY+G+I model of substitution. The ML tree (Fig. 3-4) displayed several branches with shared phylogeny of sequences from the same tissue. For instance, all thymus-derived sequences formed a separate cluster. Furthermore, three tonsil samples appeared on one discrete branch, while the two remaining tonsil sequences lay within the thymus group. A third cluster was formed by several PBMC derived sequences. Conversely, isolates originating from the bone marrow, the large intestine and the salivary gland were distributed more heterogeneously. Sequences derived from the large intestine appeared at two positions. Two were closely related to the ancestor of the tonsil cluster, while the remaining sequence clustered within the PBMCs group. Similarly, the salivary gland derived sequences appeared to be most closely related to virus extracted from PBMCs, maybe suggesting that virus in the blood stream resembles variants transmitted via saliva. The highest sequence similarities were noted between bone marrow derived sequences and isolates from PBMCs. In fact, all sequences originating from bone marrow had an identical counterpart derived from PBMCs, suggesting that bone marrow (and also salivary gland and large intestine) permit the influx of virus or infected PBMCs or that tissue derived virus infected PBMCs in the periphery.

Next, we analysed the amino acid composition of the tissue derived sequences (Table 3-5). The samples originating from the tonsil contained several mutations, mainly in V5 and gp41, which were present in no other tissue, e.g. G599E, M628I and E768K. However, these isolates were very heterogenic with only one mutation (N448K) present in all sequences. Conversely, the thymus samples proved very homogeneous with most mutations occurring in all six sequences. Some of these amino acid substitutions like the K296R mutation in V1/V2 and the I360M change in C3 almost exclusively occurred in the thymus. Furthermore, we noticed a three amino acid insertion in the V5 loop that created an additional potential N-glycosylation site. Interestingly, besides one tonsil-derived sequence, this insertion was present exclusively in thymus samples. In contrast, substitutions in virus isolated from the salivary gland, bone marrow and large intestine in most cases were shared with PBMC-derived virus. Hence, despite the limited sample size our data implies that tonsil and thymus represent compartments of isolated virus evolution, while the other tissues tested appear to allow some exchange of virus between compartments.

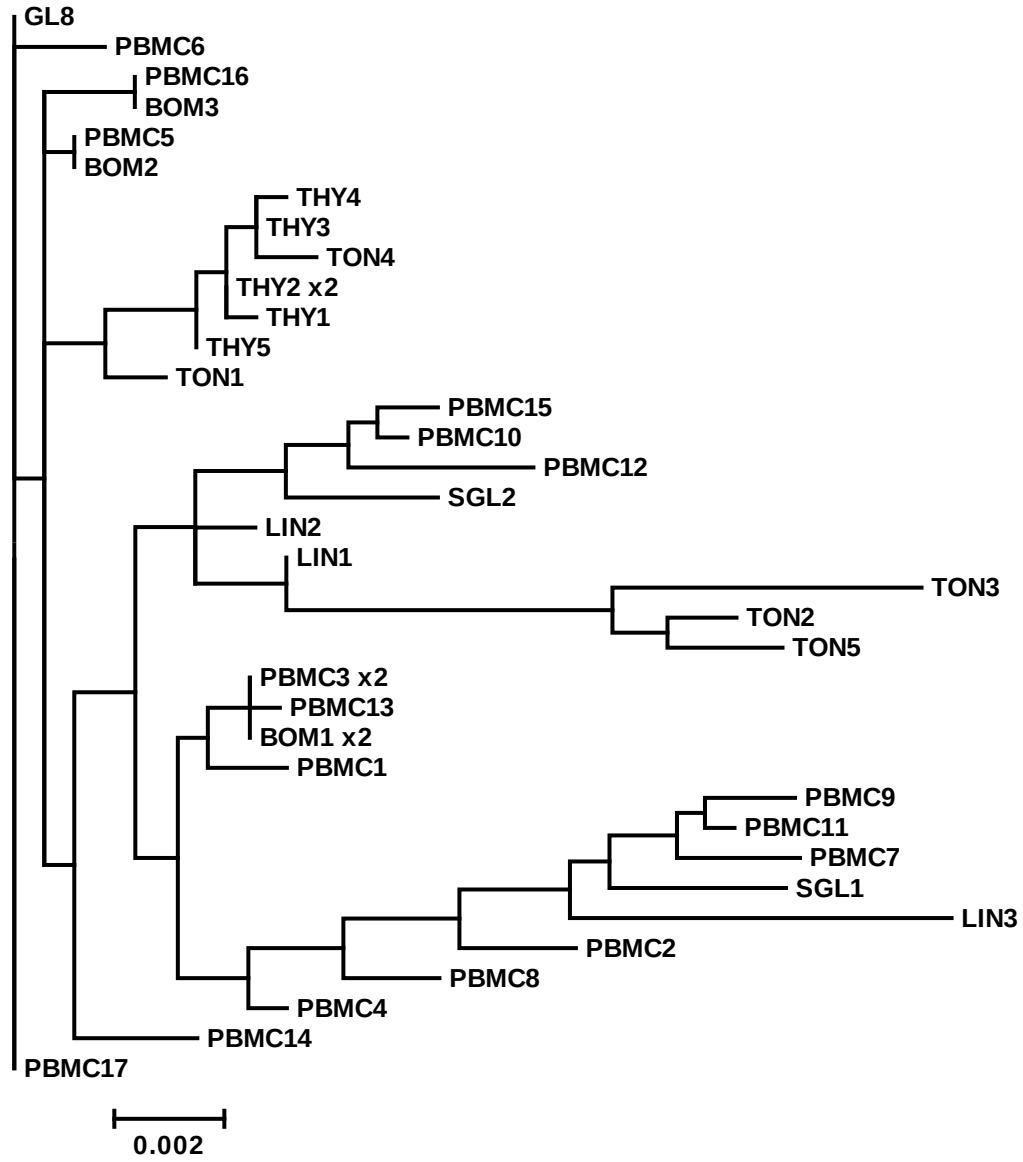


**Figure 3-4. Phylogenetic Maximum likelihood (ML) tree of tissue-derived *env* sequences.**
Proviral env sequences were derived by LD-PCR from PBMCs and tissues of cat A611 at 322 weeks p.i. A 2030 nt long sequence alignment was used to estimate an unconstrained ML tree utilising the HKY+G+I model of substitution in MEGA5. The tree is rooted on the infecting strain FIV-GL8. Repeated sequences are followed by an "x" and the number of repeats. Abbreviations: Peripheral blood mononuclear cell, PBMC; bone marrow, BOM; thymus, THY; large intestine, LIN; salivary gland, SGL; tonsil, TON.

**Table 3-5. Mutations in the *env* gene from tissues of long-term infected cat A611.**

| Location[a] | Mutation[b] | Comment[c] | BOM (4)[d] | SGL (2)[d] | THY (6)[d] | TON (5)[d] | LIN (3)[d] | PBMC (18)[d] |
|---|---|---|---|---|---|---|---|---|
| C1 | E225K | charge 2+ | | | | 1 | | 4 |
| V1/V2 | R246K | | | | | 1 | | |
| | R252K | | | | | 2 | | |
| | A268D | charge 1- | | | | 3 | 1 | |
| | I278T | | | | | 2 | | |
| | K296R | | | | 5 | 1 | | |
| | V299I | | | 1 | | | | 5 |
| | Y313H | charge 1+ | | 1 | | | | |
| C3 | I360M | | | | 5 | | | |
| V3 | D372N | charge 1+ | 1 | | | | | 2 |
| | D372E | | | | | | | 1 |
| | V373I | | 4 | | 6 | 2 | | 10 |
| | L386S | | 2 | 2 | | | 2 | 13 |
| | R397G | | | | | 1 | | |
| | E409D | | | | | | | 1 |
| | G431E | charge 1- | | | 6 | 4 | 2 | 2 |
| C4 | N448K | del. N-x-S/T; charge 1+ | 2 | | 6 | 5 | 1 | 6 |
| | N448S | del. N-x-S/T | | 2 | | | 1 | 4 |
| | K451R | | | | | | 1 | 3 |
| V4 | S483P | del. N-x-S/T | | 2 | | 1 | 1 | 8 |
| | S483L | del. N-x-S/T | | | | | | 3 |
| C5 | L502S | | | | | | 1 | |
| | T507S | | | | | | 1 | |
| | S533C | | | | | | 1 | |
| V5 | M545I | | | | | 3 | 1 | |
| | 550 +NST | insert. N-x-S/T | | | 6 | 1 | | |
| | S554G | | | 1 | | | 1 | 4 |
| | S554N | | | | | 2 | | |
| | N556T | | | | | 1 | | |
| | N556H | charge 1+ | | | | | | 4 |
| | N556S | | | 1 | | | | |
| | 557 -S | | | | | | | 3 |
| | V558G | | 2 | 2 | | 3 | 3 | 12 |
| | V558I | | | | | | | 3 |
| | K559E | charge 2- | | | | 1 | | |
| | M560L | | | | | 3 | | |
| | N565S | | | 1 | | | 1 | 5 |
| | L582F | | | | | | | 1 |
| | G599E | charge 1- | | | | 3 | | |
| gp 41 | R608S | charge 1- | | 1 | | | | 5 |
| | M628I | | | | | 3 | | |
| | H648Q | charge 1- | | 2 | | 3 | 3 | 8 |
| | T651A | | 3 | 2 | | 3 | 3 | 13 |
| | V655M | | | | 6 | 2 | | |
| | I676M | | | | | | 1 | |
| | P709L | | | 1 | | 3 | 3 | 11 |
| | H726Q | charge 1- | | | 2 | 1 | | |
| | K761R | | | | | 3 | | |
| | E768K | charge 2+ | | | | 3 | | |
| | D771E | | | | | | | 1 |
| | I790V | | | | | 1 | | |
| | E834V | charge 1+ | | | | 3 | | 1 |
| | V836I | | | | | 2 | | |
| | C847Y | | | | | 1 | | |

Amino acids are numbered from the first methionine of the *env* ORF. The number of sequences per tissue with a particular mutation is shown.

[a] Location in *env* gene equivalent to variable loop (V) and conserved region (C) of HIV *env*.

[b] Insertions and deletions are indicated with +/- followed by the amino acids.

[c] Major mutations that altered the charge of the protein or led to a deletion or insertion of potential N-glycosylation sites (N-x-S/T).

[d] Analysed tissue: BOM, bone marrow; SGL, Salivary gland; THY, thymus; TON, tonsil; LIN, large intestine; PBMC, peripheral blood mononuclear cell. Brackets contain number of sequences obtained by LD-PCR.

### 3.2.4. The influence of APOBEC3 on viral evolution

As part of the innate immune system APOBEC3 (A3) proteins are active during all stages of infection. A3 proteins execute their anti-viral function mainly by deamination of cytidine to uracil on nascent minus strand viral DNA during reverse transcription, resulting in G-to-A hypermutations on the plus strand proviral DNA (Mangeat et al., 2003; Sheehy et al., 2002; Zhang et al., 2003). Vif-deficient FIV is highly sensitive to feline A3 *in vitro,* but is protected from the detrimental effects of A3 in the presence of Vif (Munk et al., 2008; Zielonka et al., 2010b). Hitherto the influence of A3 on wild-type FIV *in vivo* is not known, A3 may contribute to the inhibition of viral replication, conversely A3 could possibly induce mutations at a sub-lethal level that accumulate over time and increase viral variability (reviewed in (Munk et al., 2012)) or A3 may, due to the action of Vif, be inactivated completely.

To assess the involvement of A3 in viral evolution *in vivo* we compared the frequency of G-to-A mutations during early and late infection with the frequency of the inversely directed A-to-G mutation that most likely resulted from the low fidelity of viral RT. PBMC-derived *env* sequences from animals A773, A775 and A613 exhibited comparably low frequencies of G-to-A mutations, which did not exceed A-to-G mutation (Table 3-6), while quasispecies isolated from A612 displayed elevated G-to-A mutation frequencies that only slightly dominated over A-to-G mutations. Thus, the influence of A3 on viral evolution in these animals appears rather limited. Conversely, G-to-A substitutions in quasispecies derived from animals A774 and A611 exceeded the inversely directed mutation considerably. In both cats the frequency of G-to-A mutations was highest among all animals of the respective group. In fact, G-to-A mutations in isolates from short-term infected cat A774 were detected more frequently than in long-term infected animal A613 even though the average frequency of mutations (excluding G-to-A and A-to-G substitutions) was ten times higher in variants isolated from A613. Hence, A3 most likely contributed to the variability of PBMC derived quasispecies in animals A774 and A613. Overall this data suggests a minor influence of A3 on viral evolution in PBMCs which appears to depend on strong inter-animal variations, yet two out of six animals displayed signatures of A3 activity.

**Table 3-6. Mutation frequencies (per 1 kb) in full length *env* sequences (2565 nt) isolated from PBMCs of short-term and long-term infected cats (including repeated sequences)**

| | 12 weeks post-infection | | | 322 weeks post-infection | | |
|---|---|---|---|---|---|---|
| mutations | A773 | A774 | A775 | A611 | A612 | A613 |
| G-to-A | 0.00 | 0.42 | 0.03 | 1.23 | 0.45 | 0.27 |
| A-to-G | 0.03 | 0.14 | 0.03 | 0.80 | 0.39 | 0.73 |
| others [a] | 0.06 | 0.01 | 0.03 | 0.29 | 0.07 | 0.10 |

[a] average frequency of mutations other than G-to-A and A-to-G

Cats express five A3 proteins that have been shown *in vitro* to preferentially mutate residues in a distinct dinucleotide context (Munk et al., 2008). The activity of the highly anti-viral feA3H and feA3CH mainly results in GA→AA, GC→AC and GG→AG mutations, while the three weakly restrictive feA3C proteins preferentially mutate GT→AT residues (Munk et al., 2008). We analysed the dinucleotide context of mutated guanines in quasispecies of animals A774 and A611. Viral isolates from both cats displayed a similar distribution of frequencies of edited dinucleotides (Figure 3-5). The majority of G-to-A mutations occurred in a GT context, followed by GA residues, while only a minor fraction of edited GG and GC dinucleotides was detected. This data suggests feA3C proteins as the main source of G-to-A mutations in PBMCs and is consistent with the high expression of feA3C mRNA in feline PBMCs (Troyer et al., 2013).

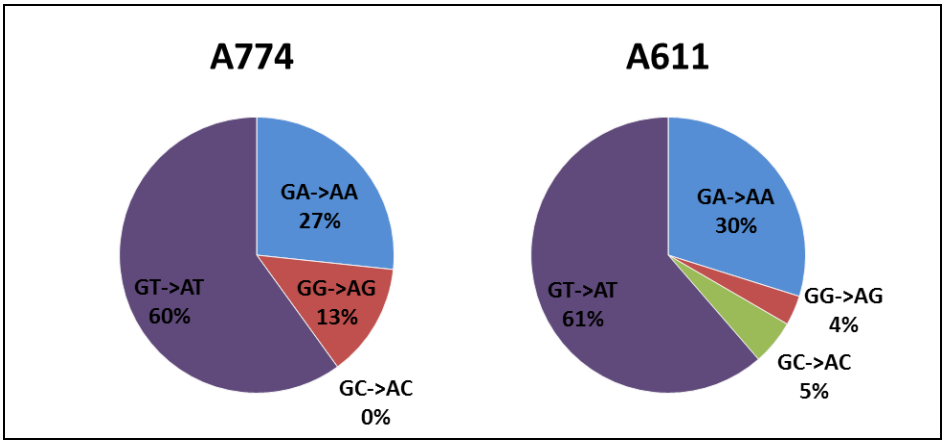


**Figure 3-5. Dinucleotide sequence preferences for G-to-A mutations in quasispecies isolated from PBMCs of animals A774 and A611.**

Percentages of mutated dinucleotides is depicted for edited G residues of sequences described in 3.1.2.

We next analysed the occurrence of G-to-A mutations in isolates originating from tissues of animal A611 using the dataset described previously (3.1.3.). FIV sequences derived from large intestine and salivary gland displayed G-to-A mutation frequencies ranging below that of A-to-G mutations (Table 3-7), indicating only a minor influence of A3. In contrast, sequences isolated from PBMCs, bone marrow, thymus and tonsil exhibited a reversed distribution of mutations with roughly twice as many G-to-A mutations compared to the inversely directed mutation, suggestive of a considerable impact of A3 on viral evolution. Interestingly, sequences originating from the tonsil displayed the highest overall G-to-A mutation frequency, exceeding the same mutation in PBMC derived isolates by almost three fold. These results indicate a strong tissue variation of A3 induced mutations and are consistent with the high expression of A3 in lymphoid tissues and the low expression in non-lymphoid tissues (Dietrich, 2013; Troyer et al., 2012).

**Table 3-7. Mutation frequencies (per 1 kb) in full length *env* sequences (2565 nt) isolated from tissues of A611 (including repeated sequences).**

| mutations | BOM | LIN | THY | TON | SGL | PBMC |
|---|---|---|---|---|---|---|
| G-to-A | 0.78 | 0.78 | 1.17 | 3.20 | 1.17 | 1.23 |
| A-to-G | 0.39 | 1.30 | 0.71 | 1.56 | 1.36 | 0.80 |
| others [a] | 0.08 | 0.29 | 0.09 | 0.37 | 0.41 | 0.29 |

Abbreviations: Peripheral blood mononuclear cell, PBMC; bone marrow, BOM; thymus, THY; large intestine, LIN; salivary gland, SGL; tonsil, TON

[a] average frequency of mutations other than G-to-A and A-to-G

We next analysed the dinucleotide context of mutated guanines in bone marrow, thymus and tonsil derived sequences. Isolates from bone marrow and thymus displayed a strong overrepresentation of edited GT residues, followed by GA and GG dinucleotides (Figure 3-6), indicating primarily activity of feA3C. In contrast, in tonsil derived quasispecies the majority of editing was detected at GA residues, while approx. 40% of mutations occurred in a GT context, suggesting the activity of feA3H and/or feA3CH in addition to the action of feA3C. The tissue expression of A3 mRNA appears to vary considerably between individual cats (Dietrich, 2013; Troyer et al., 2012), however feA3C generally is expressed at high levels which is consistent with the dinucleotide context described here.

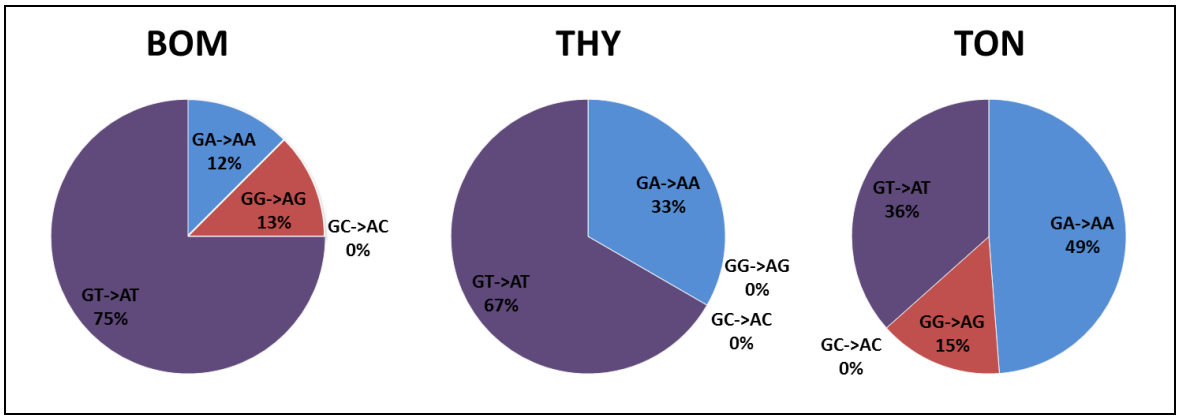


**Figure 3-6. Dinucleotide sequence preferences for G-to-A mutations in quasispecies isolated from tissues of animal A611.**
Percentages of mutated dinucleotides are depicted for edited G residues of env sequences (see 3.1.3.) extracted from bone marrow (BOM), thymus (THY) and tonsil (TON) of cat A611.

In summary our data suggests that the influence of A3 on the evolution of FIV is subjected to strong inter-animal and inter-tissue variation with limited activity in large intestine and salivary gland, while an enhanced A3 signature was detectable in lymphoid tissues, especially the tonsil. Compared to *in vitro* studies with FIVΔ*vif* (Munk et al., 2008), the overall frequency of G-to-A mutations *in vivo* was low, possibly indicating mutations at a sub-lethal degree which is consistent with the activity of the weakly mutative feA3C and confirmed by the GT dinucleotide context of editing. Yet, due to the low tissue sample size which originated from a single cat, care must be taken when drawing conclusions from this analysis. Also it should be noted here that viral evolution is subjected to other constrains like pressure from the adaptive immune system which may conceal the influence of A3 especially in the long-term infected cats.

# 3.3. Phenotype of FIV Env variants from cat A613

## 3.3.1. Analyses of PBMC-derived FIV Env variants

### *3.3.1.1. Characterisation of viral variants from cat A613*

Hitherto our analysis had concentrated on viral genotype; we next extended our investigations on the viral phenotype. We decided to clone *env* sequences isolated from PBMCs of cat A613 as this animal had displayed the lowest proviral load of all long-term

infected cats (Table 3-1), suggestive of a strong immune pressure acting on the viral evolution.

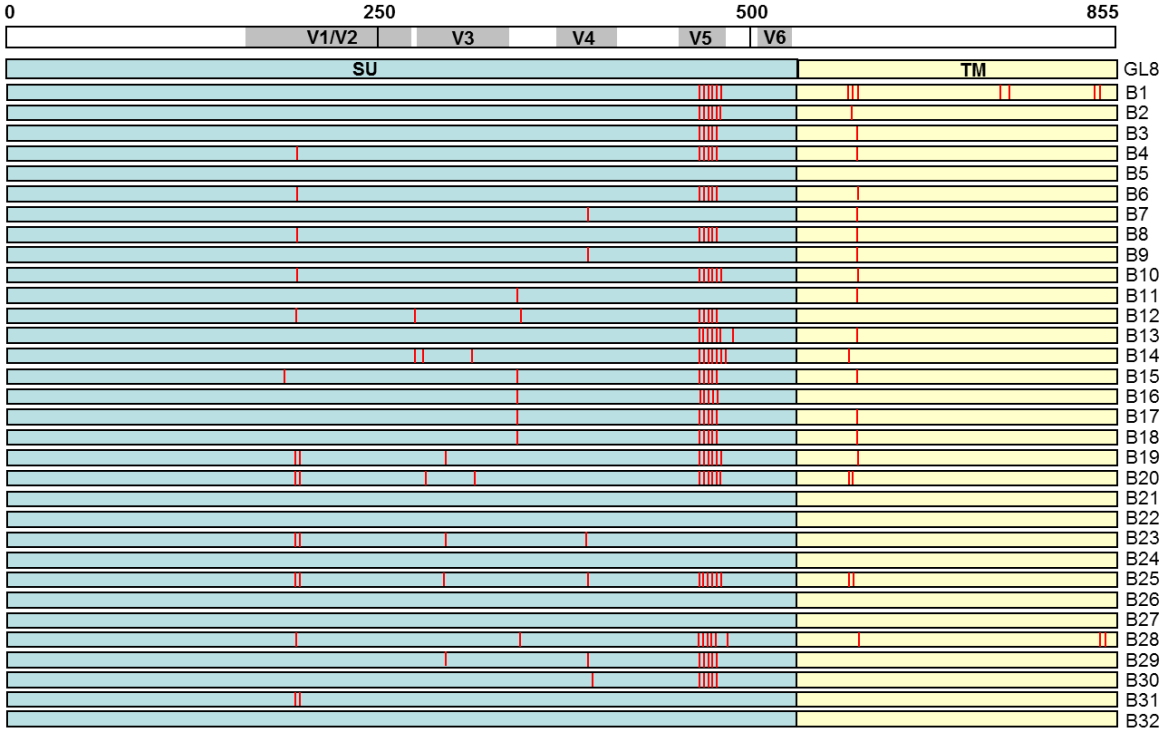


**Figure 3-7. Location of mutations in Env proteins of A613-derived viral variants.**
Mutations (marked in red) are presented relative to a linearised scheme of SU (blue) and TM (yellow) of FIV-GL8, with amino acid positions indicated above. Adapted from (Willett et al., 2010).

Thus, 32 unique viral *env* sequences isolated from PBMCs of cat A613 were cloned (an additional set of LD-PCRs had been performed to gain more viral *env* sequences). These *env* genes contained several mutations throughout the whole sequence (Figure 3-7). Hotspots of mutations were located in the V1/V2 loop (L265S, A268D and N269G/K/A), the V5 loop and the TM (H648Q, T651A and V655M) (Figure 3-8). The variety of substitutions, deletions or insertions within the V5 loop was exceptional and might indicate strong selective pressure acting on this region. We assessed the functionality of the amplified viral sequences by cloning the *env* gene into the molecular clone of FIV-GL8, pGL8-Mya, and transfection into HEK293T cells. Subsequently the virus containing supernatant was utilised to infect the feline T cell line, Mya-1, and infectivity was monitored by p24 ELISA. All Env proteins allowed productive infection of Mya-1 cells (data not shown), thus none contained a functional defect.

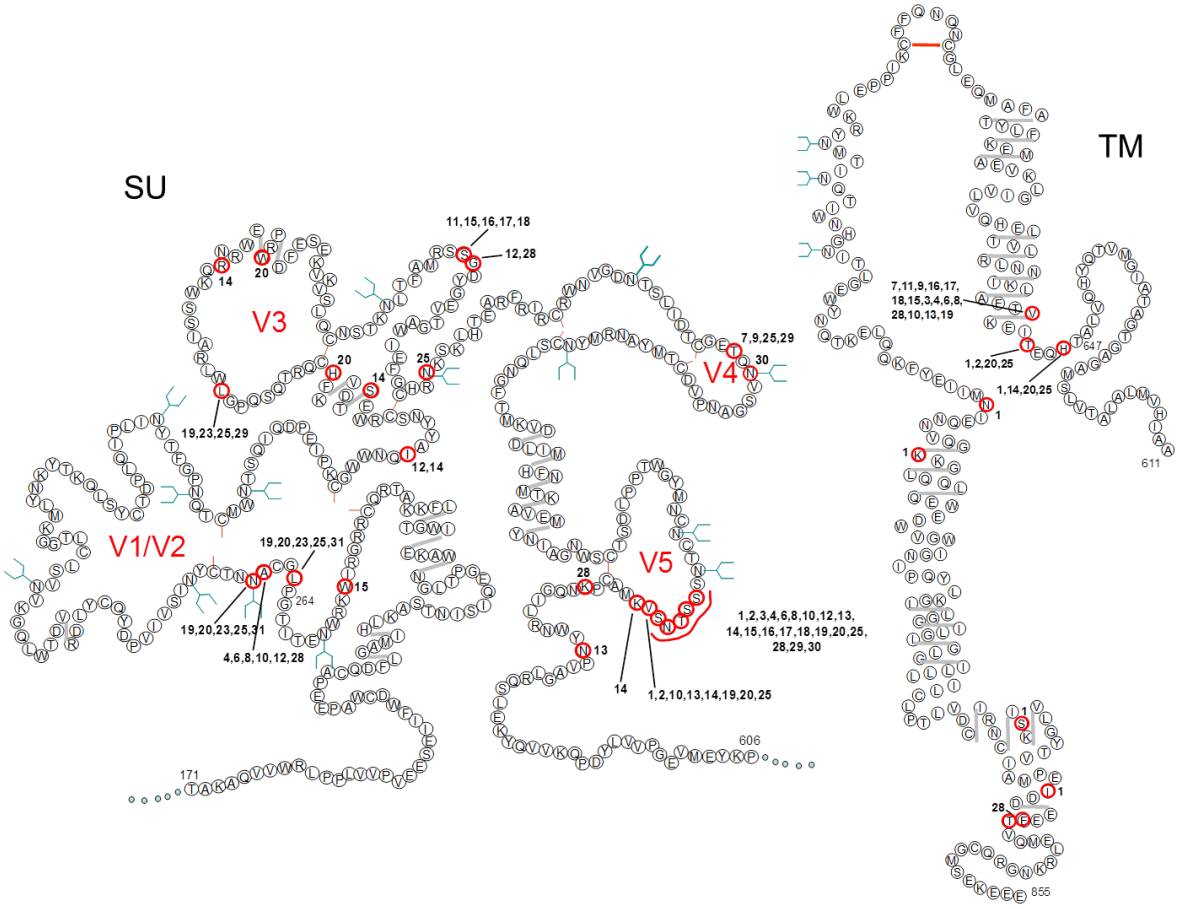


**Figure 3-8. Schematic representation of FIV gp120 and gp41.**
Location of mutations are illustrated by red circles with individual variants indicated. Also displayed are predicted N-glycosylation sites (blue "Y"), cystine bridges (red lines) and predicted alpha-helix formation (grey line). Adapted from (Willett et al., 2010).

Subsequent examination of Env properties focused on receptor interactions. We compared the distribution of AA substitutions, deletions and insertions of the 32 sequences and decided to use nine variants that contained most of the existing alterations. Accordingly, Env variants B12, B14, B19, B23, B25, B28, B30, B31 and B32 were subcloned into the expression vector VR1012. The isolates B23, B31 and B32 were closely related to FIV-GL8, in fact B32 was identical to FIV-GL8, while B23 and B31 shared the same V5 sequences as FIV-GL8, but displayed mutations in the 269NNT271 motif. The other variants were more distantly related to GL8 and contained V5 lengths polymorphisms.

The VR1012 Env expression plasmids and a plasmid encoding HIV *gag, pol* sequences and a luciferase gene were cotransfected into HEK293T cells to produce HIV particles pseudotyped with FIV Env proteins. These HIV(FIV) pseudotypes, were utilised to

infect target cells carrying different types of entry receptors or to examine the interaction with soluble entry receptor protein, receptor ligands or antibodies. Infectivity was quantified by measuring luciferase triggered luminescence three days post-infection.

#### *3.3.1.2. Recognition of complex domains on entry receptor CD134*

The infection of host cells requires the binding of virus to its attachment receptor CD134. Yet, certain FIV strains interact with different domains on CD134 (Willett et al. 2006a, b). For instance FIV-B2542, an isolate from a late stage of infection, only requires feline CRD1 expressed in the background of human CD134 for successful infection, suggesting a relatively flexible interaction with CD134. In contrast, FIV-GL8, isolated from an early stage of infection, depends on additional domains of feline CD134 and fails to utilise the chimeric receptor to enter target cells (Willett et al., 2006a; Willett et al., 2006b). It has been proposed that the character of the receptor interaction may evolve *in vivo* from a "complex" high affinity interaction during early infection towards a more "simple" receptor utilisation during late stages of infection (Willett et al., 2008).

We tested the ability of the A613 derived HIV(FIV) pseudotypes to infect MCC cells expressing either feline CD134, a feline CRD1 x human CD134 chimaera or human CD134. Luciferase activity was quantified three days p.i. and the ratio of CPM (counts per minute) for infection of cells carrying feline CD134 and chimeric CD134 was calculated and used as means of quantifying interactions between virus and receptor. Infection with FIV-B2542 and FIV-GL8 served as controls for prototypic "simple" or "complex" interaction with CD134 and resulted in high (ratio of 5) or low (ratio of 117) infectivity on cells expressing chimeric CD134, respectively (Figure 3-9). Viral variants similar to FIV-GL8 (B23, B31 and B32) displayed only little interaction with chimeric CD134, indicated by ratios of 223, 138 and 112. In contrast, variants B14, B28, B30 exhibited a low dependence for additional domains on CD134 as shown by relatively high infectivity on MCC cells carrying chimeric CD134 and ratios ranging from 4 to 11. The emergence of such variants that like B2542 only depend on feline CRD1 for successful infection is consistent with an *in vivo* evolution towards a more "simple" interaction with CD134.

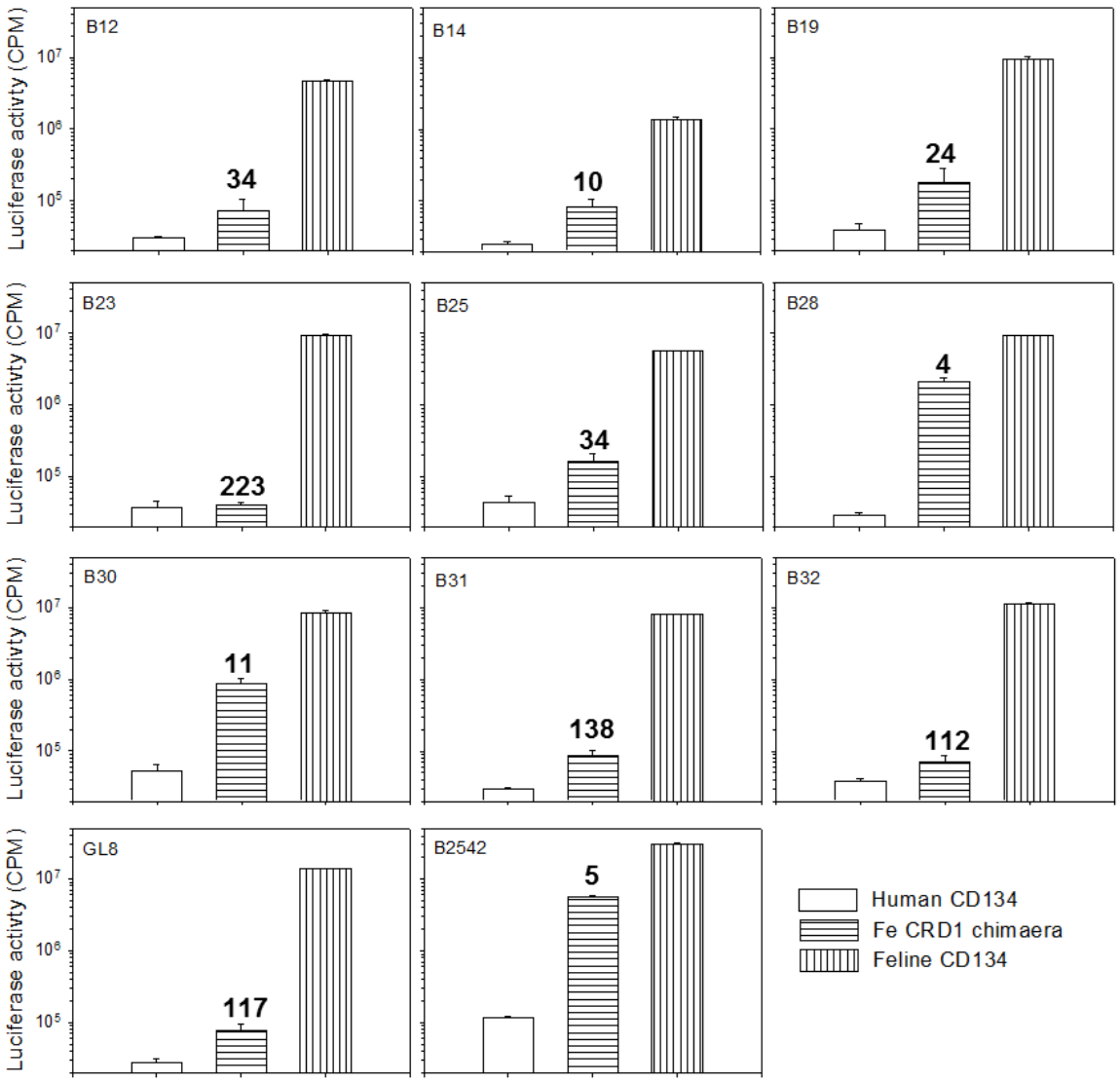


**Figure 3-9. Receptor usage of Env variants isolated from cat A613.**
MCC cells were stably transduced to express either human CD134, feline CD134 or a chimeric CD134 consisting of human CD134 and feline CD134 CRD1. Cells were infected with HIV(FIV) luciferase pseudotypes bearing Env from viral variants isolated from cat A613 or reference strains FIV-GL8 and FIV-B2542. Luciferase activity was quantified three days p.i. and displayed as counts per minute (CPM). Numbers indicate ratios of luciferase counts on cells expressing feline CD134 divided by counts on cells expressing chimeric CD134. Each infection was performed in triplicate and error bars indicate standard error. Results are representative for at least two independent experiments. Adapted from (Willett et al., 2010).

In subsequent experiments six variants (B14, B19, B28, B30, B31 and B32) were analysed further for their sensitivities to antagonism by diverse inhibitors of the virus-receptor interaction. In these experiments variant B32 (identical to GL8) served as a reference strain.

### *3.3.1.3. Inhibition by anti-CD134 AB, 7D6*

Previous studies have shown that the anti-CD134 monoclonal Ab 7D6 is able to block infection with FIV and that the extent of inhibition was strain-dependent (Willett et al., 2007). If the character of the Env-receptor interaction evolves *in vivo* this would likely be reflected by changes in the sensitivity to antagonism by 7D6.

In an inhibition assay CD134 expressing Mya-1 cells were preincubated with 7D6. Subsequent infections with pseudotyped virons resulted in marked differences between FIV-GL8 like viruses (B32, B31) and more distantly related variants (B14, B19, B28 and B30) (Figure 3-10A); the former being largely insensitive to 7D6, reaching a maximal inhibition of approx. 40% at antibody concentrations of 2 µg/ml, whereas at higher concentrations the inhibitory effect decreased (as has been noted previously (Willett et al., 2007)). In contrast, variants B14 and B28 were inhibited even at lowest concentrations of 7D6 and completely blocked at concentrations of 2 µg/ml and above. Variants B30 and B19 showed an intermediate inhibition profile. These results suggest that variants B14 and B28 acquired mutations *in vivo* that increased their sensitivity to antagonism by anti-CD134 AB, 7D6.

### *3.3.1.4. Inhibition by soluble CD134*

Earlier studies had suggested that FIV can bind to soluble feline CD134 (sFc-CD134) and depending on affinity of virus to the soluble receptor infection of target cells can be inhibited (Willett et al., 2009). To assess whether our viral variants displayed differences in their susceptibility to antagonism by soluble CD134, we preincubated Mya-1 cells with sFc-CD134 and added the HIV(FIV) pseudotypes. Again considerable differences between the variants were noted (Figure 3-10B). Isolates similar to FIV-GL8 (B32, B31) but also the more distantly related variants B19 and B30 were strongly inhibited by sFc-CD134. Infectivity of these variants in the presence of the inhibitor appeared almost indistinguishable ranging around 40-50% at 2 µg/ml of sFc-CD134 and reaching complete inhibition at maximum sFc-CD134 input concentration of 50 µg/ml. In stark contrast, variants B28 and B14 appeared largely insensitive to sFc-CD134 mediated inhibition, displaying high infectivity of 90-95% at 2 µg/ml sFc-CD134 and 20-40% infectivity at maximum concentration of soluble receptor, thus indicating changes in the Env-receptor interaction that evolved *in vivo*. Interestingly, the two variants (B14 and B28) that were

most resistant to inhibition by soluble receptor were most sensitive to antagonism by the anti-CD134 Ab.

### *3.3.1.5. Inhibition by receptor ligand*

The natural ligand of CD134 can be produced as a soluble trimeric protein (sFc-TNC-CD134L) and has been shown to prevent infection of late stage isolates FIV-B2542 and FIV-PPR. Yet, strains from early stage infection, such as FIV-GL8, were relatively resistant to inhibition by sFc-TNC-CD134L (Willett et al., 2009; Willett et al., 2007). We next asked if the FIV variants had evolved differences in their sensitivity to sFc-TNC-CD134L mediated inhibition. Mya-1 cells were preincubated with the ligand and HIV(FIV) pseudotypes added. Only modest inhibitory effects on the infectivity of all six variants were noted (Figure 3-10C), however B14 and B28 were most sensitive to antagonism, which is consistent with the distinct sensitivities of these variants to 7D6 and sFcCD134-mediated inhibition.

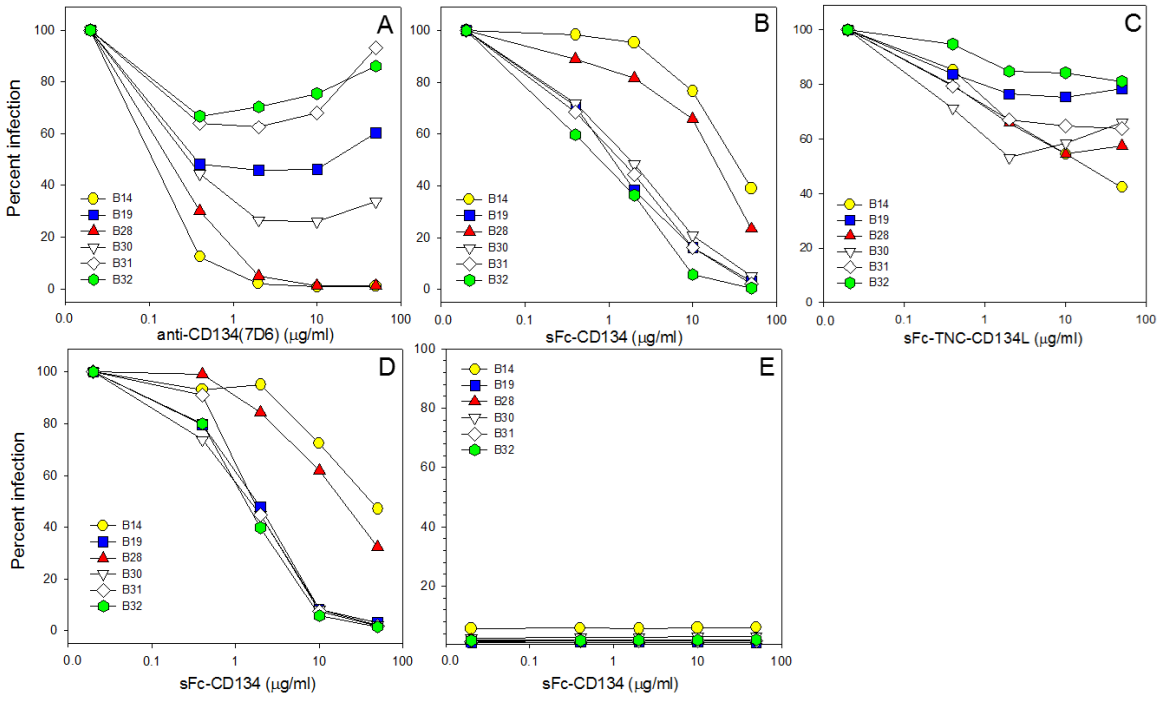


**Figure 3-10. Inhibition of A613 Env variants by antagonists to the Env-receptor interaction.**
Mya-1 cells (A-C) were pre-incubated with indicated concentrations of anti-CD134 AB (7D6), soluble CD134 (sFcCD134) or CD134 ligand (sFc-TNC-CD134L) before addition of HIV(FIV) pseudotypes carrying the Env protein of B14, B19, B28, B30, B31 and B32. MCC cells stably expressing CD134 (D) or CD134 negative MCC cells (E) were infected with HIV(FIV) pseudotypes following pre-incubation with sFcCD134. Luciferase activity was quantified three days p.i. Changes in viral infectivity are depicted as percent infection relative to the infectivity in the absence of inhibitor. Values represent means of triplicate estimations and are typical for at least two separate experiments. Adapted from (Willett et al., 2010).

### *3.3.1.6. Infection of FIV variants is strictly CD134 dependent*

Previous reports have indicated that pre-incubation of FIV with soluble CD134 receptor may trigger conformational changes in Env that would allow infection of CD134-negative cells via a direct interaction with CXCR4 (de Parseval et al., 2004; de Parseval et al., 2006). Since variants B14 and B28 had been largely insensitive to inhibition by sFcCD134 on Mya-1 cells (Figure 3-10B), we hypothesised that a direct utilisation of CXCR4 may have enabled these variants to partially overcome inhibition by soluble CD134.

To verify this hypothesis MCC cells, a feline cell line naturally expressing CXCR4 but not CD134, and MCC-CD134 which had been transduced to express feline CD134, were infected with HIV(FIV) pseudotypes following pre-incubation with increasing amounts of sFcCD134. Similar to results obtained on Mya-1 cells (Figure 3-10B), infection with viral variants B19, B30, B31 and B32 on MCC-CD134 cells was inhibited efficiently by soluble CD134, whereas variants B14 and B28 appeared largely insensitive (Figure 3-10D). Even though Mya-1 cells express approximately 100-fold less surface CD134 than MCC-CD134 (Willett et al., 2007) the actual inhibition curves of viral variants were very similar on both cell lines. Thus, it seem likely that the outcome of this assay is dependent mainly on the interaction of virus with soluble CD134 and that the level of surface bound CD134, in the range tested, does not determine the degree of inhibition.

When we assessed the infectivity of sFcCD134 pre-treated HIV(FIV) pseudotypes on CD134-negative MCC cells we did not observe an enhanced infectivity in the presence of increasing levels of sFc-CD134. Thus, these results indicate that none of the viral variants acquired the ability to infect CXCR4 expressing cells in the absence of CD134 and that pre-incubation with sFcCD134 did not trigger conformational changes in the Env that would allow direct utilisation of CXCR4. Hence, the different sensitivities of isolates B19, B30, B31 and B32 and variants B14 and B28 to antagonism by sFcCD134 and CD134 ligand most likely mirror an *in vivo* evolution of the direct interaction of Env and CD134.

### *3.3.1.7. Sensitivity of viral variants to inhibition by CXCR4 antagonists*

Given the apparent differences in the utilisation of the main receptor CD134 we next investigated whether the viral variants differed in their interaction with the co-receptor CXCR4. Mya-1 cells (CXCR4 low) or CLL-CD134 cells (CXCR4 high) were infected

with HIV(FIV) pseudotypes bearing the Env proteins of viral variants or FIV-GL8 in the presence of increasing amounts of the CXCR4 antagonist AMD3100 (Donzella et al., 1998). All six pseudotypes proved sensitive to AMD3100, consistent with the obligatory usage of CXCR4 for viral entry (Figure 3-11). Considerably lower concentrations of AMD3100 were needed to inhibit infection on Mya-1 cells, which is consistent with the lower expression of CXCR4 on these cells making CXCR4 the limiting factor for infection. Interestingly, on both cell lines only one variant, B14, displayed an increased sensitivity to the CXCR4 antagonist. Thus not only the interaction of B14 with the main receptor CD134 but also with the co-receptor CXCR4 evolved *in vivo*.

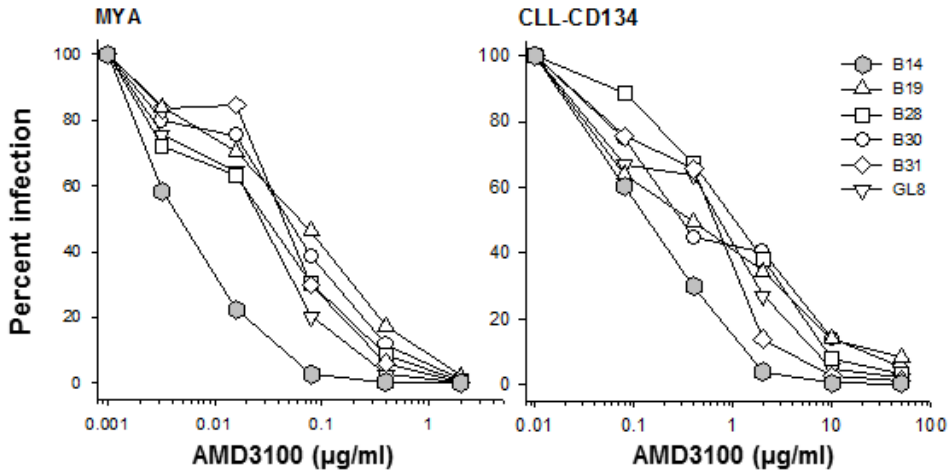


**Figure 3-11. Sensitivity of A613 Env variants to antagonism of the virus-CXCR4 receptor interaction.** MYA-1 or CLL-CD134 cells were incubated with the indicated concentrations of CXCR4 antagonist AMD3100 and subsequently infected with HIV(FIV) pseudotypes bearing the indicated Env proteins. Each point represents triplicate infection and is expressed as percent infection relative to no inhibitor control. Each graph is typical for at least two individual experiments.

### *3.3.1.8. Sensitivity to neutralising antibodies*

Following infection with FIV, cats may develop a neutralising antibody response which suppresses viral replication during the asymptomatic phase of infection. In HIV infected individuals such immune pressure may drive the emergence of escape mutants with altered cell tropism (McKnight and Clapham, 1995). In light of variable receptor interactions of our viral variants we asked whether escape from NAb response could be responsible for the *in vivo* Env evolution.

We compared the sensitivity of HIV(FIV) pseudotypes bearing the Env of nine unique viral isolates or FIV-GL8 to homologous post-mortem plasma *in vitro.* FIV-GL8 and closely related isolates B23, B31 and B32 proved highly susceptible to neutralisation by

the PM plasma of cat A613 (Figure 3-12A). In stark contrast, variants B12, B14, B19, B25, B28 and B30 were insensitive to neutralisation by the plasma

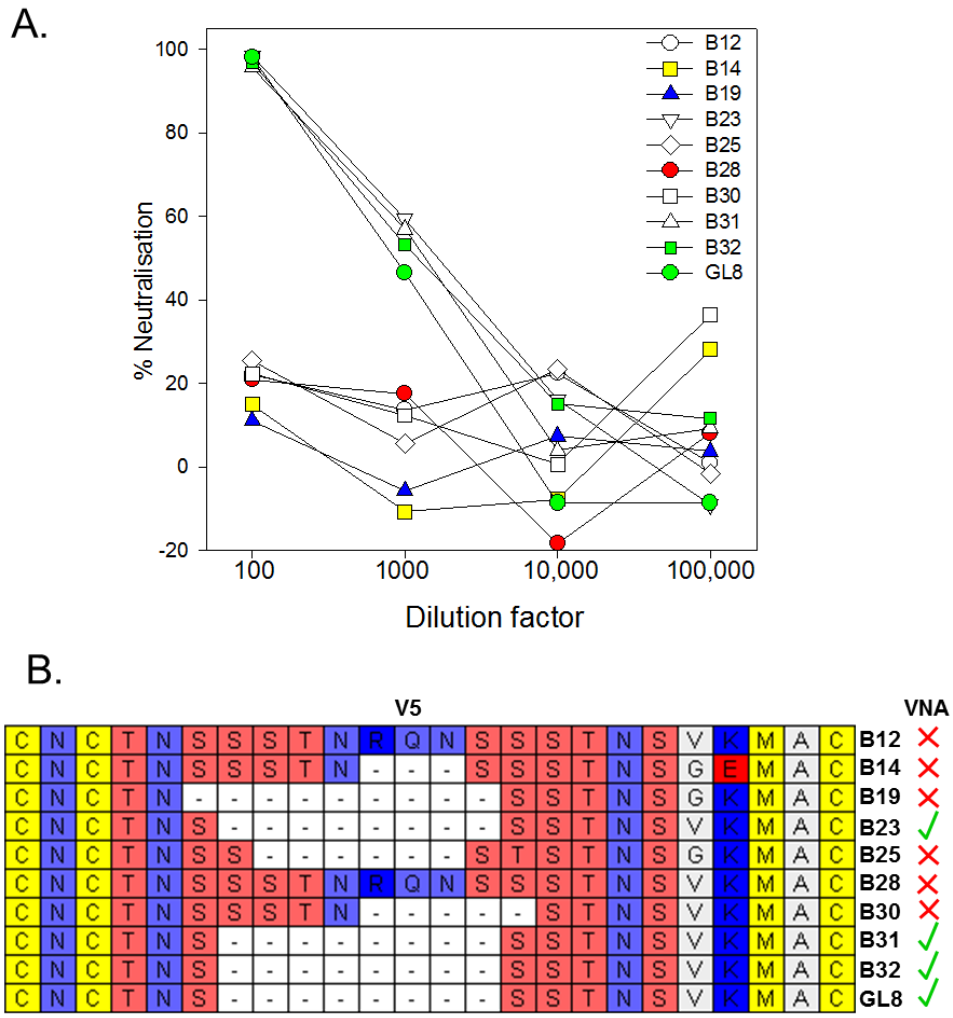


**Figure 3-12. Sensitivity of A613 derived viral variants to neutralisation by homologous plasma correlates with variability in V5 loop of Env.**

A. HIV(FIV) pseudotypes bearing the Env of the indicated variants were incubated with dilutions (1:100, 1:1000, 1:10000, 1:100000) of the post-mortem plasma of cat A613. Subsequently virus was added to CLL-CD134 cells and luciferase activity determined 72 hrs p.i. Values represent triplicate measurements and are presented as percent neutralisation relative to no plasma control. Experiment was performed at least twice. B. Amino acid sequence alignment of the V5 region of indicated viral variants. Amino acids are colour coded by chemical properties: acidic (red), basic (dark blue), hydrophobic (white), sulphur-containing (yellow), hydroxyl (pink) or amido (light blue). Isolates sensitive to virus neutralising AB (VNA) are indicated by a tick, while resistant variants are marked by a cross. Adapted from (Willett et al., 2010).

We compared the amino acid sequences of the isolates and FIV-GL8 to identify residues responsible for the resistance. Even tough, we failed to detect single amino acid changes accountable for the protection, we noted a strong correlation between the length polymorphisms in V5 and the resistance to neutralisation. All variants carrying insertions (B12, B14, B25, B28 and B30) or deletions (B19) in V5 were protected from

NAb, whereas isolates displaying V5 sequences identical to that of FIV-GL8 (B23, B31 and B32) were neutralised efficiently (Figure 3-12B). This data suggests that the V5 loop might be a main immunogenic target for the humoral immune response and that V5 directed NAb may drive the evolution of escape mutants in FIV infection.

### *3.3.1.9. Exchange of V5 loop confers resistance to neutralising antibodies*

All sequences carrying deletions or insertions in V5 had proven insensitive to neutralising antibodies from cat A613. We sought to analyse if V5 was the sole determinant for this protection. Therefore, a FIV-GL8 mutant termed GL8-ABSN, was generated that encoded unique non-coding digestion sites in the *env* gene allowing the individual exchange of a region comprising the V4 and V5 loop. Next, chimeric *env* sequences were constructed by exchanging the V4-V5 region of GL8-ABSN with the analogous sequences (nts. 1366-1848 of *env* gene) of isolates B14, B19 and B28. HIV(FIV) pseudotypes carrying the chimeric Env proteins were prepared and used in a neutralisation assay against PM plasma of cat A613. The GL8-ASBN mutant displayed neutralisation sensitivity comparable to wild-type GL8, confirming the integrity of the amino acid sequence following mutagenesis.

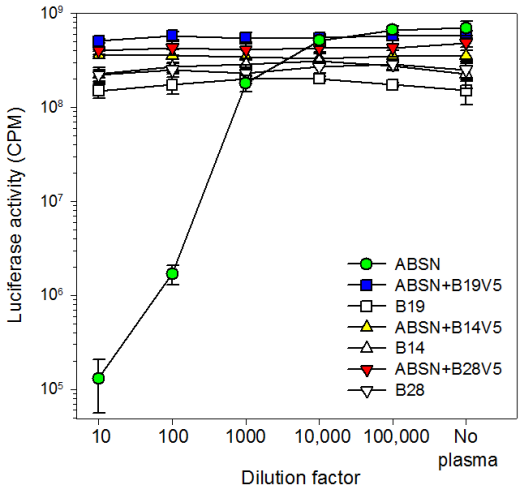


**Figure 3-13. Resistance to neutralisation by homologous plasma can be transferred by exchange of V5 loop.**

Neutralisation of FIV-GL8 encoding synonymous mutations in Env (GL8 "ASBN") that introduced restriction sites enabling the exchange of regions encompassing the V4/V5 loop was compared to neutralisation of variants B14, B19 and B28 or to chimeric Env in which the V4/V5 region of ASBN had been replaced by the analogous regions of B14, B19 and B28. HIV(FIV) pseudotypes bearing the indicated Env were incubated with dilutions (1:100, 1:1000, 1:10000, 1:100000) of PM plasma of cat A613 and plated onto CLL-CD134 cell. Luciferase activity was determined three days p.i. Each point resembles mean of triplicate (+/- standard error) and is representative for at least two independent experiments. Adapted from (Willett et al., 2010).

In contrast, the exchange of V4-V5 sequences of GL8-ABSN with the corresponding regions of variants B14, B19 or B28 resulted in resistance to neutralisation by the PM plasma. Given that these viral variants did not contain mutations in their V4 loop and only differed in their V5 sequences, the V5 region appears to be the main target of NAb in the PM plasma of cat A613.

### *3.3.1.10. Receptor interaction of FIV chimeras*

We next assessed whether mutations in the V5 loop influenced the virus-receptor interaction. We compared the sensitivity of GL8-ASBN and chimeric GL8-ASBN, carrying the V4-V5 sequences of isolates B14, B19 or B28, to inhibition by anti-CD134 antibody, soluble CD134 or CD134 ligand. In good agreement with our previous assays (Figure 3-10), HIV(FIV) pseudotypes bearing the reference GL8-ASBN Env displayed a low sensitivity to 7D6 (Figure 3-14A), while being strongly inhibited by sFcCD134 (Figure 3-14B). In contrast, the B14 Env conferred a reversed phenotype and rendered the pseudotypes highly sensitive to 7D6 and largely resistant to sFcCD134. Interestingly, chimeric GL8-ASBN, containing the V4-V5 region of B14, exactly mirrored the inhibition curves of variant B14, suggesting a strong contribution of the V5 loop to the enhanced sensitivity to 7D6 and the decreased sensitivity to sFcCD134. The Env of isolate B14 rendered pseudotypes comparably sensitive to CD134 ligand (Figure 3-14 C), yet the substitution of B14 V4-V5 failed to fully confer such phenotype onto GL8-ASBN.

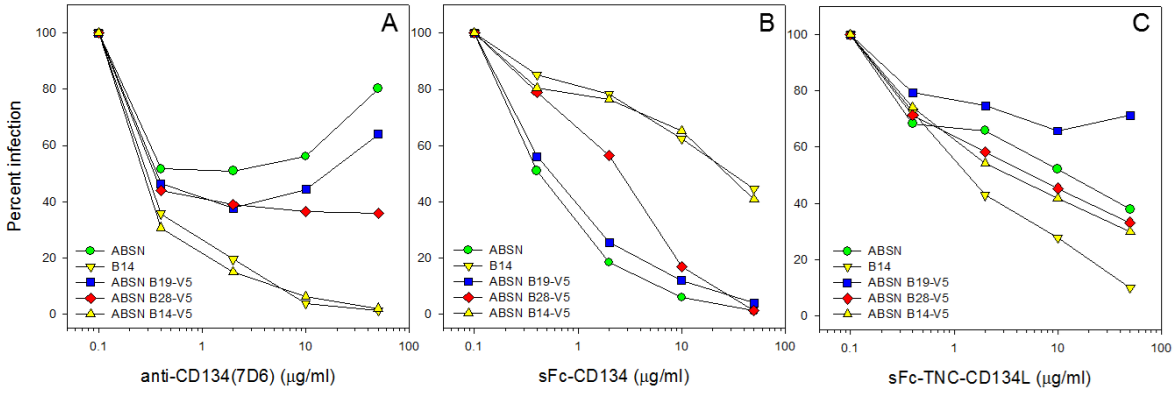


**Figure 3-14. Sensitivity of FIV-GL8-V5 mutants to antagonists of the virus-receptor interaction.** Sensitivity to antagonism by anti-CD134 antibody (A), soluble CD134 (B) and CD134 ligand (C) was compared between GL8-ASBN, B14 and chimeric ASBN encoding the V4-V5 loop of variants B14, B19 and B28. HIV(FIV) pseudotypes were added to Mya-1 cells pre-incubated with the indicated concentration of inhibitors. Each point indicates mean of three replicates and is expressed as percent infection relative to no inhibitor control. Each graph is representative of at least two individual experiments. Adapted from (Willett et al., 2010).

The influence of the B28 and B19 derived V4-V5 regions was less marked. Similar to B14, variant B28 had displayed an enhanced sensitivity to 7D6 and reduced sensitivity to sFcCD134 (Figure 3-10). The substitution of the B28 V4-V5 region into GL8-ASBN recapitulated this phenotype, yet compared to the B14 V4-V5 the effect was more marginal, suggesting that additional regions outside the V5 loop may account for the B28 phenotype. The exchange of the B19 V4-V5 region did not considerably alter the phenotype of GL8-ASBN, which is consistent with similar properties of B19 and GL8 in our previous assays using receptor antagonists (Figure 3-10). These data suggests that changes in the V5 loop that allow evasion from NAb may strongly influence the nature of the Env-receptor interaction.

## 3.3.2. Analyses of thymus-derived FIV from long-term infected cat A613

### *3.3.2.1. Genotype of thymus-derived FIV from cat A613*

The tissue analysis of cat A611 had displayed proviral sequences within the thymus that substantially differed from PBMC-derived sequences (Figure 3-4), indicating that viral evolution in thymus is subjected to different constrains than in the blood stream or other tissues. Since we had investigated the phenotypical properties of PBMC-derived variants from cat A613 extensively (see 3.2.1) we next wanted to examine isolates from the thymus of this cat. However, we failed to amplify virus using our LD-PCR protocol and had to use undiluted genomic thymus DNA for bulk amplification and subsequent cloning. We then sequenced the V5 loop of several clones to identify unique sequences carrying insertions or deletions of various lengths. Using this approach we managed to amplify seven unique full length *env* sequences from the thymus of cat A613. The *env* genes were aligned to *env* sequences derived from PBMCs of cat A613 (see 3.1.2.) and a ML tree was estimated using MEGA5 and the HKY+G+I model of substitution (Figure 3-15). Similarly to the sequences originating from PBMCs, where four isolates (613PM14) were identical to FIV-GL8, the thymus samples also included one variant (Thy7) indistinguishable from FIV-GL8. Analogous to virus isolated from cat A611 (Figure 3-4) we noted that PBMC derived virus from cat A613 had diverged further away from the parental virus FIV-GL8 than sequences originating from the thymus. Furthermore, we noticed the separate clustering of three thymus samples (Thy3, 5 and 6). However, in contrast to the sequences isolated

from A611 there was also some intermingling of thymus and PBMC derived sequences in cat A613, e.g. Thy1, 2, 4 and 613PM3, 9 clustered together. Yet, the majority of PBMC sequences did not appear to be closely related to virus isolated from the thymus which mirrors our results from cat A611. It should be noted that sequences Thy1 and Thy2 differ only by the length of their V5 insert, but as the pairwise comparison algorithm during tree estimation does not take into account insertions these two sequences appear as identical on the tree (Figure 3-15).

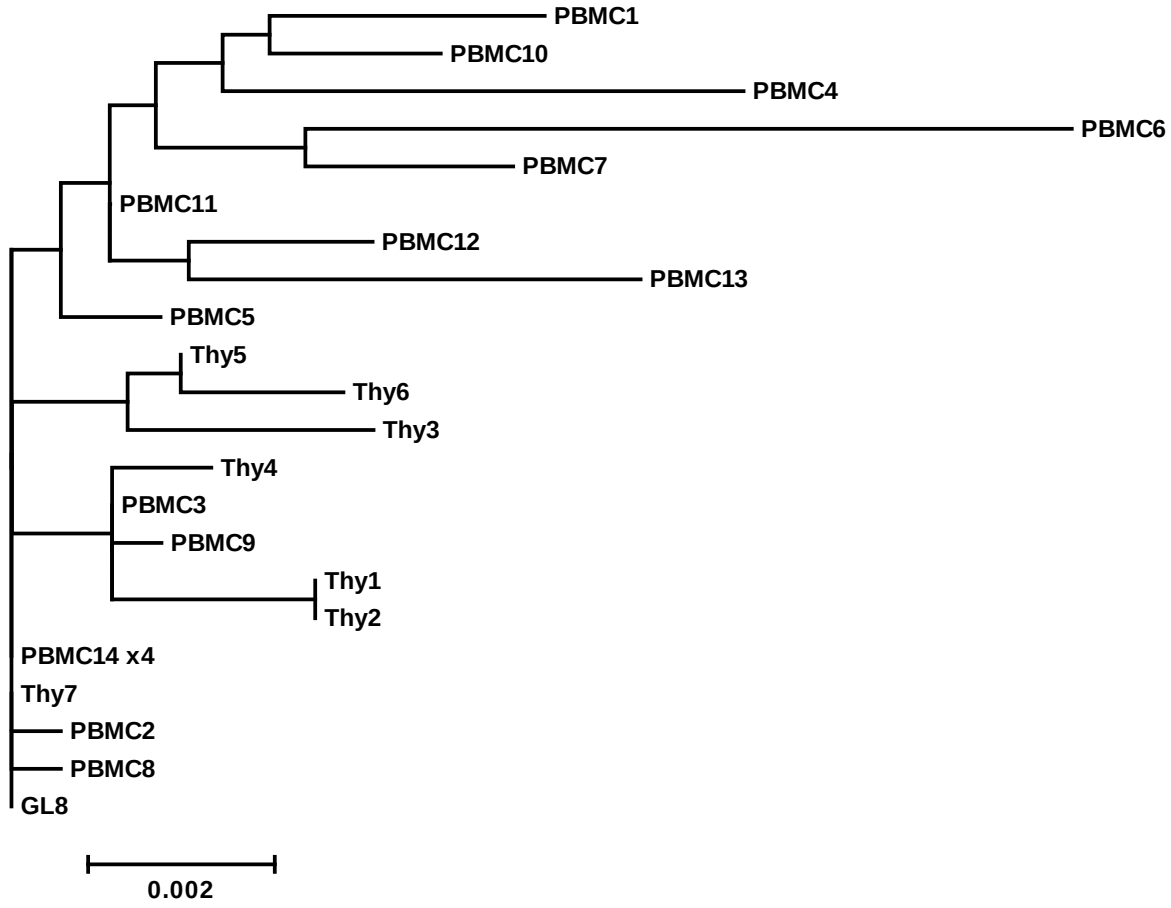


**Figure 3-15. Phylogenetic Maximum likelihood (ML) tree of PBMC and thymus-derived *env* sequences.** Proviral *env* sequences were derived from PBMCs (see 3.1.2) and thymus of cat A613 at 322 weeks p.i. The unconstrained ML tree was estimated in MEGA5 using the HKY+G+I model of substitution. The tree is rooted on the infecting strain FIV-GL8. Repeated sequences are followed by an "x" and the number of repeats. Abbreviations: peripheral blood mononuclear cell, PBMC; thymus, Thy.

By comparing amino acid sequences between thymus-derived samples from cat A611 (Table 3-5) and A613 (Table 3-8) we aimed to identify mutations that would be typical of the thymus. We found four residues that appeared to be overrepresented. An I/M mutation at position 360 was present in five out of six thymus samples (but in no other tissue) from A611 and was mutated in Thy3 from A613 although with a different

substitution (I/R). Furthermore, a G431E mutation was present in Thy1 and Thy2 from cat A613 and in all thymus samples from A611, yet it also occurred in the tonsil (4/5), large intestine (2/3) and PBMCs (2/18) of that cat. Moreover, a V655M mutation in gp41 was found in all thymus and two tonsil samples from A611 (but no other tissue) and was present in Thy1, Thy2 and Thy4 of cat A613 but also occurred at low frequency in PBMCs (2/18). The V5 loop appeared to carry a thymus signature since insertions appeared in thymus-derived virus of both cats (but not in the PBMCs of A611), however, insertions in the V5 loop also occurred in PBMCs of cat A613.

**Table 3-8. Mutations of the Env protein in thymus-derived variants of cat A613**

| Location[a] | AA position[b] | GL8[c] | Thy1[d] | Thy2[d] | Thy3[d] | Thy4[d] | Thy5[d] | Thy6[d] | comment[e] |
|---|---|---|---|---|---|---|---|---|---|
| V1/V2 | 268 | A | D | D | | | | | charge 1- |
| C3 | 360 | I | | | R | | | | charge 1+ |
| V3 | 397 | R | | | G | | | | charge 1- |
| | 431 | G | E | E | | | | | charge 1- |
| V5 | 555 | T | +NSTNST | +NST | +NSSST | | +NSSST | +SRQNSSST | ins. N-x-S/T |
| | 557 | S | | | | - | | | |
| | 558 | V | | | G | | | | |
| | 559 | K | | | E | E | | E | charge 2- |
| gp41 | 648 | H | | | N | | N | N | charge 1- |
| | 655 | V | M | M | | M | | | |
| | 680 | V | | | | | | L | |

[a] Location in *env* gene equivalent to variable loop (V) and conserved region (C) of HIV *env*.
[b] Amino acids are numbered from the first methionine of the *env* ORF.
[c] Amino acid present in FIV-GL8 at the indicated position.
[d] Substituted amino acids are shown. Insertions and deletions are indicated with +/- followed by the amino acids.
[e] Mutations that altered the charge of the protein or led to an insertion of potential N-glycosylation sites (N-x-S/T).

Next, we investigated the phenotypic properties of the thymus derived samples. The *env* sequences had been cloned into the molecular clone of FIV-GL8, pGL8-Mya and were used for the transfection of HEK293T cells and subsequent infection of Mya-1 cells utilising the virus containing supernatant. All *env* genes proved functional as p24 ELISA indicated productive infection (data not shown).

### *3.3.2.2. Receptor usage of thymus derived FIV*

The thymus expresses relatively little CD134 (Willett et al., 2007). We therefore wished to investigate how the adaption to such environment impacts on the phenotype of the virus. Therefore, we tested the receptor usage of each of the thymus isolates. HIV(FIV) pseudotypes bearing the Env of thymus-derived variants or control strains FIV-

GL8 and FIV-B2542 were used for the infection of MCC cells expressing either the human or feline CD134 or the chimeric feline CRD1 x human CD134 receptor. Three variants (Thy1, Thy2 and Thy4) displayed a CRD1-dependent interaction with feline CD134 and were able to infect MCC cells expressing a chimeric receptor comprising feline CD134 CRD1 in the context of human CD134 (fCD134xhuCD134) at a similar efficiency as late stage infection isolate FIV-B2542 (Figure 3-16). Variant Thy7 resembled the phenotype of FIV-GL8 closely, being unable to utilise the chimeric fCD134xhuCD134 receptor, which was expected as both viruses shared the same sequence.

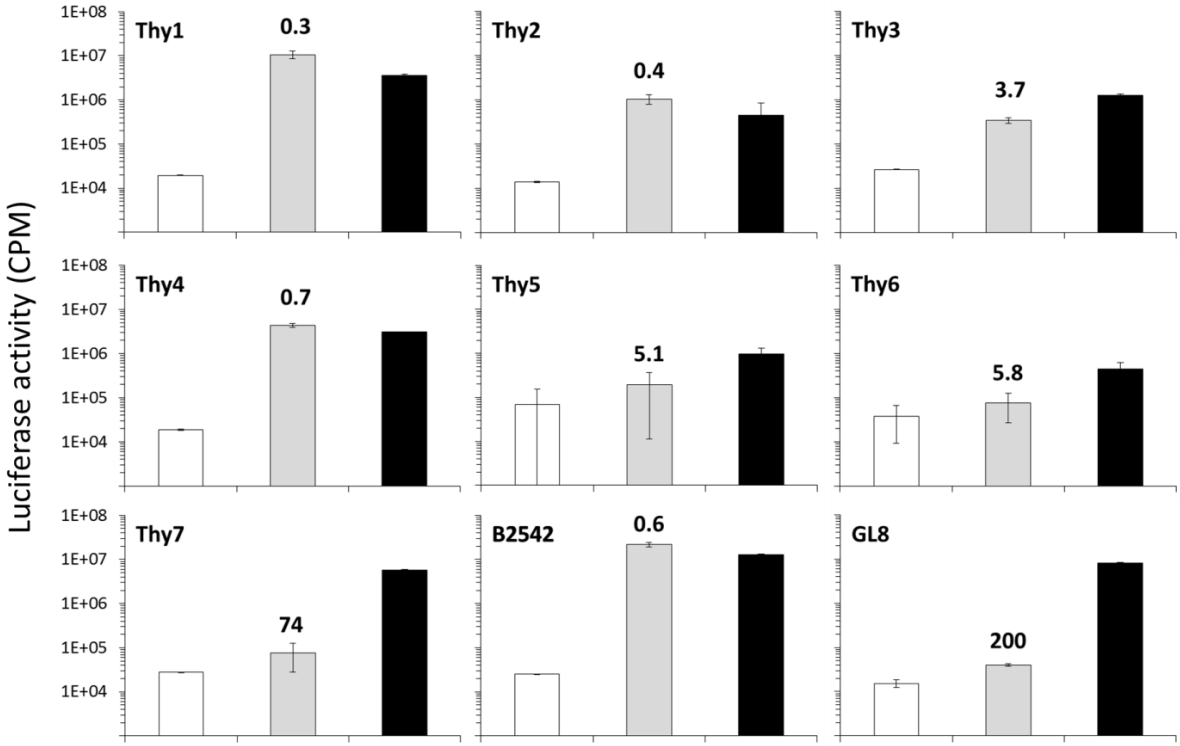


**Figure 3-16. Receptor usage of thymus-derived Env isolates from cat A613.**
MCC cells stably expressing human CD134 (white bars), a feline CRD1 x human CD134 chimaera (grey bars) or feline CD134 (black bars) were infected the HIV(FIV) pseudotypes bearing Env proteins from variants originating from the thymus of cat A613. Luciferase activity was quantified 72 hrs post-infection. The ratios of CPM on cells expressing feline CD134 divided by counts on cells expressing chimaeric CD134 are indicated in the graph. For controls FIV strains GL8 and B2542 were used. Each value represents the average of triplicate infection of a single experiment. Error bars indicate standard deviation.

Variants Thy3, Thy5 and Thy6 displayed a somewhat intermediate phenotype. Interestingly, Thy1, Thy2 and Thy4 had formed a cluster on the ML tree (Figure 3-15) that was distinct from the group formed by Thy3, Thy5 and Thy6. Investigation of amino acid differences between these groups proved little informative. The only mutations that distinguished these two groups of viruses lay within the TM domain. Thy3, 5 and 6 carried

a H648N mutation while variants Thy1, 2 and 4 displayed a V655M substitution. All other mutations were shared by both groups or were not present in all members of one group. Furthermore the V5 loop insertions differed in between isolates making it difficult to predict which mutation might have influenced the outcome of the receptor usage assay.

### *3.3.2.3. Sensitivity of thymus derived FIV to neutralising antibodies*

We have previously demonstrated that PBMC derived variants from cat A613 that carried a length polymorphism in V5 were resistant to neutralisation by homologous plasma (Figure 3-12). We next wanted to investigate if this general phenomenon also granted protection to the thymus derived isolates. We compared the sensitivity of HIV(FIV) pseudotypes bearing the thymus derived Env variants to neutralisation by the A613 PM plasma (Figure 3-17). Only one isolate (Thy7) was neutralisation-sensitive, which was expected as its sequence was identical to the infecting strain FIV-GL8. All other isolates resisted neutralisation. Since these variants carried insertions and deletions of various lengths in their V5 this experiment confirms our previous results in that a V5 length polymorphism appears to protected FIV from neutralisation by homologous plasma.

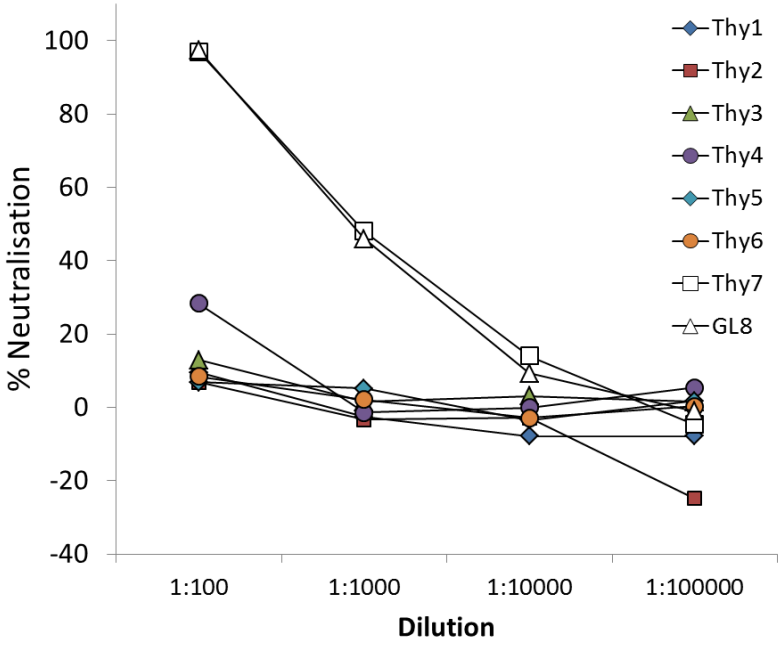


**Figure 3-17. Sensitivity of thymus-derived FIV to neutralisation by homologous plasma from cat A613.** HIV(FIV) pseudotypes bearing the Env of variants isolated from the thymus of cat A613 were incubated with the indicated dilution of homologous plasma before virions were applied to Mya-1 cells. 72 hrs post-infection luciferase activity was quantified. Each point represents the mean of triplicate infection of a single experiment. Values are expressed as percent neutralisation relative to no plasma control.

## 3.4. Infection of cats with an artificial quasispecies comprised of viruses from long-term infection

Having established the *in vitro* phenotype of selected PBMC derived viral variants (see 3.2.1) from cat A613, we next asked how the apparent evolution that certain isolates had undergone would impact on the viral phenotype *in vivo*. Cat A613 had been infected for six years but remained clinically healthy, thus in nature it would likely have engaged with other cats and may have transmitted FIV. Natural transmission of FIV infection usually occurs by biting and most likely allows the transfer of quasispecies rather than of single viral variants. Hence, we decided to compare the *in vivo* infectivity of an artificial quasispecies, consisting of six distinct variants isolated from A613, with infectivity of a clonal preparation of the parental virus FIV-GL8 (identical to B32). To account for FIV-GL8-like viruses that were still detectable in cat A613 at 322 weeks p.i. (see 3.2.1), we included variants B31 and B32 in the mixed inoculum. The remaining four viral variants comprising the artificial quasispecies showed characteristics of late stage virus displaying altered receptor utilisation (B14, B19, B28 and B30) and changes in their sensitivity to antagonists of the Env-receptor interaction (B14 and B28) (Figure 3-10, 3-18).

Would the altered receptor interaction of these variants allow the establishment of reservoirs more efficiently than with FIV-GL8-like virus or would differences in fitness between viruses lead to variants being outcompeted by others?

Two groups of cats comprising four animals each were infected with equal tissue culture infectious doses of 10,000. Infection of group 1 animals (822, 823 and 824) was carried out with a clonal preparation of B32 (identical to FIV-GL8), while group 2 animals (825, 826, 827 and 828) were infected with a mix containing equal amounts of the above mentioned variants so that total number of tissue culture infectious virus was equal to group 1. Infection proceeded for 21 weeks and blood samples were taken at defined time points and post-mortem.

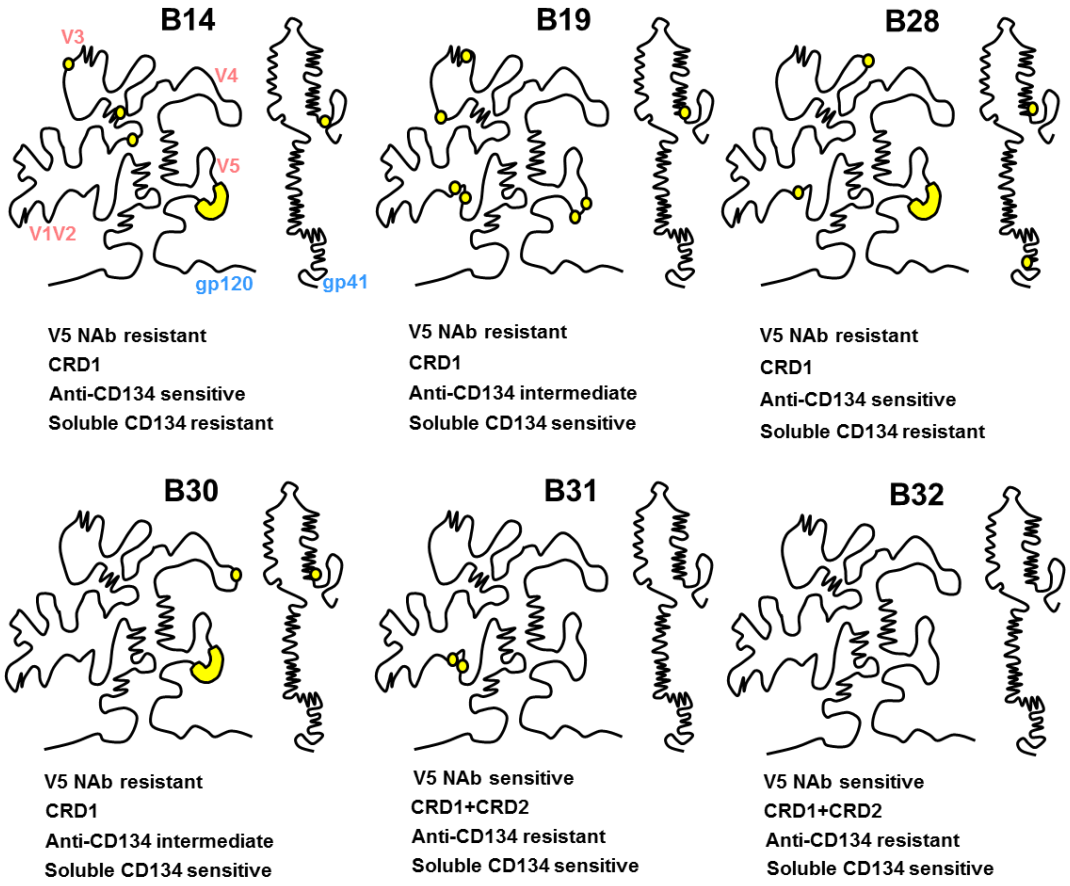


**Figure 3-18. Location of non-synonymous mutations on Env proteins of variants comprising the artificial quasispecies.**

Schematic representation of gp120 and gp41. Yellow circles indicate single mutations, yellow stretches areas of multiple changes. Each Env is characterised by i) its sensitivity to neutralisation by homologous plasma, ii) dependency on simple (CRD1) or complex (CRD1+CRD2) domains on CD134 for successful infection, iii) sensitivity to inhibition by anti-CD134 antibody or iv) soluble CD134 receptor. Adapted from (Willett et al., 2013).

## 3.4.2. CD4:CD8 ratio

We first analysed numbers of CD4+ and CD8+ cells in both FIV infected groups and a group of age-matched uninfected animals. Following infection a significant decrease in the CD4:CD8 ratio was apparent in both groups as compared to control animals (Figure 3-19). However, no statistically significant differences in CD4:CD8 ratios between group 1 and group 2 were detected at any time point that was analysed.

The reduced CD4:CD8 ratios resulted from a decrease in CD4+ cells and an expansion of the population of CD8+ cells as has been reported previously (Willett et al., 1993). A continuous decline in numbers of CD4+ cells was apparent in group 1, leading to approx. 40% reduction by week 21. Animals in group 2 also displayed a decrease in CD4+ T cell numbers by week 21, however, the reduction was less dramatic. The percentage of

CD8+ T cells clearly increased from 3 weeks p.i. onwards and had almost doubled in both FIV infected groups by 12 weeks p.i. However, at subsequent time points numbers of CD8+ cells in group 1 declined to levels of the control group, while the percentage of CD8+ cells in group 2 remained elevated. Thus, even though CD4:CD8 ratios were almost identical for both groups, infection with clonal FIV-GL8 led to a strong reduction in CD4+ cells while inducing a transient increase in CD8+ cells, whereas inoculation of animals with the quasispecies resulted in a mild decrease of CD4+ cells and a sustained expansion of CD8+ cells.

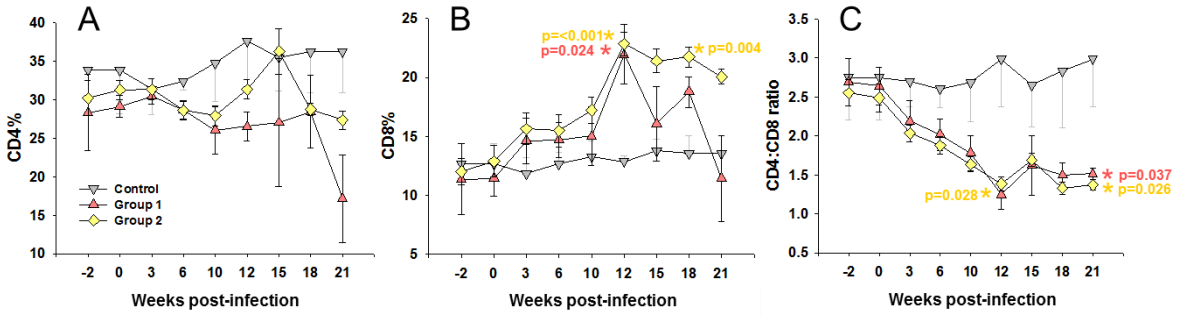


**Figure 3-19. Variation in CD4+ and CD8+ lymphocyte population following FIV infection.**
Group 1 animals had been challenged with clonal FIV-GL8 (B32), whereas cats in group 2 had been inoculated with a reconstituted quasispecies comprising variants B14, B19, B28, B30, B31 and B32, while control cats remained unchallenged. PBMC derived CD4+ (A) and CD8+ (B) lymphocyte subsets were analysed by flow cytometry and the CD4:CD8 ratio (C) calculated. All values are group means +/- standard error. Statistical significant differences between infected and uninfected control groups are indicated by p-values (Student's t-test). Adapted from (Willett et al., 2013).

## 3.4.3. Total proviral load

Next we quantified proviral loads in PBMCs of group 1 and 2 animals. For the generation of the inoculum the *env* variants had been cloned into the pGL8-Mya vector, hence, the *gag* gene of each virus preparation was identical. We utilised a qPCR targeting a part of *gag* that had been found to be conserved among diverse FIV strains previously (Klein et al., 2001), thus, alterations to this sequence during the course of infection seemed unlikely.

Comparison of the area under the curve for the 21-week infection period revealed no significant difference between group 1 and 2; in both groups viral titres were detectable as early as 3 weeks post-infection and plateaued at 10 weeks p.i. (Figure 3-20A). However, cats infected with the clonal preparation of B32 (FIV-GL8) generally achieved higher viral titres (plateau at ~$8x10^4$ copies per $10^6$ cells) than cats receiving the

quasispecies preparation (plateau at ~3x$10^4$ copies per $10^6$ cells). The only exception to this occurred three weeks post-infection when proviral load in group 1 was lower than in group 2.

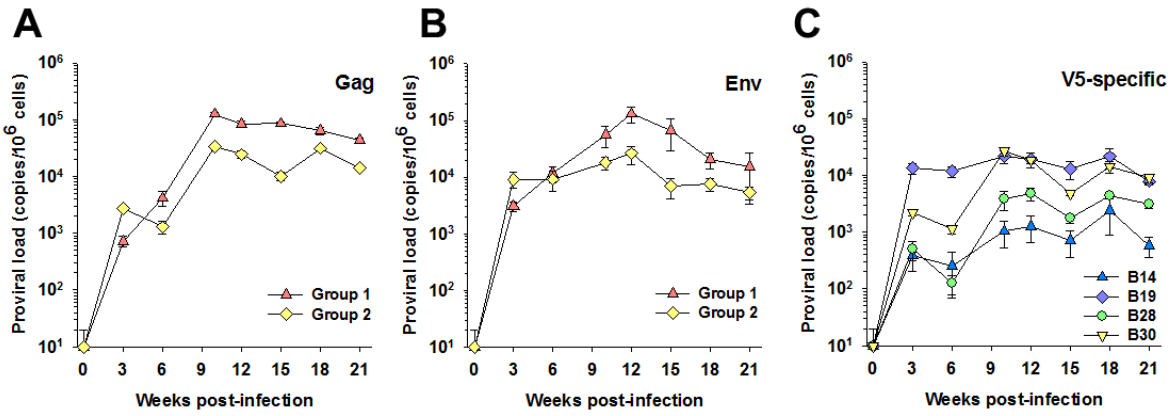


**D**

| Virus | V5 sequence | No. of clones | | | | |
|---|---|---|---|---|---|---|
| GL8 | C T N S S S T N S V K M A C | 825 | 826 | 827 | 828 | % |
| GL8 | TGTACAAATAGTAG TAGTACAAATAGTGTTAAAATGGCATGT | 48 | 45 | 34 | 52 | 84 |
| GL8v1 | TGTACAAATAGTAG TAGTACAAATAGTGCTAAAATGGCATGT | 0 | 0 | 6 | 0 | 2.8 |
| GL8v2 | TGTACAAATAGTAG TAGTACAAGTAGTGTTAAAATGGCATGT | 0 | 0 | 2 | 0 | 0.9 |
| B14 ▲ | TGTACAAATAGTAGTAGTACAAA TAGTAGTAGTACAAATAGTGGTGAAATGGCATGT | 0 | 0 | 0 | 0 | 0 |
| B19 ◆ | TGTACAAATAGTAG TACAAATAGTGGTAAAATGGCATGT | 2 | 2 | 10 | 0 | 6.5 |
| B28 ● | TGTACAAATAGTAGTAGTACAAATCGGCAAAA TAGTAGTAGTACAAATAGTGTTAAAATGGCATGT | 0 | 1 | 1 | 0 | 0.9 |
| B28v1 | TGTACAAATAGTAG TACAAATCGGCAAAA TAGTAGTAGTACAAATAGTGTTAAAATGGCATGT | 0 | 0 | 1 | 0 | 0.5 |
| B30 ▽ | TGTACAAATAGTAGTAGTACAAA TAGTACAAATAGTGTTAAAATGGCATGT | 0 | 3 | 4 | 1 | 3.7 |
| B30v1 | TGTACAAATAGTAGTAGTACAAA TAGTACAAATAGTACAAATAGTGTTAAAATGGCATGT | 0 | 0 | 0 | 2 | 0.9 |
| | 1645 1686 | | | | | |

**Figure 3-20. Proviral loads in PBMCs following FIV infection.**
Mean proviral loads (+/-SE) were estimated in group 1 (clonal infection) and group 2 (quasispecies infection) using qPCRs specific for a conserved region in *gag* (A) and *env* (B). (C) Mean proviral loads (+/-SE) for individual variants (B14, B19, B28 and B30) in group 2 were quantified utilising qPCRs targeting unique sequences within the V5 of env. All proviral load estimations were performed in triplicate and normalised to 18S rDNA. (D) Alignment of variable V5 region (as analysed in C) amplified from animals 825, 826, 827 and 828 at 21 weeks post-infection. The region spanning nucleotides 1645-1686 of the corresponding FIV-GL8 sequence is shown and the predicted amino acid sequence of FIV-GL8 is indicated above. The number of clones of each variant is displayed and newly emerging V5 mutants of GL8, B28 and B30 are indicated. Adapted from (Willett et al., 2013).

To validate the findings obtained by *gag* specific qPCR, we extracted fresh genomic DNA from PBMCs of the infected cats and performed a second qPCR targeting a conserved stretch in *env*. The outcome of this totally independent analysis confirmed our previous results indicating higher proviral loads in group 1 except for blood samples taken at three weeks post-infection where proviral load in group 2 was raised (Figure 3-20B). These findings are consistent with the lower counts for CD4+ cells in group 1, which are indicative of a more pronounced infection.

In summary, even though equal amounts of virus, as calculated by TCID50, had been administered to the cats of both groups, the *in vivo* replication of the quasispecies in group 2 appeared impaired.

## 3.4.4. Proviral load of FIV-V5 mutants

We next asked whether the lower proviral load in group 2 was due to weaker replication of the quasispecies *per se* or if single variants within the quasispecies replicated less well than others. Although the mixed variants used in group 2 were highly similar, the length polymorphism in V5 allowed the estimation of individual proviral loads by qPCR. We were able to establish four selective qPCRs, targeting V5 of variants B14, B19, B28 and B30 (Figure 2-1). Unfortunately it was not feasible to selectively quantify proviral loads of B31 and B32 using the V5 region due to non-specific amplification of the remaining variants.

Throughout the infection, B19 and B30 achieved highest titres levelling off at ~$10^4$ copies per $10^6$ PBMCs (Figure 3-20C). Variant B19 reached its plateau as soon as three weeks post-infection, while B30 did not achieve peak titres until 10 weeks post-infection, indicating a slightly impaired replication. More strikingly, despite matched doses of all viruses in the inoculum, variants B28 and B14 achieved significantly lower proviral loads (~$3x10^3$ copies per $10^6$ PBMCs for B28 and ~$1x10^3$ copies per $10^6$ PBMCs for B14) indicating some replicative disadvantage.

Given the high specificity of V5 qPCRs detecting B28 and B30 (see Material and Methods), estimates for these variants are most likely to be accurate. The qPCRs for B19 and B14 were more prone to false amplification of competing templates. Yet, the total proviral load as estimated by *gag* specific PCR suggested viral copy numbers too low to interfere with specific amplification of B19 and B14. Thus quantification of B19 and B14 is likely reliable. Nevertheless, during the 21 week period of infection, the variants may have acquired mutations in their V5 sequences that may have impacted on the outcome of the qPCR analysis. To assess the emergence of mutations in V5 and to confirm the reliability of the qPCR results we amplified V5 sequences from PBMCs extracted post-mortem from group 2 animals. The amplicons were cloned and their nucleic acid sequences determined. The majority of amplicons were identical to the V5 regions of the input viruses, only 11 out of 214 showed variations in their nucleotide sequence (Figure 3-

20D). GL8-like variants (B31, B32 and two additional closely related variants found in cat 827, GL8v1 and GL8v2) were most abundant; accounting for 88% of the population, indicating that by week 21 p.i. isolates identical or similar to FIV-GL8 were predominant in the blood of group 2 animals. Variant B19 was present in 6.5 % of analysed clones, followed by B30 with a frequency of 4.6 %. Analysis of proviral load using V5 specific qPCR had revealed significantly lower titres for variants B28 and B14 (Figure 3-20C) and indeed B28 could be identified only three times by direct sequencing, while B14 was absent from this analysis, correlating with lowest titres as detected by qPCR. Overall the sequencing data is in good agreement with the qPCR results, confirming an impaired replication of variants B14 and B28 *in vivo*.

### 3.4.5. Humoral immune response

Cat A613 had mounted a strong NAb response against FIV-GL8 (Figure 3-12), that probably led to the emergence of the V5 escape mutants (Figure 3-13). Hence, a humoral immune response against B14 and B28 in group 2 animals could possibly be responsible for the impaired replication of these variants. However, given the lower proviral loads of B14 and B28 evident as early as three weeks p.i. it appeared rather unlikely that NAb would be involved in the restriction of these variants. To assess whether a humoral immune response contributed to the impaired replication of variants B14 and B28, we first confirmed the existence of antibodies binding to viral proteins.

Western blots were prepared from FIV-GL8, pelleted by ultracentrifugation from supernatant of infected Mya-1 cells, and probed with sequential plasma samples of group 1 and 2 animals (Figure 3-21). The capsid protein was recognised by plasmas of all cats as early as 3 weeks p.i., while sero-activity to the matrix protein developed between week 3 and 6. Antibodies to the Env protein emerged later but were detectable in most cats by week 10 to 12.

We next tested the efficiency of these plasmas to neutralise HIV(FIV) pseudotypes bearing the Env of FIV-GL8 or variants. Plasma samples of group 1 animals failed to neutralise particles carrying FIV-GL8 Env, while the control plasma from cat A613 reduced viral infectivity efficiently (Figure 3-22). Efficiency of the humoral immune response increases during prolonged infection, thus the cats may have mounted an early weak NAb response that may have been overcome by the high amount of viral particles used in the

assay. To account for this possibility the neutralisation assays were performed with 10 and 100-fold reduced viral input, but still no neutralisation could be detected (data not shown).

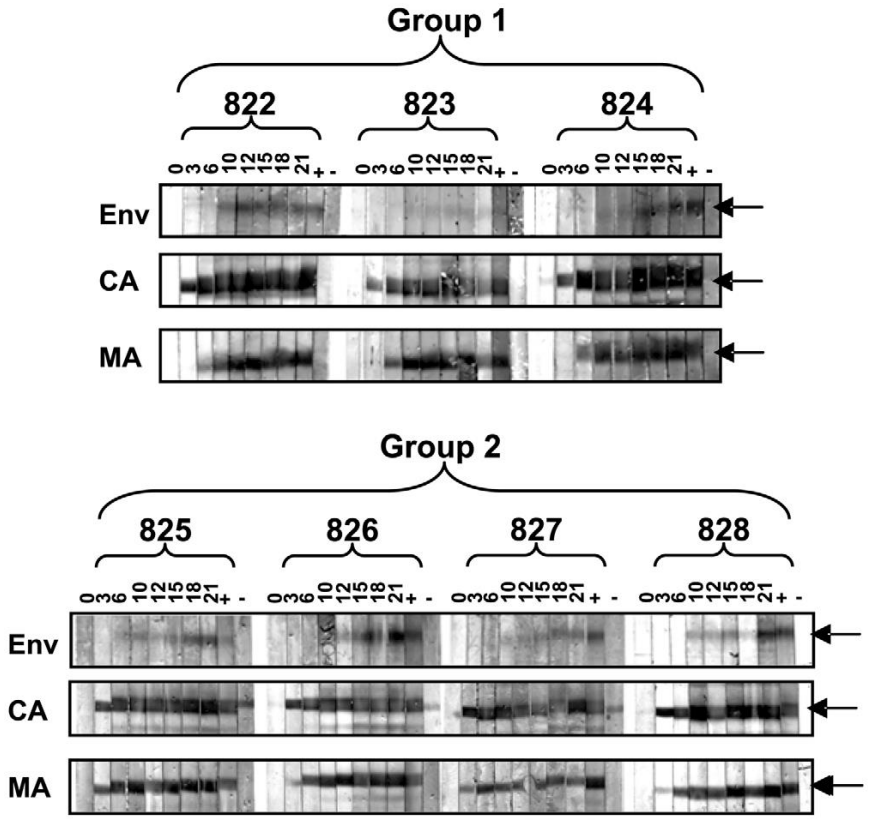


**Figure 3-21. Development of antibodies response following FIV infection.**
Western blot from purified FIV-GL8 was probed with plasmas from group 1 and 2 animals collected at 0, 3, 6, 10, 12, 15, 18 and 21 weeks post-infection or positive (+) or negative (-) control plasmas. Arrows indicate bands corresponding to envelope glycoprotein (ENV), capsid (CA) and matrix (MA) protein. Adapted from (Willett et al., 2013).

Next we analysed the efficiency of group 2 plasmas to neutralise each viral variant. The A613 control plasma reduced infectivity of B31 and B32 approx. 100-fold, but was ineffective against B14, B19, B28 and B30, confirming our earlier results (Figure 3-12). As noted with group 1, no neutralising antibody response to any of the viral variants could be detected using sequential plasma samples from group 2 animals (Figure 3-23 right panel). And again the plasmas failed to reduce infectivity of 100-fold diluted viral particles (data not shown). The V5 specific qPCRs of individual variants in group 2 cats had revealed lowest proviral loads for B14 and B28 in each cat (Figure 3-23 middle panel), yet these results did not correlate with the humoral immune response. Thus our data does not support a contribution of NAb to the impaired replication of B14 and B28.

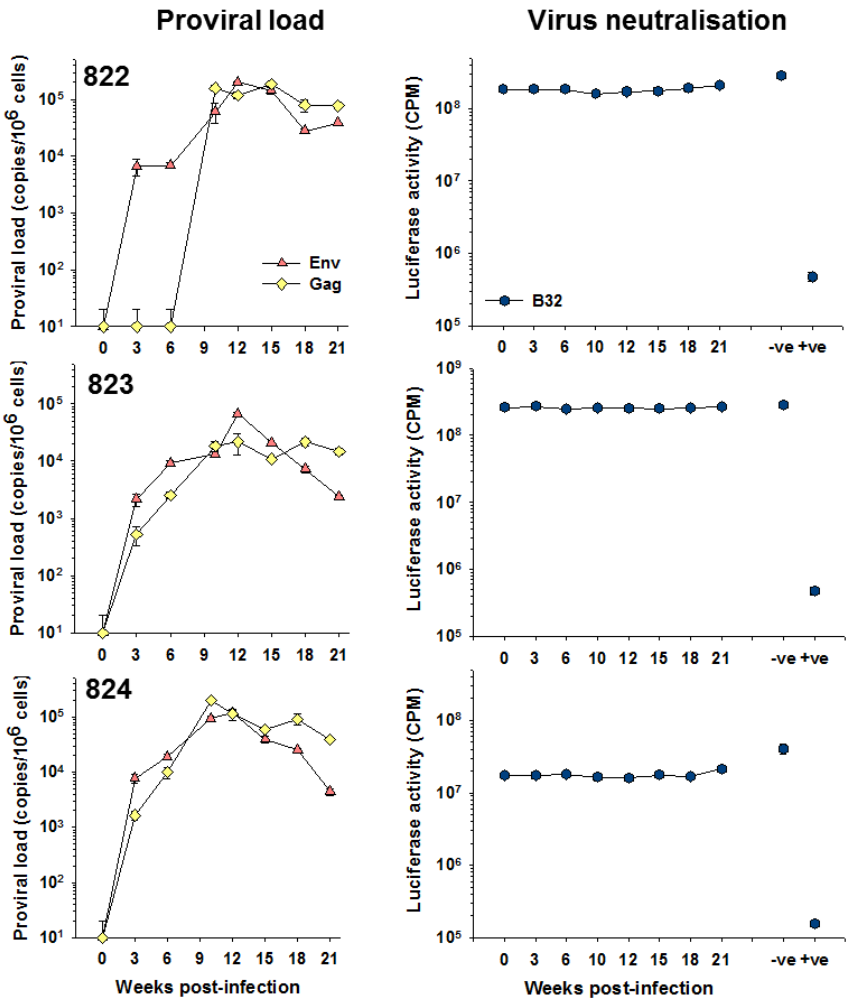


**Figure 3-22. Proviral load and NAb response following clonal infection with FIV-GL8 (group 1).**
Left panel: Proviral loads in individual group 1 animals (822, 823 and 824) were estimated by *gag* and *env* specific qPCR. Right panel: HIV(FIV) pseudotypes bearing the B32 (FIV-GL8) Env were incubated with 1:100 dilutions of sequential plasma (collected at 0, 3, 6, 10, 12, 15, 18 and 21 weeks post-infection) from infected group 1 cats or control plasma from cat A613 collected post-mortem (+ve) or pooled plasma from unchallenged cats (-ve). Subsequently, pseudotypes were applied to MYA-1 cells and luciferase activity quantified 72 hrs p.i. All estimations of proviral load and luciferase activity represent mean of triplicate (+/- standard error). Adapted from (Willett et al., 2013).

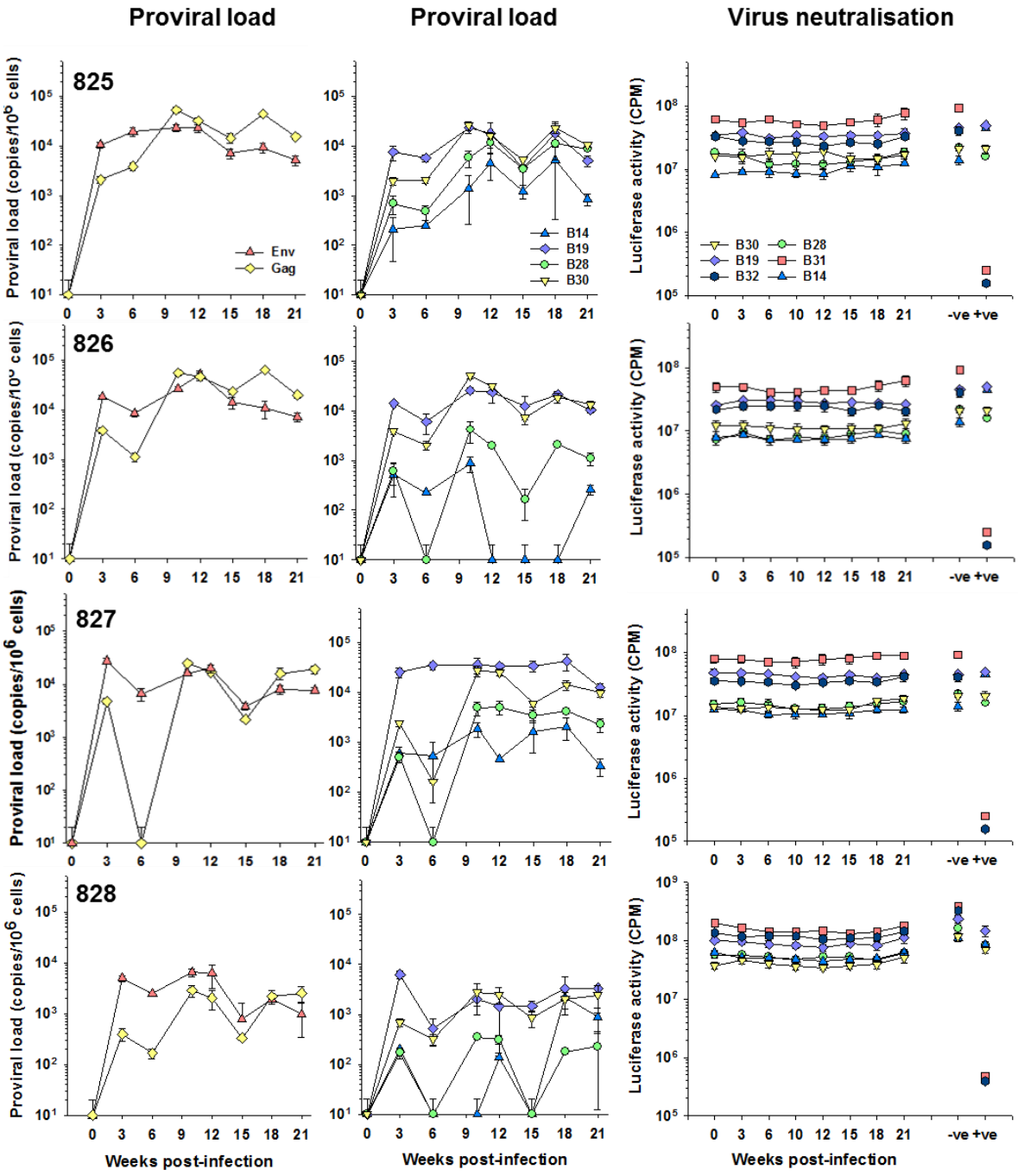


**Figure 3-23. Proviral load and NAb response following infection with artificial quasispecies (group 2).** Left panel: Total proviral loads in individual group 2 animals (825, 826, 827 and 828) were estimated by *gag* and *env* specific qPCR. Middle panel: Proviral loads of viral variants B14, B19, B28 and B30 in individual group 2 animals were estimated by V5 specific qPCRs. Right panel: HIV(FIV) pseudotypes bearing the Env of B14, B19, B28, B30, B31 or B32 were incubated with 1:100 dilutions of sequential plasma (collected at 0, 3, 6, 10, 12, 15, 18 and 21 weeks post-infection) from infected group 2 cats or control plasma from cat A613 collected post-mortem (+ve) or pooled plasma from unchallenged cats (-ve). Subsequently, pseudotypes were applied to MYA-1 cells and luciferase activity quantified 72 hrs p.i. All estimations of proviral load and luciferase activity represent mean of triplicate (+/- standard error). Adapted from (Willett et al., 2013).

### 3.4.6. Cellular immune response

During the acute phase of HIV and FIV infection a cellular immune response to the virus develops that is thought to contribute substantially to the restriction of viral replication. Furthermore, the induction of virus specific CD8+ T cells is rapid and may be detected prior to the detection of neutralising antibodies (Borrow et al., 1994; Koup et al., 1994; Wilson et al., 2000). Animals in group 1 and 2 displayed an increase in numbers of CD8+ T cells as early as 3 weeks p.i. (Figure 3-19), which may have represented a population of activated T cells responding to infection.

To assess whether the infected animals had mounted a FIV-specific cellular immune response, we performed ELISpot assays to detect interferon gamma (IFNy) production (Dean et al., 2004; Paillot et al., 2005) from lymphocytes extracted from popliteal (PLN) and mesenteric (MLN) lymph nodes, PBMCs or spleens collected from the infected cats post-mortem. Viral antigen was generated by treatment of FIV-GL8 with Aldrithiol™-2 (AT-2), which covalently modifies zinc finger residues in the viral nucleocapsid thereby inactivating the virus without disturbing the structural integrity of the Env protein (Rossio et al., 1998).

The IFNy responses displayed considerable inter-animal and inter-tissue variation (Figure 3-24). In group 1, animals 823 and 824 showed a strong activation of spleen-derived cells by viral antigen, while IFNy responses of PLN and PBMC samples were moderate and absent in MLN. In contrast, a high number of IFNy producing cells were detected in PBMC samples of cat 822 but only a weak activation of spleen-derived cells and no responses in PLN and MLN samples were noted. All animals that had received the mixed inoculum (group 2) displayed a moderate IFNy response in spleen and PBMC samples, while in PLN and MLN only a weak or no activation by viral antigen was noted. Solely samples derived from cat 826 revealed a high number of IFNy producing cells in MLN and PBMCs. Interestingly, proviral loads of B14 had been very low in animal 826 thus cellular immune response may have contributed to impaired viral replication in this cat.

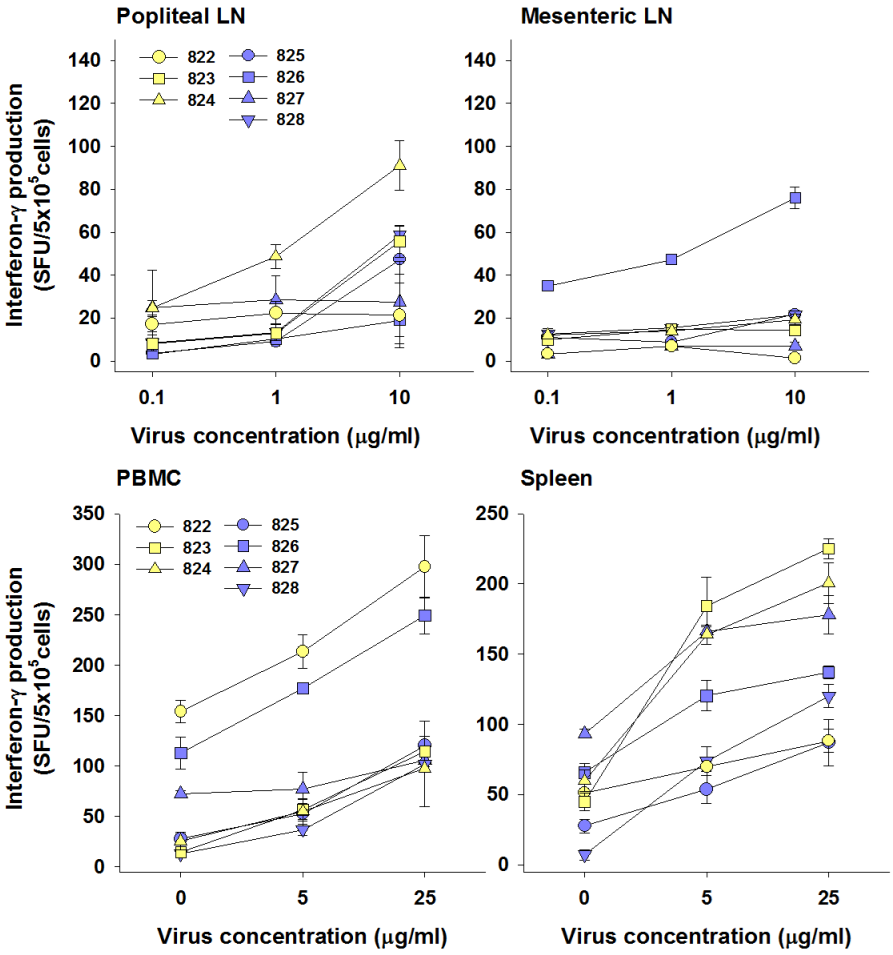


**Figure 3-24. Cellular immune responses in lymphoid tissues following FIV infection.**
PBMCs, spleen, popliteal and mesenteric lymph node were extracted at post-mortem from cats infected with clonal B32 (822, 823, 824) or an artificial quasispecies (825, 826, 827 and 828). IFNy production following incubation of T cells with AT-2-inactivated FIV-GL8 indicated T cell activation and was quantified by IFNy-ELISpot. Each value indicates triplicate measurement of spot forming units per 5x105 cells (+/- SE). Adapted from (Willett et al., 2013).

The efficiency of viral restriction by cellular immune responses may strongly depend on the epitopes recognised by the T cells. As all viral preparations used for the infection comprised identical *gag* and *pol* sequences we reasoned that any differences in the T cell response would be directed against the Env protein. Thus, we next asked whether the animals differed in the determinates on Env recognised by the cellular immune response. To map the T cell epitopes, spleen derived lymphocytes from group 1 and 2 animals were tested against 17 pools of 10 overlapping 15 amino acid long peptides, covering the entire Env protein. Following detection of an IFNy response to a peptide pool, single peptides comprising the respective pool were incubated with lymphocytes to fine map the epitopes.

Cellular responses to peptide pools generally were greater than to the virus preparation which probably was owed to the increased presentation of respective epitopes by the peptides. Each animal displayed IFNy responses to at least one peptide pool but mostly two pools were recognised. Within both groups the majority of cats differed in the peptide pools that induced an IFNy response, however several pools were recognised by cells from animals of different groups.

In group 1 (clonal infection), cells from animal 822 reacted to pools P8 and P9, cat 823 to pools P12 and P15, while lymphocytes from 824 responded solely to pool P14 (Figure 3-25). Among animals receiving the quasispecies inoculum (group 2) lymphocytes from 826 recognised three peptide pools P2, P10 and P14, cells from 827 reacted to pools P8 and P9, while 825 and 828 elicited a response to single pools P9 and P15, respectively.

Separation of pools into single peptides revealed epitopes consisting of stretches of successive peptides or single peptides. For example, responses to pool P8 by lymphocytes of animals 822 (group 1) and 827 (group 2) could be mapped to peptides G2-G5 (Figure 3-25), while the epitope in pool P14, recognised by cats 824 (group 1) and 826 (group 2) comprised a single peptide K11.

Transferring the location of recognised peptides onto the predicted structure of FIV gp120 and gp41 (Figure 3-26A) revealed epitopes in gp120 at the leader-SU junction (B4-5), the V3 loop (G2-5), a region between the V3 and V4 loop (H2-5) and a sequence subsequent to the V5 loop (J5), while epitopes in gp41 mapped to the-alpha helical structure of the extracellular region (K11) and a region spanning the V7 loop and the principle immunodominant domain (PID) (L9-L10), which is a immunogenic structure that is conserved among FIV isolates (Flynn et al., 1997; Pancino and Sonigo, 1997).

In total six T cell epitopes were detected, of these three were recognised by lymphocytes from two cats (from different groups) (Figure 3-26B), while a single epitope was detected by cells from three animals, suggesting a possible immunodominance of these epitopes. However, this analysis failed to produce epitopes that would be specific for group 2 and thus did not explain the impaired replication of variants B14 and B28. To account for differences in the V5 sequences of variants used for the infection of group 2 animals, additional ELIspot analyses were performed using peptides encoding the variant specific V5 sequences. Yet, none of the peptides induced an IFNy response, suggesting that the V5 loop may not represent a T cell epitope (data not shown).

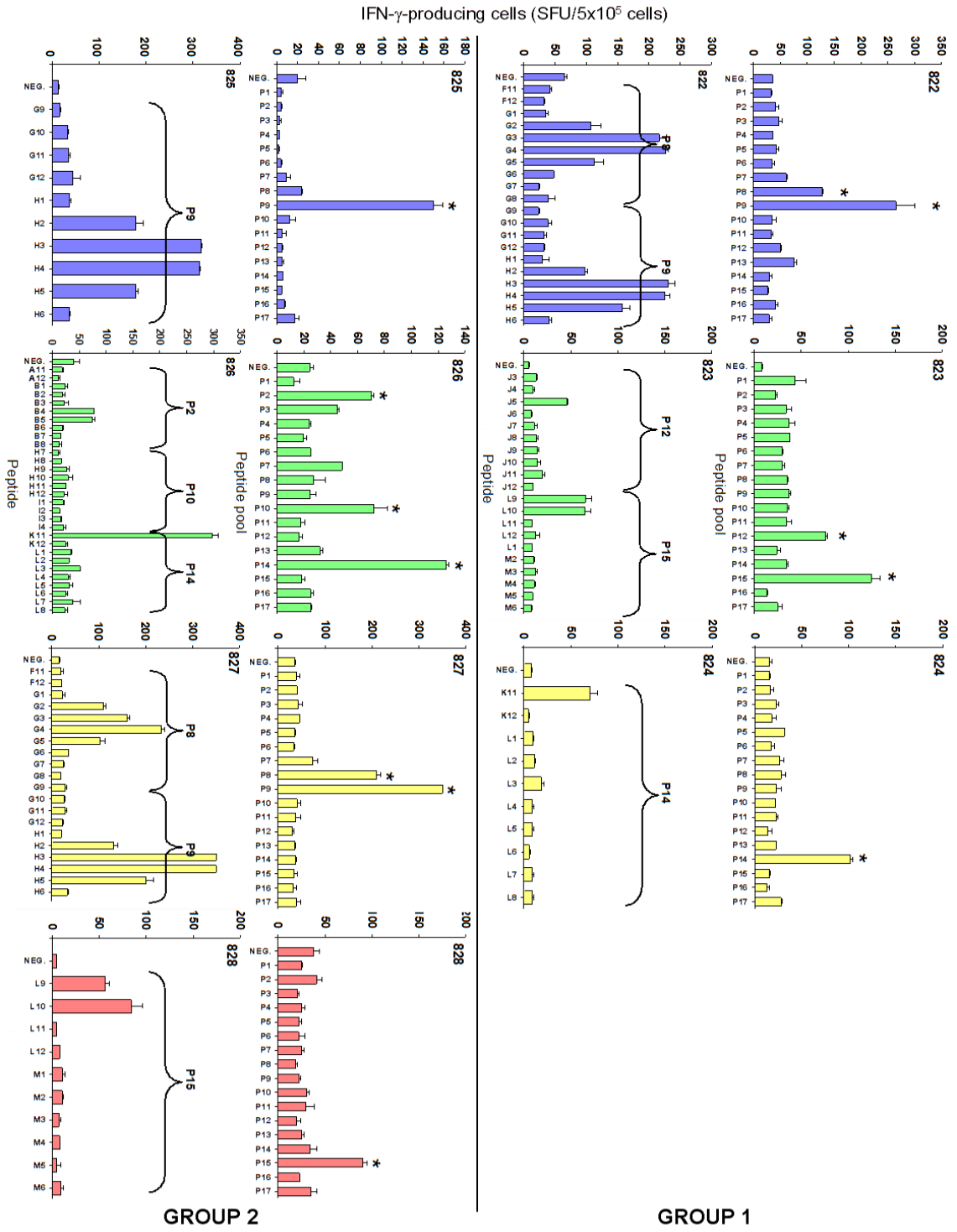


**Figure 3-25. Epitopes of T cell response to FIV infection.**

T cell epitopes of lymphocytes extracted from spleens of group 1 (clonal infection) and group 2 (quasispecies infection) animals were mapped by IFNγ ELISpot using 17 peptide pools (P1-P17) spanning the FIV-GL8 Env protein. Each pool consisted of 10 x 15-mer peptides overlapping by 10 amino acids. Once pools induced strong responses (*), single peptides comprising the respective pool were analysed separately to identify the individual epitopes. Adapted from (Willett et al., 2013).

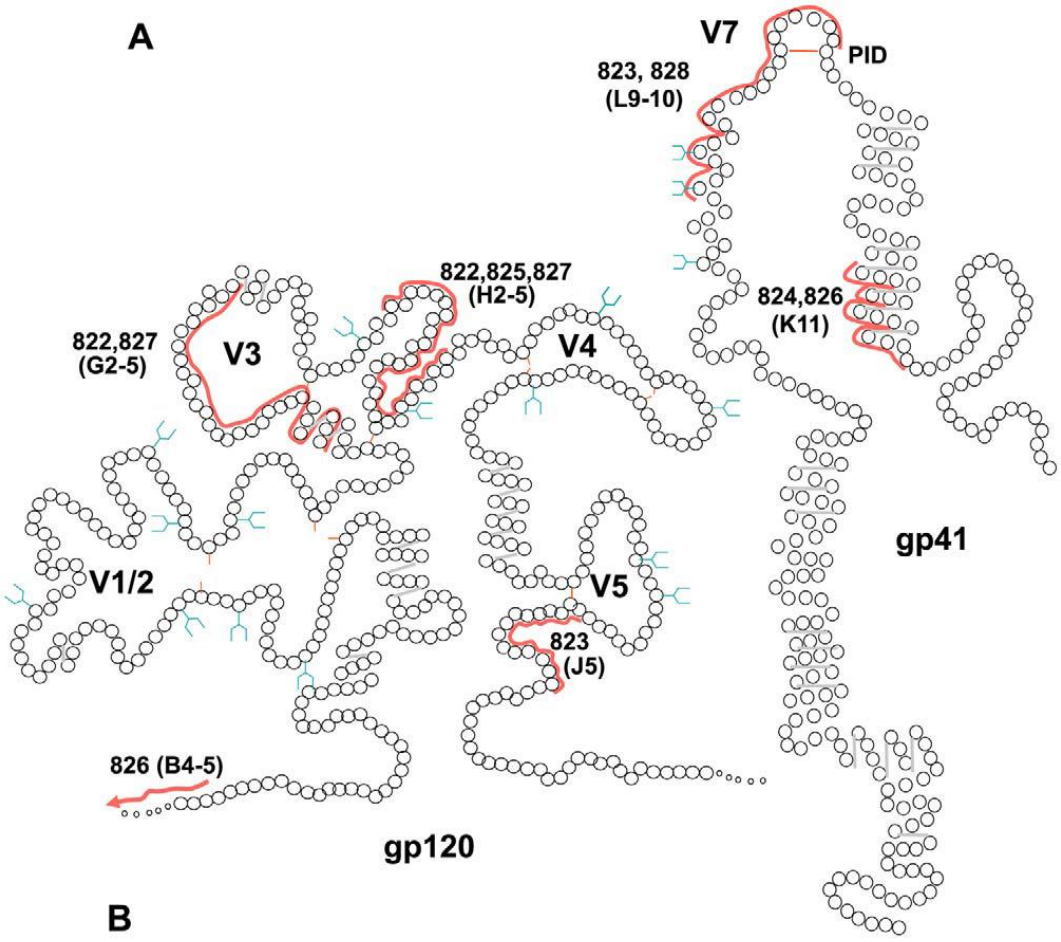


| Peptides | Sequence | Animal # |
|---|---|---|
| B4-5 | EEGNAGKFRRARFLRYSDET | - 826 |
| G2-G5 | CRWESTDVKFHCQRTQSQPGLWLRA | - 822,827 |
| H2-H5 | AMRSSGDYGEVTGAWIEFGCHRNKSKLHTE | - 822,825,827 |
| J5 | ACPKNQGILRNWYNP | - 823 |
| K11 | TIEKVTEALKINNLR | - 824,826 |
| L9-10 | NQFFCKVPPELWKRYNMTIN | - 823,828 |

**Figure 3-26. Location of T cell epitopes on schematic representation of FIV Env.**
(A) Circles represent single amino acids, while red lines mark T cell epitopes recognised by cells of the indicated cats. Name of individual peptides is given in brackets. (B) Amino acid sequence of peptides recognised by cells of the indicated animals. Adapted from (Willett et al., 2013).

In summary the data suggests that while an early cellular immune response is induced by FIV infection it is unlikely to account for the selective failure of variants B14 and B28 to replicate *in vivo*. Thus in the absence of an obvious humoral or cellular immune pressure particularly directed against B14 and B28, the differences in the virus-receptor interaction (Figure 3-9) and sensitivity to antagonists of the virus-receptor interaction (Figure 3-10) of these variants may indicate a deficiency in the process of viral entry and may account for an impaired replication *in vivo.*

# 4. Discussion

## 4.1. Evolution of FIV in long-term infected cats

Apprehending the evolution of retroviruses is crucial for decoding their interaction with the immune system and developing efficient therapy and prophylaxis. Lentiviruses are constantly evolving. The low fidelity of the RT and the high virus turn-over allow the production of highly adaptive quasispecies (Mansky and Temin, 1995; Perelson et al., 1996). Variants with mutations that enable faster replication or allow immune evasion undergo positive selection and expansion. Hence, investigating the changes viral populations acquire during infection enables the identification of genomic regions that remain constant and regions that are highly variable, including those that may pose a replicative advantage or protect from immune pressure.

In our first animal study the evolution of a molecular clone of FIV-GL8 was determined in the acute and chronic phase of infection. The use of a homogenous source of virus for the initial infection rather than a natural isolate may have decreased the overall variability of the quasispecies but it allowed the direct comparison of viral sequences to the inoculum, thus facilitating the quantification of the rate of evolution and identification of sites that were under positive or negative selection. Utilising PBMCs to study integrated viral DNA sequences enabled us to identify archival viral variants within the PBMCs rather than concentrating solely on the most recent quasispecies circulating in the blood. Further useful information could probably have been gained from samples of these animals obtained at later time points, when disease may have progressed to the terminal stage of infection, however such samples were not available.

In early infection FIV mainly targets activated CD4+ helper T cells and monocytes/macrophages consistent with the expression of considerable amounts of the primary receptor CD134 and the co-receptor CXCR4 on these cell types (de Parseval et al., 2004; Shimojima et al., 2004; Willett et al., 2003; Willett and Hosie, 2008; Willett et al., 2007). However, at later stages of infection the cell tropism expands to B cells and CD8+ T cells (Dean et al., 1996; English et al., 1993), which express low levels of CD134 (Willett et al., 2007). Adaptations within the Env enable utilisation of weakly expressed CD134 facilitating the infection of such broad variety of cells. Furthermore, quasispecies are

shaped by the action of the adaptive immune system during chronic infection. Neutralising Ab may force the virus to change its surface structure to evade the immune pressure, whereas pressure from cytotoxic T cells may favour low Env expression on infected cells resulting in viral particles with less Env protein (Asmal et al., 2011; Gnanakaran et al., 2011). The variability of FIV is likely to derive from a combination of such host factors but is also influenced by viral factors. For instance, a study using clonal SIV to infect macaques described a strong correlation between replication kinetics and viral evolution. A fast replicating virus diverged from its parental strain to a level of 0.9% (after 40 weeks) and 1.4% (after 75 weeks). In contrast, a slowly replicating virus reached a divergence of only 0.2% and 0.6% after 40 and 75 weeks, respectively (Eastman et al., 2008). Comparing these values to our study, it appears that FIV-GL8 diverges to similar levels as the slowly replicating SIV. In comparison to other FIV studies utilising clonal virus preparations, we found long-term infection with FIV-GL8 to result in a highly diverse population of viruses. Previous reports describing infection periods of more than 2 years (Huisman et al., 2008; Motokawa et al., 2005) or 9 years (Ikeda et al., 2004), respectively found relatively few single amino acid substitutions within the V3, V5 loop and gp41. Such a low number of mutations may possibly result from the poor replication of the FIV strains utilised, however, the replication kinetics of these isolates are not known. Yet, for the strain AM6 utilised by Huisman and colleagues (Huisman et al., 2008), *in vivo* data is available allowing a comparison to FIV-GL8. During a vaccination study unvaccinated control groups were challenged with either AM6 or FIV-GL8. The cats receiving FIV-GL8 displayed 10-fold higher proviral loads than unvaccinated animals infected with AM6, suggesting a higher replication efficiency of FIV-GL8 *in vivo* (Hosie et al., 2000). These findings are in agreement with a hypothesis that has been proposed for HIV-1 and HIV-2 in which the higher rate of replication of HIV-1 is responsible for its increased evolutionary rates (MacNeil et al., 2007).

Our data revealed a higher evolutionary rate and mean divergence per year for the short-term infected cats compared to the long-term infection group. While this may seem surprising initially, it is likely that this actually reflects faster evolution of the virus during the initial burst of viral replication which is not constrained by the adaptive immune response. However, during chronic infection, evolution slows down as a balance between replication efficiency and immune evasion is found. There is only sparse information

available on evolutionary rates of FIV and most reports analysed only variable regions within the *env* gene. Thus, the evolutionary rate of V1/V2 has been estimated with 3.4 x $10^{-3}$ substitutions per site per year (Greene et al., 1993), while the V3-V6 region ranged between 3.1 and 6.6 x $10^{-3}$ substitutions per site per year (Hayward and Rodrigo, 2010). These values are comparable to our rates of evolution of 6.7 x $10^{-3}$ substitutions per site per year in the short-term and 0.9 x $10^{-3}$ substitutions per site per year in the long-term infected group.

Of the long-term infected cats variants isolated from A612 displayed the lowest viral diversity. Interestingly this cat also possessed the highest viral burden and the lowest CD4:CD8 ratio. Thus, animal A612 might have failed to mount an efficient adaptive immune response to FIV which is consistent with the low titres of NAb that have been reported in this cat (Hosie et al., 2011). Hence, unconstrained viral replication may have diminished the population of CD4+ T helper cells and induced the expansion of CD8+ T cells, resulting in the reduced CD4:CD8 ratio.

Interestingly, even after six years of infection FIV-GL8 sequences could be recovered from two cats, suggesting that FIV-GL8 efficiently replicates *in vivo* while being protected from the immune response. However, investigations into the humoral immunity of cat A613 have revealed a highly efficient NAb response to the founder virus (Fig. 3-12; (Hosie et al., 2011)). How is it possible that 4 out of 17 sequences from cat A613 were identical to FIV-GL8? During acute infection FIV quickly establishes reservoirs in several tissues (Beebe et al., 1994; Liu et al., 2006; Ryan et al., 2003). These reservoirs might be poorly accessible for the humoral immune system (e.g. brain, testis) and may allow FIV-GL8 to persist in its original form. However, limited exchange of lymphocytes would carry the virus to the periphery. The thymus and bone marrow represent the primary tissues for the generation and selection of lymphocytes. Indeed we were able to recover FIV-GL8 from the thymus of cat A613. Furthermore, in animal A611 the bone marrow was recognised as a tissue with limited viral evolution containing FIV which was almost identical to FIV-GL8 (Fig. 3-4). Hence FIV-GL8 may reside in these tissues (and possibly other tissues that have not been tested) and may infect lymphocytes that transiently locate into those compartments, while free virus in the periphery would be cleared quickly by NAb. This could be clarified by analysis of cell-free virus circulating in the plasma, where an absence of FIV-GL8 in animal A613 would be expected.

The envelope glycoprotein of FIV has several functions, one is the protection from the humoral immune response which is accomplished by amino acid substitution, length polymorphism and extensive glycosylation. In this study we found high diversity located in the variable loops of gp120 but also in gp41. The other important function of Env is the recognition of susceptible cells, which is achieved by binding to the primary receptor CD134 and co-receptor CXCR4. Subsequent conformational changes bring the viral envelope and host cell plasma membrane into close proximity, resulting in membrane fusion. Certain residues in the V3 homologue of FIV Env have been shown previously to alter the usage of CXCR4. In fact, mutations of either residue 407 or 409 that increase the net charge by substitution of glutamate for lysine are thought to render the virus independent from CD134 by direct interaction with CXCR4 (de Parseval and Elder, 2001; Hosie et al., 2002; Verschoor et al., 1995). Two variants isolated from cat A613 displayed such E407K substitution making CD134 independence possible. Furthermore, one variant isolated from animal A611 displayed an E409D mutation in this position, yet an impact on CD134 usage seems unlikely as this substitution did not result in a change of charge. Provided such mutations would grant a considerable fitness advantage we would expect them to occur more frequently in the quasispecies. However, previous reports indicated that strains with a reduced dependency for CD134 are readily neutralised by the humoral immune response (Hu et al., 2012; Osborne et al., 1994) and therefore may be restrained in the peripheral blood. It is possible that such virus could be tolerated in other privileged tissues, however we did not detect these mutations in any of the A611 tissue variants nor in the thymus samples of A613, suggesting that these variants may reside in compartments other than the ones tested or that this mutation occurs infrequently *in vivo*. Hence, we did not include isolates carrying these mutations in later assays. It is possible that CD134 independent variants emerge frequently during infection but are cleared quickly by neutralising antibody. Such a transient existence may turn into continual re-emergence once the AIDS-like state of disease is reached.

We noticed a hot-spot of mutation in the V4 region of variants isolated from cat A611. In total 11 (out of 18) viral sequences derived from PBMC displayed either an S483P or an S483L mutation that would disrupt the potential N-linked glycosylation site at position 481. Furthermore, one sequence isolated from cat A613 also contained a deletion of that site however by an N481K substitution. The asparagine at position 481

has previously been associated with the conversion of a neutralisation-sensitive to a neutralisation-resistant FIV-strain (Bendinelli et al., 2001; Cammarota et al., 1996), therefore the changes in cat A611 might indicate humoral immune pressure acting on the quasispecies. Interestingly, the tissue derived virus from animal A611 displayed a limited number of substitutions at position 483. Only one tonsil and large intestine and two salivary gland samples carried the mutation suggesting an enhanced necessity for this mutation in the periphery.

Another Env region that has previously been linked to resistance to neutralising Ab is the V5 loop. For instance an FIV isolate acquiring an additional N-linked glycosylation site at position 557 was partly resistant to NAb (Bendinelli et al., 2001). In our study the region close to residue 557 was highly diverse. One sequence from cat A613 carried a N551S mutation that led to the deletion of a potential N-glycosilation site, while another sequence showed an S553N substitution which in the sequence context deleted the N-glycosylation site at position 551 while simultaneously creating a new one at residue 553. Most striking were length polymorphisms seen in variants from cat A613 and to a lesser extent, cat A611. At position 555 three different insertions of two or three amino acids were found in four sequences isolated from cat A613, while cat A611 harboured three sequences with a deletion of a single amino acid at residue 560. These highly diverse changes indicate a strong pressure on the virus to change its V5 sequence which is consistent with our detection of the V5 loop as the major target of NAb in cat A613.

Additionally we observed several mutations in gp41. Even though gp41 is well hidden beneath gp120, it is immunogenic in HIV infected individuals and some of the strongest broadly neutralising antibodies for HIV, e.g. 2F5, 4E10, target the so-called membrane-proximal external region of gp41 (Zwick et al., 2005)). Peptides to the corresponding region in FIV efficiently blocked infection *in vitro,* but failed to induce neutralising antibodies following peptide vaccination (Giannecchini et al., 2004; Giannecchini et al., 2007; Giannecchini et al., 2003). Similarly, in our study this region did not appear to be under strong immune pressure as only two mutations arose; D771E in A611 and V773A in A775. The majority of gp41 mutations were located at residues 648 and 651 and were present in all long-term infected cats. These mutations might stem from immune evasion, may enable more efficient entry or were necessary to countervail changes that occurred in gp120 (Vahlenkamp et al., 1997).

## 4.2. Tissue variability

Retroviruses can efficiently disseminate into confined tissues of their host. For example, HIV crosses the blood-brain barrier and replicates in the brain where it damages cognitive function (Gonzalez-Scarano and Martin-Garcia, 2005). Such growth in discrete compartments results in separate evolution as the virus has to adapt to the existing conditions (e.g. receptor expression). Hence, it has been observed that compartmentalisation of HIV between brain and lymph node may be associated with differences in sensitivity to entry inhibitors, macrophage tropism and resistance to neutralising antibodies (Brown et al., 2011). Thus, similar to alteration in the Env-receptor interaction that we observed in connection with humoral immune pressure, tissue growth conditions may also influence viral phenotype.

We observed a three amino acid insertion in the V5 loop of all A611 thymus isolates that conferred an additional potential N-linked glycosylation site. Similarly, the majority of thymus samples from A613 harboured V5 insertions of varying size. It remains undetermined whether the V5 length polymorphism in the thymus arose due to selection pressure from neutralising antibodies or if the inserts were acquired in the periphery and enabled a more efficient infection of thymus cells. Given the absence of a strong humoral immune response to FIV-GL8 in cat A611 (Hosie et al., 2011), the latter scenario might be more favourable. However, proviral loads in the thymus of animal A613 were extremely low (4 copies per $10^6$ cells), conversely FIV yielded more than 1000-fold higher titers in the thymus of cat A611 (16529 copies per $10^6$ cells), while cat A612 ranged in-between (1616 copies per $10^6$ cells). Given that the majority of isolates from thymus of A613 harboured V5 inserts, it appears that such length polymorphism *per se* did not confer a replicative advantage in the thymus. Thus, either the slightly different positions of the V5 insertions of A611 and A613 variants, possibly coupled with additional mutations, are responsible for deviating tissue proviral loads or selection pressure other than humoral immunity might be at play in the thymus of animal A613 (but not A611), limiting viral spread.

In HIV infection, tissues quickly become infected and are thought to constitute reservoirs which shed particles into the periphery. Thus, following prior elimination of HIV from the blood stream by anti-retroviral drugs that often fail to penetrate into certain

tissues, virus might quickly recur once therapy is interrupted. FIV also rapidly infiltrates tissues, thus virus may be detected in the brain as early as 14 days post-infection (Liu et al., 2006; Ryan et al., 2003). Similarly, FIV DNA in thymus and tonsil has been detected at 28 days p.i., however, virus-induced hyperplasia in tonsil was noted as early as 5 days p.i. (Beebe et al., 1994). In our study thymus and tonsil isolates from cat A611 displayed signatures of compartmentalisation. Given that these tissues do not possess an immunological barrier, the separate evolution of virus may be the result of different populations of susceptible cells or variable levels of receptor expression (Willett et al., 2007). Possibly the tissue variants regularly re-enter the periphery but are unable to thrive in PBMCs, yet certain immunological changes (e.g. cytokine induced regulation of receptor expression, B cell activation) may possibly allow their replication in the blood at later stages of infection. In contrast to thymus and tonsil all bone marrow derived samples in our study had an identical PBMC derived counterpart, suggesting a regular exchange of cells or virus between these tissues. It has been demonstrated that a high proportion of non-T cells and non-B cells which are CXCR4+ is infected in the bone marrow (Troth et al., 2008). Even though these cells have not been further characterised they might represent monocytes/macrophages, which are thought to be a major reservoir of FIV (Beebe et al., 1994; Dow et al., 1999) consistent with the proposed reservoir function of the bone marrow (Troth et al., 2008). Given that FIV did not evolve far from ancestral FIV-GL8 in the bone marrow of A611 this tissue may actually contribute to conservation of original FIV-GL8 during chronic infection.

Compartmentalisation may also be of importance for the transmission of virus. HIV variants in the blood stream have been shown to differ from virus in the semen and in the majority of cases virus isolated from semen mononuclear cells most closely resembled variants transmitted to the recipient (Zhu et al., 1996). Given that genital fluids are the main route of HIV transmission, understanding the composition of quasispecies in these compartments is essential for efficiently fighting the virus. In felids, the transmission of FIV occurs mainly by biting during fighting or mating. FIV has been isolated from saliva of infected cats (Yamamoto et al., 1988), however it has not been investigated whether the saliva borne virus originates form the salivary glands or from the tonsil. Our study is the first to show that virus in these compartments differs substantially. While variants isolated from the salivary gland clustered with PBMC derived virus, tonsil isolates were

most distantly related to virus in the blood stream. Thus, the origin of salivary gland borne virus may determine the variability of transmitted virus.

## 4.3. APOBEC3

The cytidine deaminase APOBEC3 is a viral restriction factor that has been shown *in vitro* to inhibit the replication of diverse retroviruses including lentiviruses (e.g. HIV and FIV), spumaviruses (feline foamy virus, FFV), gamma-retroviruses (murine leukemia virus, MLV) and beta-retroviruses (mouse mammary tumor virus, MMTV) (Browne and Littman, 2008; Mangeat et al., 2003; Munk et al., 2008; Okeoma et al., 2007). The contribution of APOBEC3 to immune protection from retroviral infection *in vivo* has been demonstrated previously in the mouse model. APOBEC3 knock-out mice were more susceptible to infection with MMTV and MLV than their wild type counterparts (Okeoma et al., 2010; Okeoma et al., 2007; Santiago et al., 2008; Takeda et al., 2008). However, these murine retroviruses do not possess Vif-like proteins to counteract APOBEC3 and therefore might be more vulnerable to effects of the restriction factor. Lentiviral Vif targets APOBEC3 proteins of the viral host species for degradation in the proteosome thereby evading its anti-viral activity (Mehle et al., 2004; Wang et al., 2011; Yu et al., 2003). Vif proficient primate and feline lentiviruses have been found to resist inhibition by APOBEC3 *in vitro*, but were restricted efficiently in the absence of Vif (Munk et al., 2008; Sheehy et al., 2002; Zielonka et al., 2010a). Yet, the influence of APOBEC3 on *in vivo* infection with wild-type lentivirus remains unclear. For primate lentiviruses an inverse correlation of disease progression and APOBEC3 expression has been reported (Kourteva et al., 2012; Mussil et al., 2011). However, other studies do not support such findings (Amoedo et al., 2011). Furthermore, APOBEC3 expression in HIV-exposed seronegative individuals was found to be higher than in seropositive patients or healthy control subjects. Additionally, PBMCs of these seronegative individuals were less susceptible to *ex vivo* infection with HIV than control cells from healthy donors (Biasin et al., 2007). In stark contrast to these anti-viral effects, there is evidence that APOBEC3 might actually be beneficial for the virus. Limited packaging of APOBEC3 into Vif competent viruses may lead to poor editing of viral genomes possibly adding further variety to a viral quasispecies, such has been shown to result in a quicker adaptation to anti-retroviral drugs *in vitro* (Fourati et al., 2010; Kim et

al., 2010; Mulder et al., 2008). The retroviral mutation rate of approximately three substitutions per genome per cycle ensures the viral integrity in a slowly changing environment (Mansky and Temin, 1995). However increasing the mutation rate may boost the viral adaptability in a rapidly evolving environment (Munk et al., 2012). Such increase in mutation rates may be accomplished by a balanced interaction of Vif with the cytidine deaminase APOBEC3.

Approximately 90% of viral particles produced by human CD4+ T cells following *ex vivo* infection with wild-type HIV do not carry any G-to-A mutations, while ~8% are inactivated by hypermutation. However, the remaining 1-2% particles harbour a limited number of G-to-A mutations (20-40 per genome) (Gillick et al., 2013) resulting mainly in the production of defective genomes (Armitage et al., 2012). *In vitro* experiments with HIV$\Delta$vif showed that a single molecule of human APOBEC3G (hA3G) is sufficient to efficiently mutate the virus and *in silico* calculations have estimated that as little as nine hA3G mediated G-to-A mutations per genome would be sufficient to induce a lethal stop codon in 50% of viral offspring (Armitage et al., 2012). These estimates do not take into account the likely negative effects of non-synonymous mutations on viral proteins and possible disadvantageous impact of synonymous mutations on viral RNA secondary structure (Sanjuan et al., 2004; Wang et al., 2008), thus inactivation of virus may be even more pronounced. However, recombinational processes may actually rescue the defective virus. Superinfection of host cells with virus containing APOBEC3 and virus devoid of APOBEC3 may result in the integration of both, the edited and the non-edited viral DNA into the cellular genome. Subsequently, the two viral genomes (mutated and non-mutated) may be packaged into the same novel particle. Upon infection of the successive target cell, template switching of RT, which occurs 2-13 times per reverse transcription (Neher and Leitner, 2010; Zhuang et al., 2002), may produce recombined functional genomes. Given the remarkably fast replication dynamics of HIV of approximately $10^{10}$ new particles per day (Perelson et al., 1996), a small number of functional virions with increased variability may emerge. Hence, anti-viral and pro-viral effects of APOBEC3 may possibly exist in parallel. During acute infection the anti-viral effects will predominate, however if the adaptive immunity is unable to clear the infection, low-editing induced mutations may accumulate over time and increase viral variability.

Little is known about the effects of feline APOBEC3 on FIV *in vivo*. Our data indicated that viral sequences in both the long-term infected cat A611 and the short-term infected cat A774 were subjected to APOBEC3-mediated editing. The quasispecies isolated from these cats were the most heterogeneous of the two study groups and this diversity would largely be reduced if G-to-A mutations were excluded from the analyses. In animal A611 there appeared to be no obvious link between the proviral load at post-mortem and the action of APOBEC3 as viral copy numbers ranged between proviral loads in cat A612 and A613. As a component of the innate immune response, the action of APOBEC3 is likely to mainly support the immune system during the early phase of infection before an adaptive immune response has been mounted. Indeed animal A774 displayed the lowest proviral load of its group at 12 weeks post-infection. Similarly, the early infection of A611 was clearly retarded. Proviral loads in animals A612 and A613 were detectable as early as 6 weeks post-infection (Figure 4-1), while viral replication in A611 could not be detected until week 12 p.i. (Hosie et al., 2002). The significance of the delayed onset of viral replication in cat A611 is unclear as it did not seem to influence proviral loads over a prolonged period of infection (Fig 4-1). However, this may also reflect the inability of cat A611 to mount an efficient humoral immune response against FIV-GL8 (Hosie et al., 2011). In summary, it appears that quasispecies in A611 have experienced both the restrictive effects of APOBEC3 during early infection and the increases of variability throughout the chronic phase of infection, even though this did not elevate proviral loads.

Why did only 2 out of 6 cats display signs of APOBEC3-mediated editing? The animals used in our study were out-bred cats, thus it is possible that differences in the levels of APOBEC3 expression or polymorphisms of APOBEC3 influenced the interaction with FIV. There are relatively few studies investigating APOBEC3 expression in felids. Levels of feA3H mRNA may vary up to three fold in PBMCs extracted from out-bred cats and expression is inducible by interferons, which may lead to variable level of APOBEC3 (Dietrich, 2013; Troyer et al., 2012). Unfortunately, data concerning the expression of APOBEC3 in our study animals was not available, therefore the inter-animal variation in expression levels is unknown. Moreover, in HIV-infected humans a polymorphism in hA3G has been linked to faster disease progression and decline in CD4+ T cells (An et al., 2004).

The occurrence of such polymorphisms in felids has not been investigated and thus cannot be excluded from our study group.

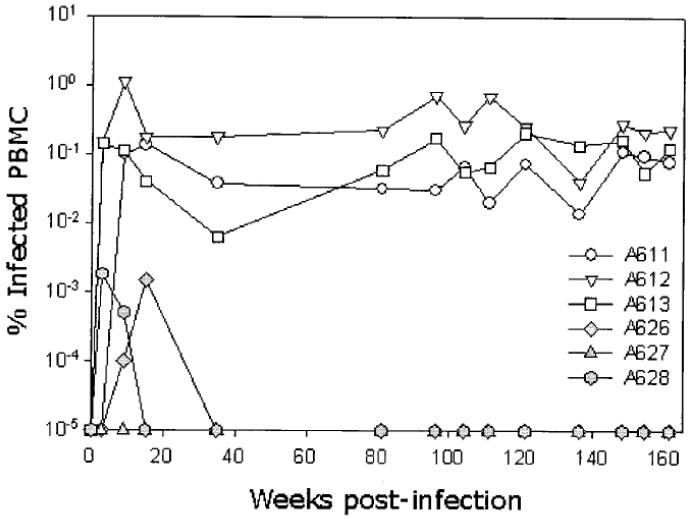


**Figure 4-1. Sequential proviral loads in cats during acute and chronic phase of FIV-infection.**
Animals were infected intra-peritonially with either FIV-GL8 (A611-A613, open symbols) or FIV-PET (A626-A628, closed symbols). Proviral load in PBMCs was estimated using real-time PCR and is expressed as percent infected PBMCs. Reproduced from (Hosie et al., 2002).

Samples isolated from PBMCs, bone marrow, tonsil and thymus displayed the highest levels of G-to-A mutations in relation to the reverse mutation. Interestingly, the dinucleotide context of editing varied between these tissues suggesting the activity of different APOBEC3 subtypes. In felids five APOBEC3 proteins are known. FeA3C which exists in three closely related isoforms is highly active against FFV and SIVΔvif, but is inefficient against FIVΔvif (Dietrich, 2013; Munk et al., 2008; Zielonka et al., 2010a). Conversely, feA3H and feA3CH display only weak activity against FFV, but are active against SIVΔvif and FIVΔvif (Munk et al., 2008). However, activity against SIV results in 100-fold reduction, while anti-FIV activity is 10-fold weaker and is completely abolished in the presence of Vif. Certain human APOBEC3 proteins have been shown to be highly specific in the dinucleotide context of editing; while activity of hA3G results in GG-to-AG mutations, hA3F modifies GA to AA (Harris et al., 2003; Wiegand et al., 2004). The activity of feA3H and feA3CH is less specific and results in the mutation of GC, GG and GA dinucleotides, while GT-to-AT mutations are uncommon (Munk et al., 2008; Stern et al., 2010). In stark contrast, even though editing activity is very limited, feA3C was found to mainly mutate GT residues (Munk et al., 2008). Our analysis of PBMC derived sequences

yielded elevated levels of GT-to-AT mutations, suggesting primary activity of feA3C, consistent with feA3C mRNA levels that exceed feA3H expression by 4-fold and feA3CH by 1000-fold (Troyer et al., 2012). In general, the thymus and tonsil appear to express more APOBEC3 mRNA than the bone marrow, which is consistent with the lower levels of editing in samples isolated from this compartment. Furthermore, expression of feA3H in thymus and tonsil may be up to 50-fold higher than in the bone marrow (Dietrich, 2013), which may explain the appearance of edited GG and GA dinucleotides.

Lentiviruses have evolved a broad spectrum of accessory proteins to disable anti-viral mechanism of their host species. HIV and FIV rely mainly on Vif for counteracting APOBEC3. The interaction of Vif and APOBEC3 is a highly complex process involving several host proteins that are necessary to target APOBEC3 to ubiquitination and proteasomal degradation (Kobayashi et al., 2005). Thus, each step may offer a potential interference of new anti-viral substances that would increase the number of available APOBEC3 molecules, resulting in pronounced hypermutation (Cen et al., 2010; Zuo et al., 2012). However, there is also research to the contrary aimed at decreasing mutation rates by blocking APOBEC3 and thus reducing sub-lethal editing of HIV by APOBEC3 (Li et al. 2012). Accordingly, limited viral variability would render the virus more susceptible to the adaptive immune response and decrease drug resistance. It remains unclear which of these strategies will prove most successful.

## 4.4. Phenotype of FIV Env variants from cat A613

In our phenotype analysis we described the evolution of the Env-receptor interaction of FIV-GL8 variants isolated from animal A613 at 322 weeks post-infection. A shift in cell tropism occurring in the course of FIV infection has been reported previously (Dean et al., 1996; English et al., 1993). The molecular mechanisms underlying this shift are as yet unknown. All FIV isolates described to date utilise CXCR4 as their co-receptor, thus, unlike HIV where a switch from CCR5 dependence to CXCR4 usage is possible, such a shift seems implausible for FIV. X4 variants of HIV arise in approx. 50% of HIV infected individuals and their emergence is often linked with disease progression (Shankarappa et al., 1999; Zhang et al., 1998), however advancement towards AIDS may also occur in the absence of X4 tropic viruses. Thus evolution of the co-receptor interaction may influence

the disease but is not a necessity for development of AIDS. Furthermore, the broadened cell tropism of X4 variants may come at the cost of increased sensitivity to humoral immune responses, thus during early infection viral replication might be suppressed. Given that determinants for receptor usage and neutralisation sensitivity may be shared, evasion of the adaptive immune response may drive the evolution of the Env-receptor interaction and result in a shift in cell-tropism (McKnight and Clapham, 1995). In this study we presented evidence for the evolution of the Env-receptor interaction *in vivo*. The inoculum for the initial infection, FIV-GL8, is thought to be an early stage virus with a "complex", high affinity interaction with CD134. At post-mortem, 322 weeks post-infection viral variants had emerged that evaded neutralisation by homologous plasma and that differed in the way they interacted with CD134.

Why should FIV alter the way it interacts with its main receptor? Studies of HIV and SIV have demonstrated not only the *in vivo* evolution of the co-receptor usage with disease progression (Shankarappa et al., 1999), but also altered interactions between the virus and its main receptor CD4. For example, intra-patient variation in the V1/V2 and V3 loop can modulate co-receptor binding but may also influence the interaction with the primary receptor (Nabatov et al., 2004). Given that FIV depends solely on CXCR4 as a co-receptor, the observed changes in the interaction with CD134 may provide a mechanism by which FIV can expand its cell tropism.

Variants B14 and B28 successfully utilised CRD1 of CD134 for infection. They displayed an increased sensitivity to inhibition by CD134 ligand or anti-CD134 antibody, 7D6, and were comparably resistant to inhibition by soluble receptor sFc-CD134. Thus the mutations acquired by these variants seemed not simply to reduce the affinity of Env for CD134 but also changed the nature of the interaction with the receptor. Two types of interaction with CD134 may be classified as either "complex" (involving both CRD1 and CRD2) or "simple" (solely depending on CRD1) (Willett and Hosie, 2008). Possibly the "complex" interaction is of high affinity and involves the binding of trimeric Env to trimeric CD134, while the simple interaction is less stringent and may function by engagement of Env with either trimeric or monomeric CD134. The high affinity interaction may not distinguish between cellular and soluble CD134 receptor so that strong binding of sFc-CD134 compromises recognition of the cellular receptor, while the reduced affinity of the "simple" interaction may allow the virus to detach from soluble sFc-CD134 to bind

to cellular CD134. Furthermore, receptor multimerisation on cell surfaces may be induced through association with the ligand (Vila-Coro et al., 1999). Given the low sensitivity of the "complex" phenotype to inhibition by CD134L, such viruses may displace the ligand from the receptor and may exhibit enhanced infectivity on target cells in the proximity of soluble ligand *in vivo* (for example helper T cells exposed to CD134L-expressing antigen presenting cells). In contrast, viruses depending solely on CRD1 for attachment are more sensitive to CD134L and may be inhibited *in vivo* by endogenous soluble ligand.

Several variants isolated post-mortem were resistant to neutralisation by homologous plasma from cat A613. Interestingly these variants shared a length polymorphism in the V5 region which appeared to afford protection from neutralisation independent of the number of inserted amino acids in V5. The exchange of the V5 loop of neutralisation-resistant variants into the neutralisation-sensitive FIV-GL8 rendered the virus resistant to NAb, confirming that protection was afforded by mutations of the V5 loop. Repeating these assays with different target cell lines (Mya-1 and MCC-CD134) led to similar results (not shown), thus our observations seem not to stem from a bias in our system. A linear peptide encompassing the V5 loop of B28 was recognised by the post-mortem plasma of cat A613 (data not shown), confirming that an immune response was induced by that region even in the neutralisation-resistant variants. However, we were unable to detect antibodies in the p.m.-plasma binding to linear peptides derived from the V5 loop of FIV-GL8 (data not shown), suggesting a conformational epitope recognised by the Nab.

In our study the V5 loop appears to be the single main target for the humoral immune system. Such targeting of single epitopes has been reported previously for the V4 and the V5 loop of FIV (Bendinelli et al., 2001; Giannecchini et al., 2001; Samman et al., 2010; Siebelink et al., 1995). For instance, a mutation of residue 560 in V5 in conjunction with a mutation at position 483 (V4) is thought to disrupt a conformational epitope of NAb and conferred neutralisation resistance to the FIV strain 19k1 (Siebelink et al., 1995). Furthermore, the creation of two potential N-linked glycosylation sites in the V4 (K481N) and the V5 loop (S557N) was involved in the conversion of a neutralisation sensitive FIV strain to a neutralisation resistant phenotype (Giannecchini et al., 2001; Pistello et al., 2003). The targeting of the V5 loop by NAb is not confined to clade A strains only. For instance, the Japanese isolate NG4 (clade B) has been shown to escape neutralisation by a

deletion of two amino acids in V5 (Samman et al., 2010). Among known FIV isolates the V5 loop is a highly variable region with substitutions as well as length polymorphisms (Fig 4-2).

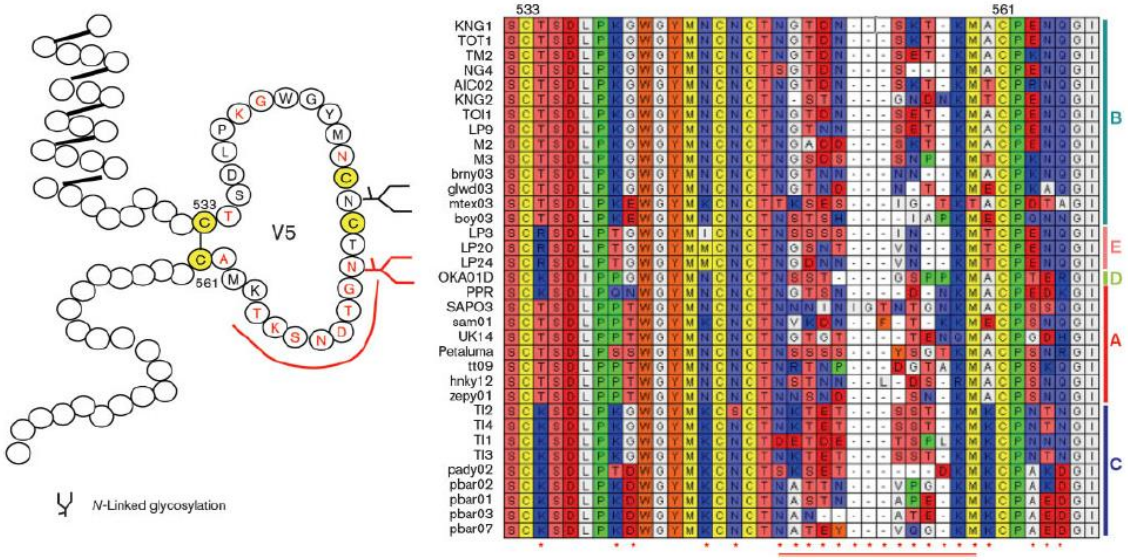


**Figure 4-2. Amino acid alignment of the V5 loop from diverse FIV strains.**
Virus clades are denoted right hand from the alignment. Between loop forming cysteine residues at position 533 and 561 extensive variation is apparent. Highly variable residues are marked by an asterisk. Amino acid colours specify side chains: white, hydrophobic; red, acidic; light blue, amido; dark blue, basic; orange, aromatic; pink, hydroxyl; yellow, thiol; green, proline. Reproduced from (Samman et al., 2010).

The V5 length polymorphisms detected in our study resulted largely from reiteration of nucleotide sequences encoding threonine and serine residues. Both bear hydroxyl side chains that allow O-linked gylcosylation. In comparison to N-linked glycosylation the effects of a potential O-linked glycosylation are believed to have only a minor impact on the glycan shield of HIV, which is owed to the comparably lower molecular size of O-linked oligosaccharides. However, due to the variety of possible oligosaccharides for O-linked glycosylation, such carbohydrate side chains may still be efficient at shielding neutralising epitopes, especially when occurring in close proximity (Bernstein et al., 1994). Furthermore, X-ray crystallography studies on HIV gp120 have suggested that N- and O-linked glycosylation influences the local conformation of Env but also may affect the secondary structure of more distant parts of Env. Such changes, in turn, would render epitopes less accessible for the interaction with NAb (Huang et al., 1997).

## 4.5. Reduction in viral diversity following experimental transmission of an artificial FIV quasispecies

The interaction of FIV with its primary receptor CD134 may be of high affinity involving CRD1 and 2 ("complex") or of low affinity involving solely CRD1 ("simple"). While the "complex" phenotype predominates in pathogenic primary isolates during early infection (e.g. FIV-GL8), the "simple" interaction is believed to be more prominent among isolates from late, chronic infection (Willett and Hosie, 2008). In our first animal study we demonstrated that following clonal infection with "early" isolate FIV-GL8, a broad variety of viral variants had evolved *in vivo*. Our subsequent investigation into the viral phenotype revealed certain variants that displayed features of "late" isolates. In our second animal study we sought to illustrate the situation of natural transmission by infection of naïve cats with an artificial viral quasispecies comprising our "late" isolates and FIV-GL8-like "early" variants.

In HIV infected individuals, high viral diversity during the early phase of infection has been linked to accelerated disease progression with increased viral loads and reduced CD4+ T cell counts (Sagar et al., 2003). However, the diversity of an HIV quasipecies is greatly reduced following mucosal transmission (Margolis and Shattock, 2006; Zhu et al., 1993) and even virus that was transmitted directly to the blood stream might be subjected to specific filtering mechanisms (Spijkerman et al., 1995). Similarly, we observed the preferential replication of FIV-GL8-like virus, while "late" stage variants failed to thrive following intra-peritoneal infection. This block in replication of "late" isolates did not stem from a humoral immune response as we could not find neutralising Ab against any of the variants during the 21 week study period. Previous data indicated that the development of efficient NAb to FIV-GL8 may require several months. Specifically, the humoral immune response in cat A613 took 100 weeks before efficiently neutralising FIV-GL8, while cats A611 and A612 failed to mount a strong response (Hosie et al., 2011). In the current study we were able to detect Env binding antibodies by immunoblotting. However, utilising HIV(FIV) pseudotypes bearing the Env protein of each variant within the inoculum, we did not observe a neutralising antibody response in any of the cats at 21 weeks post-infection. Thus the weakly replicating isolates were not

specifically targeted by the humoral immune response. Of note, although we did not detect NAb directly, using the V5 bulk cloning approach for quantification of variants (Fig. 3-20D) we discovered new mutations in the V5 loop that accounted for ~5% of the total sequences isolated. These changes included substitutions but also length polymorphisms of up to three amino acids. Such variation might indicate some immune pressure to change the V5 loop and in the absence of CTL epitopes mapping to the V5 loop an as yet undetectable humoral immune response may contribute to this process.

FIV infection induced significant cellular immune responses in animals from both study groups by 21 weeks post-infection. However, there was no correlation between target sequences or level of activation and replication of individual isolates. T cell epitopes differed between cats consistent with the distinct MHC and T cell repertoires that would be expected in the outbred study group. Mapping the epitopes indicated a strong immune response to the V3 loop and the adjacent region between V3 and V4, suggesting at least some immune pressure for antigenic variation in these determinates of Env may stem from CTL responses. In contrast, no epitopes were mapped to the V5 loop, suggesting that this region failed to induce a cellular immune response, accordingly the V5 escape mutants noted in animal A613 may solely be a product of pressure from the humoral immune response.

Even though we were able to map the regions in Env targeted by the cellular immune response, no clear pattern emerged that would indicate the efficient targeting of cells infected with isolates that replicated poorly. In light of the potent cellular responses detected, there is probably some cellular element to controlling infection with FIV, however there must be additional factors to restrain replication of variant B14.

The investigation of humoral and cellular immune responses failed to explain sufficiently the lower proviral loads of the “late” isolates, making reduced *in vivo* replication kinetics a more likely cause. The viral stocks used for infection had been produced and titrated on Mya-1 cells, a feline T cell line that should resemble closely the *in vivo* target of FIV. Subsequent analysis of RT activity of virus stocks had indicated almost identical numbers of particles suggesting similar replication kinetics in Mya-1 cells. Yet, when we compared the infectivity of RT activity-matched HIV(FIV) pseudotypes carrying the envelope glcyoproteins of our variants, we found that the “late” isolates

displayed a reduced ability to infect diverse cell types (Willett et al., unpublished data), which may reflect differences in the interaction with the CD134 and CXCR4 receptors.

*Ex vivo* assays have indicated that the fitness of primary isolates of HIV-1 mapped to the *env* gene (Ball et al., 2003; Rangel et al., 2003). For example, some HIV-1 subtype B Envs conferred increased fitness compared to subtype C Env and this was associated with elevated cell surface binding, more efficient entry and a decreased sensitivity to CCR5 inhibitors and fusion antagonist (Marozsan et al., 2005). Consistent with these reports, variants like B14 and B28 may have a reduced affinity for the primary or co-receptor that decreases fitness, resulting in reduced viral replication *in vivo*.

Our *in vitro* analysis of Env phenotypes had shown an increased sensitivity to anti-CD134 antibody 7D6 by the FIV-GL8 progeny. The exact nature of the 7D6 mediated inhibition is unknown, however the low sensitivity of FIV-GL8 to the effects of 7D6 may indicate a high affinity binding of FIV-GL8 to CD134 (Willett et al., 2007). Accordingly, the "late" variants possibly possessed a reduced affinity to CD134. Furthermore, variant B14 was highly sensitive to CXCR4 antagonist AMD3100, possibly indicating reduced affinity for the co-receptor. The natural ligand for CXCR4, SDF-1, has been reported to block FIV infection (Hosie et al., 1998b), thus endogenous levels of SDF-1 may be sufficient to inhibit infection by B14. Hence, FIV-GL8 may dominate in acute infection due to a more efficient infection of primary target cells. Upon successful initial infection the resulting immunological activation is associated with lymphoid hyperplasia (Callanan et al., 1992), increased production of pro-inflammatory cytokines (Lawrence et al., 1995) and polyclonal B cell activation (Flynn et al., 1994) and may lead to up-regulation of receptor expression. Hence an environment may be created that allows the emergence of variants with reduced requirement for high affinity interactions with cellular receptors.

The fact that FIV-GL8-like viruses were more infectious *in vivo* than B14-like variants is consistent with observations that during early infection, HIV-1 tends to harbour amino acid signatures that promote Env expression on the cell surface, increase Env incorporation into nascent viral particles and result in higher viral titers (Asmal et al., 2011; Gnanakaran et al., 2011). However these signatures are lost in the course of infection under pressure from the humoral and cellular immune responses (Asmal et al., 2011; Gnanakaran et al., 2011). Late isolates like B14 may represent the final product of selection pressures on FIV-GL8 during chronic infection, however following transmission

they would be supplanted readily by FIV-GL8. Whether B14-like viruses disseminate into other tissue compartments remains to be investigated. Possible target cells would include B-cells and CD8+ T cells, however methods for the maintenance of such cells from cats are not currently available.

## 4.6. Considerations for vaccine design

Despite immense research effort, the development of an effective vaccine to combat HIV remains elusive. Vaccines may afford protection in the laboratory setting (Shiver et al., 2002) but prove unsuccessful in clinical vaccination trials (Barouch and Korber, 2010). Similarly, the commercially available FIV vaccine Fel-o-Vax® is not protective against all primary FIV strains (Dunham et al., 2006a; Dunham et al., 2006b). An ideal vaccine would induce both cell and antibody mediated immunity. The induction of a humoral immune response should result in the generation of efficient broadly neutralising antibodies. Encouraging results from previous vaccine trials have proven that it is indeed possible to protect cats against infection with primary FIV isolates (Pistello et al., 1997). However, such vaccines induced antibodies that neutralised homologous challenge virus but did not provide protection against heterologous strains (reviewed in (Hosie and Beatty, 2007)). One possible solution to this would be the development of vaccines specific for the virus strains circulating in the concerning country (Steinrigl and Klein, 2003). However such regional vaccines would be more costly to produce and may not be applicable in countries where several diverse FIV strains are prevalent. A world-wide protective vaccine would have to induce antibodies able to neutralise a wide range of primary isolates. However, such vaccines remain challenging mainly because of a low number of known conserved neutralisation epitopes and the difficulties in presenting these epitopes adequately in vaccines. The majority of antibodies generated by vaccination target non-neutralising epitopes (Richman et al., 2003), while steric factors may hinder the accessibility of neutralising epitopes to NAb, (Labrijn et al., 2003).

In our phenotype study we described a mono-specific neutralising antibody response directed against the V5 loop of FIV. Within Env, the V5 loop is highly polymorphic among diverse FIV strains (Samman et al., 2010). The variety of substitutions, insertions and deletions is indicative of strong immune pressure on the V5

loop to evolve, resulting in the emergence of escape mutants. The ability of minimal mutations to either reduce or abrogate humoral immunity is of importance for the design of efficient vaccines against FIV. Beyond question the V5 and the V4 loop are immunogenic and induce antibodies capable of neutralising virus. However, one main function of these regions appears to be the decoy of the immune system by the presentation of easily accessible targets. By the time an efficient NAb response to these targets has been mounted virus variants may have evolved that can escape the mono-specific plasma. To resolve this dilemma in an efficient vaccine the immunodominant determinants in the V5 region would have to be silenced to allow a refocusing of the immune response to conserved regions of Env. By selective deglycosylation of immunogens, cryptic epitopes may be revealed that would enable the generation of neutralising antibodies.

The importance of neutralising Ab for the suppression of HIV is unclear. Bar and colleagues showed that NAb may appear as early as two weeks after seroconversion. These NAb exhibited low titres (IC50 of 1:20 to 1:50) and their binding to several epitopes on HIV Env triggered the emergence of escape mutants, some with impaired replicative activity (Bar et al., 2012). Conversely, studies with HIV-2 describe high titers of NAb against homologous and heterologous isolates, however no correlation between viral load and NAb titer was observed (de Silva et al., 2012; Kong et al., 2012). Interestingly, plasma samples dating back as far as 15 years were able to neutralise recent autologous isolates from the same patient, indicative of low or no immune pressure from NAb to change Env (de Silva et al., 2012). Additionally, numerous reports have indicated that HIV elite controllers (patients infected with HIV displaying exceptionally low viral loads, high CD4+ counts and decelerated disease progression) do not differ from other HIV-infected patients in the quantity and quality of NAb (Bello et al., 2009; Blankson, 2010; Lambotte et al., 2009). While the reason for this is unclear it may suggest that NAb alone are not sufficient to control infection. However, it should be considered that an unknown immunological response to viral replication in elite controllers may result in low viral loads that would subsequently lead to poor immune activation and reduced levels of NAb.

In the case of the long-term FIV infected cats A611, A612 and A613 a longitudinal study of neutralisation capabilities suggested no causal link between NAb and proviral

load during the first 160 weeks of infection (Fig. 4-1; (Hosie et al., 2011; Hosie et al., 2002)). Animal A613 alone had developed a robust humoral immune response against the inoculum FIV-GL8 at week 100 post-infection. The plasma of A613 reduced infectivity of FIV-GL8 pseudotypes approx 1000 fold and this anti-viral activity was retained until the end of the study at week 322 p.i. (Fig. 3-12). Conversely, cats 611 and 612 by week 160 exhibited weak NAb that were able to reduce FIV-GL8 infectivity only 2 fold (Hosie et al., 2011). Surprisingly, the total proviral load in all three cats remained stable during week 100-160 p.i. (Fig. 4-1; (Hosie et al., 2002)), suggesting that not FIV-GL8 but escape mutants dominated in the PBMCs of A613 in that period. Possibly these escape mutants differed from our V5 variants and were replicative fit, but additional pressure by further NAb mounted at later timepoints might have led to the emergence of less fit V5 mutants. Alternatively, immune pressure by the CTL response, may have limited viral loads or induced mutations resulting in reduced replicative fitness explaining the barely detectable proviral load observed in animal A613 at post-mortem (Table 3-1).

Immunity by cytotoxic T cells is crucial for containing retroviral infection and CD8+ T cell depletion has been shown to result in elevated viral loads and augmented transmission of virus (Gaufin et al., 2010; Kane et al., 2011). Our analysis of CTL epitopes in cats at 21 weeks post-infection yielded six different regions in Env recognised by T cells. Of these, four epitopes were recognised twice or more. In light of the distinct MHC and T cell repertoires of outbred animals, such regions might be of immunodominant nature. Indeed, CTL responses to regions corresponding to peptides G2-G3, H3-H5 and J5 of the isolate FIV-NCSU have been reported previously (Dean et al., 2004). Hence, if certain regions of FIV-GL8 Env are immunodominant in principle, we would expect such T cell responses to impact on our first study group as well. Overlay of non-synonymous substitutions detected in the long-term infected cats of the first animal study (Table 3-3) with the T cell epitopes (Figure 3-26) observed in the second animal study revealed a strong correlation of regions recognised by T cells and high prevalence mutations (Figure 4-3). Solely the B4-5 epitope at the leader did not display mutations in close proximity. Thus, not only neutralising antibodies triggered an immune evasion (as observed in cat A613) but also CTL responses may have induced escape mutations. Hence T cell responses should be considered when designing a vaccine to elucidate not only NAb but also strong cellular immunity.

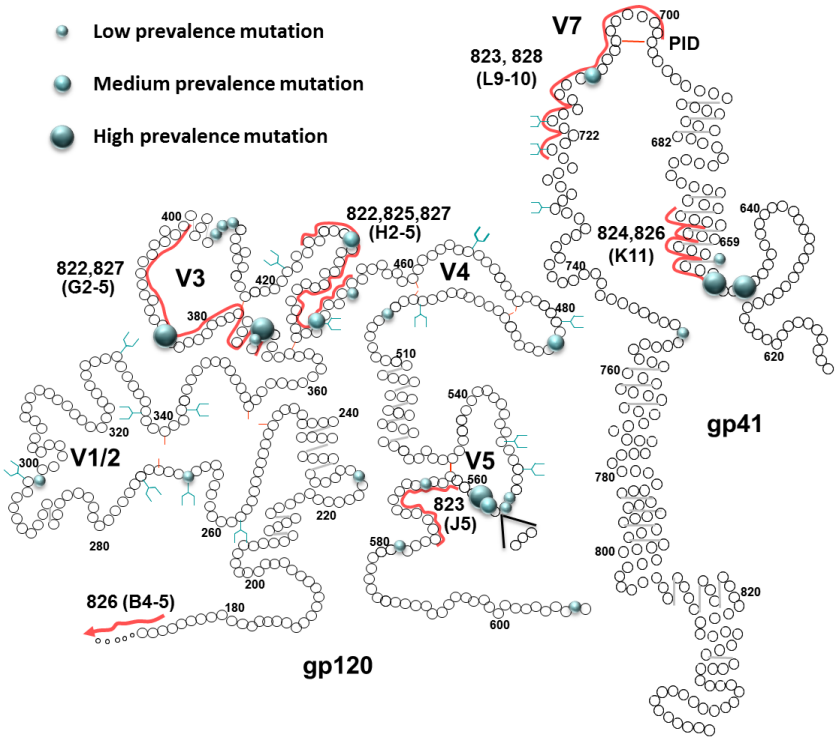


**Figure 4-3. Overlay of T cell epitopes and non-synonymous mutations.**
T cell epitopes were mapped in animals A822-A828 following infection with either clonal FIV-GL8 or FIV-GL8 derived artificial quasispecies for 21 weeks (Figure 3-26). Non-synonymous mutations were detected in animals A611-A613 at 322 weeks post-infection with clonal FIV-GL8 (Table 3-3). In the schematic FIV Env T cell epitopes are indicated by red lines. Mutations are denoted by spheres and sorted by prevalence (low: <50% of sequences mutated in one cat; medium: >50% of sequences mutated in one cat or low prevalence mutations in two cats; high: mutations in all three cats or >50% of sequences mutated in two cats). Mutations that occurred only once in a single cat were excluded from analysis.

Furthermore, the choice of virus strains is of major importance for FIV vaccine design. Experimental studies have demonstrated that FIV strains differ in their pathogenicity, ranging from relatively avirulent “laboratory adapted” strains such as FIV-PET (Talbott et al., 1989), to virulent strains such as FIV-GL8 (Hosie et al., 1995) and highly virulent FIV-CPG (Diehl et al., 1995). Limited protection against field isolates is a major concern regarding the commercially available FIV vaccine Fel-O-Vax®. While protection was afforded against low virulence strains including FIV-PET (Uhl et al., 2008), the vaccine failed to protect against more pathogenic strains such as FIV-GL8 (Dunham et al., 2006b; Hosie and Flynn, 1996). Our study indicates the use of immunogens based on pathogenic FIV-GL8-like “early” viruses as representative of the type of virus that is more likely to be transmitted and dominates during early infection. While targeting such viruses with a vaccine may not induce a sterilizing immunity, it may lead to a reduced viral burden, decelerated disease progression and decreased likelihood of transmission. The design of

vaccines that efficiently target FIV and HIV, inducing long-lasting and broad immunity remains one of the biggest obstacles in AIDS research.

# 5. Summary

Feline immunodeficiency virus (FIV) is a wide-spread pathogen of the domestic cat. In the course of FIV infection animals may develop clinical signs similar to that of human immunodeficiency virus (HIV) infected patients with acquired immunodeficiency syndrome (AIDS). This feature is unique for non-primate lentiviral infection and underlines the importance of FIV not only as a pathogen of veterinary significance but also as a valuable animal model for HIV infection. FIV enters its host cells, mainly CD4+ T helper cells, via an interaction of its envelope glycoprotein (Env) with the main receptor CD134 and the co-receptor CXCR4. The mode of interaction with these receptors differs between viral strains and by analogy to HIV, has been proposed to evolve in the course of infection. During replication retroviruses accumulate mutations through recombination between viral variants and through mis-incorporation of nucleotides due to error-prone reverse transcriptase, resulting in the emergence of a diverse viral population within the host. The appearance of such “quasispecies” is shaped by host factors such as the range of available target cells and the cellular and humoral immune system. Little is known about how FIV evolves during infection and why some cats develop immunodeficiency while others remain free of symptoms.

In this study we analysed the *in vivo* evolution of FIV following experimental infection of cats with a molecular clone of the FIV strain GL8 (FIV-GL8) for a period of either 12 weeks or 322 weeks. We identified viral variants within the viral population of long-term infected cats that displayed amino acid mutations throughout the whole Env protein. These mutations included substitutions, deletions and insertions of amino acids at residues previously described as determinants of receptor usage and resistance to humoral immune responses. Additionally, we performed phylogenetic analyses on FIV Env sequences isolated from lymphoid and non-lymphoid tissues of one long-term infected animal and present evidence for the compartmentalisation of FIV in the thymus and tonsil. Our sequence analyses also indicated that, in PBMCs, bone marrow, tonsil and thymus, FIV might be subjected to effects of APOBEC3, a viral restriction factor that induces lethal G-to-A mutations in viral genomes.

We characterised the biological properties of diverse Env variants derived from PBMCs of one long-term infected animal. We discovered variants that mirrored parental

virus FIV-GL8 in its requirement for a complex interaction with the entry receptor CD134, which is typical of virus isolated during acute infection. More importantly, we also identified variants, which displayed a simple interaction with CD134, which is characteristic for isolates from late stage infection. Further, we noted a range of sensitivities to inhibitors of viral entry and neutralising antibody. We show that this *in vivo* evolution was partly driven by escape from humoral immune response and we identified the V5 loop of FIV-GL8 Env as the major determinant of neutralisation.

Following the thorough examination of diverse viral phenotypes, we conducted an *in vivo* study to investigate whether such viral variety would be maintained following transmission. We compared the *in vivo* replication kinetics during infection with either a clonal preparation of FIV-GL8 or an artificial quasispecies comprising six viral variants that we had characterised phenotypically in the previous study. Both Group 1 (clonal infection) and Group 2 (mixed inoculum) animals displayed reduced levels of CD4+ lymphocytes and increased levels of CD8+ lymphocytes, while proviral loads were broadly similar. However, we detected marked differences in the proviral loads of single viral variants utilised in Group 2. Isolates most closely related to parental FIV-GL8 achieved higher proviral loads, while two more distantly related late stage variants failed to thrive following transmission. This block in replication did not stem from humoral or cellular immune responses as we could not detect neutralising antibodies or a correlation between detected T cell epitopes and the growth of certain isolates. However, our data indicates that the reduced replicative capability of the two late stage variants was associated with their modified interactions with the entry receptors. Our findings suggest that viral isolates with FIV-GL8-like characteristics possess an early replicate advantage and thus should be focussed on for future vaccine design.

# 6. Zusammenfassung

Das Feline Immundefizienz-Virus (FIV) ist ein weltweit verbreitetes Pathogen der Katze. FIV ist, wie das Humane Immundefizienz-Virus (HIV), ein Lentivirus und führt im Krankheitsverlauf bei infizierten Tieren zu Symptomen ähnlich dem Aquired Immune Deficiency Syndrome (AIDS) beim Menschen. Diese Analogien im Verlauf der Infektion machen FIV neben seiner veterinärmedizinischen Bedeutung zu einem wichtigen Tiermodel für die Untersuchung retroviraler Erkrankungen. FIV infiziert Wirtszellen über eine Interaktion der viralen Hüllproteine (Env) mit dem Hauptrezeptor CD134 und dem Korezeptor CXCR4. Hierbei bestehen virusstammspezifische Unterschiede in der Art der Rezeptorbindung und es wird vermutetet, dass ähnlich dem für HIV typischen Wechsel von Korezeptoren, im Verlauf der FIV-Erkrankung Veränderungen in der Env-Rezeptorinteraktion auftreten. Lentiviren ändern über den Infektionszeitraum permanent das Erscheinungsbild ihrer Hüllproteine. Mutationen ausgelöst durch Fehler in der Reversen Transkription und Rekombination von im Körper zirkulierenden Viren führen zur Entstehung variabler Viruspopulationen im erkrankten Individuum. Die Charakteristika solcher sogenannten viralen Quasispezies werden durch Wirtsfaktoren wie der Verfügbarkeit infizierbarer Zellen oder der Immunabwehr beeinflusst.

In der vorliegenden Studie wurde die Entwicklung des hüllproteinkodierenden FIV *env* Gens *in vivo* untersucht. Hierzu wurden zwei Versuchstiergruppen für 12 bzw. 322 Wochen mit einem Molekularklon des FIV-Stammes Glasgow 8 (FIV-GL8) infiziert und die Nukleotidsequenzen des *env* Gens in mononukleären Zellen des peripheren Blutes (PBMCs) analysiert. Über den Zeitraum von sechs Jahren entwickelten sich Env-Mutanten welche unter anderem Substitutionen, Insertionen und Deletionen von Aminosäuren an Stellen aufzeigten, die in früheren Studien mit der Rezeptorbindung bzw. Resistenz gegenüber neutralisierenden Antikörpern (NAbs) in Verbindung gebracht wurden. Zusätzlich offenbarte die phylogenetische Untersuchung des viralen *env* Gens in Organen einer langzeitinfizierten Katze Anzeichen einer isolierten FIV-Entwicklung in Thymus und Tonsillen. Des Weiteren deutete die Analyse viraler *env* Sequenzen aus PBMCs, Thymus, Tonsillen und Knochenmark auf eine Einwirkung des Restriktionsfaktor APOBEC3 hin, welcher durch die Induktion letaler G->A Mutationen im Virusgenom seine antivirale Wirksamkeit erzielt.

Im nächsten Schritt wurden *env* Gene von Viren einer der langzeitinfizierten Katzen kloniert und phänotypisch charakterisiert. Dabei zeigten sich isolatspezifische Unterschiede. Einige Viren interagierten, ähnlich wie das Ausgangsvirus FIV-GL8, mit dem Hauptrezeptor CD134 über zwei Bindungsdomänen. Dieses Verhalten ist typisch für Viren aus dem frühen Stadium der Infektion. Andere Virusvarianten hingegen zeigten charakteristische Eigenschaften von Viren aus späteren Stadien der Infektion. Diese infizieren Wirtzellen durch eine minimale Interaktion mit einer einzelnen Bindungsdomäne von CD134. Weiterhin zeigten die Virusisolate ein breites Spektrum an Sensitivitäten gegenüber NAbs und Inhibitoren der Rezeptorbindung. Die hierfür verantwortlichen Mutationen wurden, zumindest teilweise, durch eine gegen den V5 Loop des Env-Proteins gerichtete humorale Immunreaktion induziert.

Im Anschluss an die phänotypische Charakterisierung wurde untersucht, in welchem Ausmaß virale Diversität nach der Transmission auf ein gesundes Tier weiterbesteht. Hierzu wurden zwei Versuchstiergruppen entweder mit klonalem FIV-GL8 (Gruppe 1) oder einer künstlichen Quasispezies aus sechs Virusisolaten der Phänotypstudie infiziert (Gruppe 2). In beiden Gruppen zeigte sich der für FIV-Infektionen typische Abfall von CD4+ T-Zellen und ein Anstieg von CD8+ T-Zellen. Auch die Proviruslast war in beiden Gruppen vergleichbar hoch, jedoch zeigten sich Unterschiede im Replikationsverhalten einzelner Virusvarianten in Gruppe 2. Die mit dem Ausgangsvirus nah verwandten Isolate replizierten ähnlich gut wie FIV-GL8. Dagegen waren zwei entfernter mit FIV-GL8 verwandte, dem Spätstadiumtypus zuzuordnende Varianten, nur in geringen Mengen nachweisbar. Die verringerte Proviruslast dieser Isolate schien weder auf einer humoralen noch zellulären Immunreaktion zu basieren, da in den Tieren beider Gruppen keine NAbs nachgewiesen werden konnten und die detektierten T-Zell-Epitope keine Korrelation mit dem Wachstum bestimmter Isolate zeigten. In Anbetracht mangelnder Spezifizität der Immunreaktionen scheinen Unterschiede in der Rezeptorbindung die Ursache der verringerten Replikation der Spätstadiumisolate darzustellen. Unsere Studie legt einen Replikationsvorteil FIV-GL8-artiger Viren während der frühen Infektionsphase nahe, welcher vermutlich auch in natürlichen Infektionen auftritt. Daher sollten diese Viren bei der Entwicklung zukünftiger FIV-Impfstoffe stärker berücksichtigt werden.

# 7. Appendix 1: Primers and Probes

| Name | Sequence (5' to 3') |
|---|---|
| 1F4 | TGTAATCAACGYTTTGTKTCTCCTTACAG |
| 1R4 | CCAATAMTCWTCCCAGTCCACCCTT |
| 2F2 | TATTATTGGCARTTGCAATCTACMTTATC |
| ApaI7285F | CTGATCAATTATACGTTCGGGCCCAATCAAAC |
| ApaI7291R | CATGTTTGATTGGGCCCGAACGTATAATTG |
| AYSeqR | GCTTTYGCTATGCAAGAATTAGGATG |
| B14F | GTA CAA ATA GTA GTA GTA CAA ACA GTA GT |
| B19F | ATA TGA ATT GTA ATT GTA CAA ATA GCA GTA CA |
| B28F | CAA ATA GTA GTA GTA CAA ATC GGC AAA |
| B30F | GTA CAA ATA GTA GTA GTA CAA ATA GTA CA |
| BssHII7672R | CTACATCTAATCCTAAAGCGCGCTTC |
| BssHII7644F | ACTGAAGCGCGCTTTAGGATT |
| FIV108R | TTG GGT CAA GTG CTA CAT ATT G |
| FIV0771F | AGA ACC TGG TGA TAT ACC AGA GAC |
| FIV1010P | FAM-TAT GCC TGT GGA GGG CCT TCC T-TAMRA |
| FIV1360F | GCA GAA GCA AGA TTT GCA CCA |
| FIV1437R | TAT GGC GGC CAA TTT TCC T |
| FIV1416P | FAM-TGC CTC AAG ATA CCA TGC TCT ACA CTG CA-TAMRA |
| G8NotI8030R | GGGCGGCCGCTACCACTAAGTAATCTGGTT |
| G8V57829F | GCA TTT CAA TAT GAC AAA AGC T |
| GL8MluF | TAGACGCGTAAGATTTTTAAGGTATTC |
| GL8NdeR | AATGGATTCATATGACACATCTTCCTCAAAGGG |
| GL8NotI R | GGGCGGCCGCCATCATTCCTCCTCTTTTTCAGAC |
| GL8SalI F | GGGTCGACACCATGGCAGAAGGGTTTGCAGCA |
| MluSeqF | TAGAAGRGYAAGATWTTTAAGRTA |
| NheI8123R | TTGCAAGAGCTAGCATAACATGA |
| NheI8118F | GCTATTCATGTTATGCTAGCTCTTG |
| rDNA343F | CCA TTC GAA CGT CTG CCC TA |
| rDNA409R | TCA CCC GTG GTC ACC ATG |
| rDNA370P | FAM-CGA TGG TAG TCG CCG TGC CTA-TAMRA |
| Sal 7802 R | GCATAATAAGGTCGTCGACCTTCATAGTA |
| Sal 7799 F | GTTTACTATGAAGGTCGACGACCTTAT |
| V3R | AACCTAACCTTTGCAATGAGAAGT |
| V5R1 | GCT ACG GGG TTA TAC CAA TTT C |
| V5P1 | FAM-ATA GTG TTA AAA TGG CAT GTC CTA AAA ATC AAG GCA TCT-TAMRA |
| XF2B | TACTGCTTAGAAATATTTVTWWTAATATTTCATYTGCA |
| XR2 | CCTCAAAGGGAAGAAATCAGCTCA |
| XV5R | CCTGCYACTGGRTTRTACCA |
| XV6F | TATCAAGTDGTAAAACARCCAGADTA |
| XV6R | TAHTCTGGYTGTTTTACHACTTGATA |
| | |
| | M=A/C, K=G/T, R=G/A, Y=C/T, W=A/T, V=A/C/G, H=A/C/T, D=A/G/T |

# 8. Appendix 2: Buffers and solutions

| Name | Contents |
|---|---|
| AE Buffer | 10 mM Tris-Cl, 0.5 mM EDTA; pH 9.0. |
| LB agar | 1 % bactotryptone, 0.5% yeast extract, 1% NaCl, 1.5% agar |
| LB broth | 1% bactotryptone, 0.5% yeast extract, 0.5% NaCl; pH 7.0 |
| Loading dye (10X) | 60% glycerol, 0.25% bromophenol blue |
| PBS | 137 mM NaCl, 27 mM KCl, 2 mM KH2PO4,10.2 mM Na2HPO4; pH 7.4 |
| TBE | Tris base 89 mM, Boric acid 89 mM, EDTA 2 mM, pH 8.0 |
| TE Buffer | 10 mM Tris·Cl, pH 8.0, 1 mM EDTA |

# 9. Publications arising from this work

**Kraase M.**, Sloan R., Klein D., Logan N., McMonagle L., Biek R., Willett B. J. and Hosie M. J., 2010. Feline immunodeficiency virus env gene evolution in experimentally infected cats. Veterinary immunology and immunopathology 134, 96-106.

Willett B. J., **Kraase M.**, Logan N., McMonagle E., Varela M. and Hosie M. J., 2013. Selective expansion of viral variants following experimental transmission of a reconstituted feline immunodeficiency virus quasispecies. PloS one 8, e54871.

Willett B. J., **Kraase M.**, Logan N., McMonagle E. L., Samman A. and Hosie M. J., 2010. Modulation of the virus-receptor interaction by mutations in the V5 loop of feline immunodeficiency virus (FIV) following in vivo escape from neutralising antibody. Retrovirology 7, 38.

# 10. List of References

Aasa-Chapman M. M., Aubin K., Williams I. and McKnight A., 2006. Primary CCR5 only using HIV-1 isolates does not accurately represent the in vivo replicating quasi-species. Virology 351, 489-96.

Agace W. W., Amara A., Roberts A. I., Pablos J. L., Thelen S., Uguccioni M., Li X. Y., Marsal J., Arenzana-Seisdedos F., Delaunay T., Ebert E. C., Moser B. and Parker C. M., 2000. Constitutive expression of stromal derived factor-1 by mucosal epithelia and its role in HIV transmission and propagation. Current biology : CB 10, 325-8.

Alkhatib G., Combadiere C., Broder C. C., Feng Y., Kennedy P. E., Murphy P. M. and Berger E. A., 1996. CC CKR5: a RANTES, MIP-1alpha, MIP-1beta receptor as a fusion cofactor for macrophage-tropic HIV-1. Science (New York, N.Y.) 272, 1955-8.

Amoedo N. D., Afonso A. O., Cunha S. M., Oliveira R. H., Machado E. S. and Soares M. A., 2011. Expression of APOBEC3G/3F and G-to-A hypermutation levels in HIV-1-infected children with different profiles of disease progression. PloS one 6, e24118.

An P., Bleiber G., Duggal P., Nelson G., May M., Mangeat B., Alobwede I., Trono D., Vlahov D., Donfield S., Goedert J. J., Phair J., Buchbinder S., O'Brien S. J., Telenti A. and Winkler C. A., 2004. APOBEC3G genetic variants and their influence on the progression to AIDS. Journal of virology 78, 11070-6.

Arhel N., 2010. Revisiting HIV-1 uncoating. Retrovirology 7, 96.

Armitage A. E., Deforche K., Chang C. H., Wee E., Kramer B., Welch J. J., Gerstoft J., Fugger L., McMichael A., Rambaut A. and Iversen A. K., 2012. APOBEC3G-induced hypermutation of human immunodeficiency virus type-1 is typically a discrete "all or nothing" phenomenon. PLoS genetics 8, e1002550.

Asmal M., Hellmann I., Liu W., Keele B. F., Perelson A. S., Bhattacharya T., Gnanakaran S., Daniels M., Haynes B. F., Korber B. T., Hahn B. H., Shaw G. M. and Letvin N. L., 2011. A Signature in HIV-1 Envelope Leader Peptide Associated with Transition from Acute to Chronic Infection Impacts Envelope Processing and Infectivity. PloS one 6, e23673.

Bachmann M. H., Mathiason-Dubard C., Learn G. H., Rodrigo A. G., Sodora D. L., Mazzetti P., Hoover E. A. and Mullins J. I., 1997. Genetic diversity of feline immunodeficiency virus: dual infection, recombination, and distinct evolutionary rates among envelope sequence clades. Journal of virology 71, 4241-53.

Ball S. C., Abraha A., Collins K. R., Marozsan A. J., Baird H., Quinones-Mateu M. E., Penn-Nicholson A., Murray M., Richard N., Lobritz M., Zimmerman P. A., Kawamura T., Blauvelt A. and Arts E. J., 2003. Comparing the ex vivo fitness of CCR5-tropic human immunodeficiency virus type 1 isolates of subtypes B and C. Journal of virology 77, 1021-38.

Bar K. J., Tsao C. Y., Iyer S. S., Decker J. M., Yang Y., Bonsignori M., Chen X., Hwang K. K., Montefiori D. C., Liao H. X., Hraber P., Fischer W., Li H., Wang S., Sterrett S., Keele B. F., Ganusov V. V., Perelson A. S., Korber B. T., Georgiev I., McLellan J. S., Pavlicek J. W., Gao F., Haynes B. F., Hahn B. H., Kwong P. D. and Shaw G. M., 2012. Early low-titer neutralizing antibodies impede HIV-1 replication and select for virus escape. PLoS pathogens 8, e1002721.

Barlough J. E., Ackley C. D., George J. W., Levy N., Acevedo R., Moore P. F., Rideout B. A., Cooper M. D. and Pedersen N. C., 1991. Acquired immune dysfunction in cats with experimentally induced feline immunodeficiency virus infection: comparison of short-term and long-term infections. Journal of acquired immune deficiency syndromes 4, 219-27.

Barouch D. H. and Korber B., 2010. HIV-1 vaccine development after STEP. Annual review of medicine 61, 153-67.

Barre-Sinoussi F., Chermann J. C., Rey F., Nugeyre M. T., Chamaret S., Gruest J., Dauguet C., Axler-Blin C., Vezinet-Brun F., Rouzioux C., Rozenbaum W. and Montagnier L., 1983. Isolation of a T-lymphotropic retrovirus from a patient at risk for acquired immune deficiency syndrome (AIDS). Science (New York, N.Y.) 220, 868-71.

Beatty J. A., Willett B. J., Gault E. A. and Jarrett O., 1996. A longitudinal study of feline immunodeficiency virus-specific cytotoxic T lymphocytes in experimentally infected cats, using antigen-specific induction. Journal of virology 70, 6199-206.

Beebe A. M., Dua N., Faith T. G., Moore P. F., Pedersen N. C. and Dandekar S., 1994. Primary stage of feline immunodeficiency virus infection: viral dissemination and cellular targets. Journal of virology 68, 3080-91.

Bello G., Velasco-de-Castro C. A., Bongertz V., Rodrigues C. A., Giacoia-Gripp C. B., Pilotto J. H., Grinsztejn B., Veloso V. G. and Morgado M. G., 2009. Immune activation and antibody responses in non-progressing elite controller individuals infected with HIV-1. Journal of medical virology 81, 1681-90.

Bendinelli M., Pistello M., Del Mauro D., Cammarota G., Maggi F., Leonildi A., Giannecchini S., Bergamini C. and Matteucci D., 2001. During readaptation in vivo, a tissue culture-adapted strain of feline immunodeficiency virus reverts to broad neutralization resistance at different times in individual hosts but through changes at the same position of the surface glycoprotein. Journal of virology 75, 4584-93.

Bernstein H. B., Tucker S. P., Hunter E., Schutzbach J. S. and Compans R. W., 1994. Human immunodeficiency virus type 1 envelope glycoprotein is modified by O-linked oligosaccharides. Journal of virology 68, 463-8.

Biasin M., Piacentini L., Lo Caputo S., Kanari Y., Magri G., Trabattoni D., Naddeo V., Lopalco L., Clivio A., Cesana E., Fasano F., Bergamaschi C., Mazzotta F., Miyazawa M. and Clerici M., 2007. Apolipoprotein B mRNA-editing enzyme, catalytic polypeptide-like 3G: a possible role in the resistance to HIV of HIV-exposed seronegative individuals. The Journal of infectious diseases 195, 960-4.

Biek R., Rodrigo A. G., Holley D., Drummond A., Anderson C. R., Ross H. A. and Poss M., 2003. Epidemiology, Genetic Diversity, and Evolution of Endemic Feline Immunodeficiency Virus in a Population of Wild Cougars. Journal of virology 77, 9578-9589.

Bishop K. N., Verma M., Kim E.-Y., Wolinsky S. M. and Malim M. H., 2008. APOBEC3G Inhibits Elongation of HIV-1 Reverse Transcripts. PLoS pathogens 4, e1000231.

Bishop S. A., Stokes C. R., Gruffydd-Jones T. J., Whiting C. V. and Harbour D. A., 1996. Vaginal and rectal infection of cats with feline immunodeficiency virus. Veterinary microbiology 51, 217-227.

Blankson J. N., 2010. Effector mechanisms in HIV-1 infected elite controllers: highly active immune responses? Antiviral research 85, 295-302.

Bleul C. C., Farzan M., Choe H., Parolin C., Clark-Lewis I., Sodroski J. and Springer T. A., 1996. The lymphocyte chemoattractant SDF-1 is a ligand for LESTR/fusin and blocks HIV-1 entry. Nature 382, 829-33.

Bleul C. C., Wu L., Hoxie J. A., Springer T. A. and Mackay C. R., 1997. The HIV coreceptors CXCR4 and CCR5 are differentially expressed and regulated on human T lymphocytes. Proceedings of the National Academy of Sciences of the United States of America 94, 1925-30.

Borrow P., Lewicki H., Hahn B. H., Shaw G. M. and Oldstone M. B., 1994. Virus-specific CD8+ cytotoxic T-lymphocyte activity associated with control of viremia in primary human immunodeficiency virus type 1 infection. Journal of virology 68, 6103-10.

Brown P. O., 1997. Integration. In Coffin J. M., Hughes S. H. and Varmus H. E. (Eds.), Cold Spring Harbor Laboratory Press, Cold Spring Harbor NY.

Brown R. J., Peters P. J., Caron C., Gonzalez-Perez M. P., Stones L., Ankghuambom C., Pondei K., McClure C. P., Alemnji G., Taylor S., Sharp P. M., Clapham P. R. and Ball J. K., 2011. Intercompartmental recombination of HIV-1 contributes to env intrahost diversity and modulates viral tropism and sensitivity to entry inhibitors. Journal of virology 85, 6024-37.

Browne E. P. and Littman D. R., 2008. Species-specific restriction of apobec3-mediated hypermutation. Journal of virology 82, 1305-13.

Bukrinskaya A., Brichacek B., Mann A. and Stevenson M., 1998. Establishment of a functional human immunodeficiency virus type 1 (HIV-1) reverse transcription complex involves the cytoskeleton. The Journal of experimental medicine 188, 2113-25.

Burkhard M. J. and Dean G. A., 2003. Transmission and immunopathogenesis of FIV in cats as a model for HIV. Current HIV research 1, 15-29.

Callanan J. J., Jones B. A., Irvine J., Willett B. J., McCandlish I. A. P. and Jarrett O., 1996. Histologic classification and immunophenotype of lymphosarcomas in cats with naturally and experimentally acquired feline immunodeficiency virus infections. Veterinary pathology 33, 264-272.

Callanan J. J., Thompson H., Toth S. R., O'Neil B., Lawrence C. E., Willett B. and Jarrett O., 1992. Clinical and pathological findings in feline immunodeficiency virus experimental infection. Veterinary immunology and immunopathology 35, 3-13.

Cammarota G., Matteucci D., Pistello M., Nicoletti E., Giannecchini S. and Bendinelli M., 1996. Reduced sensitivity to strain-specific neutralization of laboratory-adapted feline immunodeficiency virus after one passage in vivo: association with amino acid substitutions in the V4 region of the surface glycoprotein. AIDS research and human retroviruses 12, 173-175.

Carpenter M. A., Brown E. W., MacDonald D. W. and O'Brien S J., 1998. Phylogeographic patterns of feline immunodeficiency virus genetic diversity in the domestic cat. Virology 251, 234-43.

Cen S., Peng Z. G., Li X. Y., Li Z. R., Ma J., Wang Y. M., Fan B., You X. F., Wang Y. P., Liu F., Shao R. G., Zhao L. X., Yu L. and Jiang J. D., 2010. Small molecular compounds inhibit HIV-1 replication through specifically stabilizing APOBEC3G. The Journal of biological chemistry 285, 16546-52.

Chams V., Jouault T., Fenouillet E., Gluckman J. C. and Klatzmann D., 1988. Detection of anti-CD4 autoantibodies in the sera of HIV-infected patients using recombinant soluble CD4 molecules. AIDS (London, England) 2, 353-61.

Cheney C. M., Rojko J. L., Kociba G. J., Wellman M. L., Dibartola S. P., Rezanka L. J., Forman L. and Mathes L. E., 1990. A FELINE LARGE GRANULAR LYMPHOMA AND ITS DERIVED CELL-LINE. In Vitro Cellular & Developmental Biology 26, 455-463.

Cheung M. C., Pantanowitz L. and Dezube B. J., 2005. AIDS-related malignancies: emerging challenges in the era of highly active antiretroviral therapy. The oncologist 10, 412-26.

Choi I. S., Hokanson R. and Collisson E. W., 2000. Anti-feline immunodeficiency virus (FIV) soluble factor(s) produced from antigen-stimulated feline CD8(+) T lymphocytes suppresses FIV replication. Journal of virology 74, 676-83.

Collman R., Hassan N. F., Walker R., Godfrey B., Cutilli J., Hastings J. C., Friedman H., Douglas S. D. and Nathanson N., 1989. Infection of monocyte-derived macrophages with human immunodeficiency virus type 1 (HIV-1). Monocyte-tropic and lymphocyte-tropic strains of HIV-1 show distinctive patterns of replication in a panel of cell types. The Journal of experimental medicine 170, 1149-63.

Connor R. I., Chen B. K., Choe S. and Landau N. R., 1995. Vpr is required for efficient replication of human immunodeficiency virus type-1 in mononuclear phagocytes. Virology 206, 935-44.

Connor R. I., Sheridan K. E., Ceradini D., Choe S. and Landau N. R., 1997. Change in coreceptor use correlates with disease progression in HIV-1--infected individuals. The Journal of experimental medicine 185, 621-8.

Corre J. P., Fevrier M., Chamaret S., Theze J. and Zouali M., 1991. Anti-idiotypic antibodies to human anti-gp120 antibodies bind recombinant and cellular human CD4. European journal of immunology 21, 743-51.

Courchamp F. and Pontier D., 1994. Feline immunodeficiency virus: an epidemiological review. Comptes rendus de l'Academie des sciences. Serie III, Sciences de la vie 317, 1123-34.

Cronn R., Cedroni M., Haselkorn T., Grover C. and Wendel J. F., 2002. PCR-mediated recombination in amplification products derived from polyploid cotton. TAG. Theoretical and applied genetics. Theoretische und angewandte Genetik 104, 482-489.

Dacheux L., Moreau A., Ataman-Önal Y., Biron F., Verrier B. and Barin F., 2004. Evolutionary Dynamics of the Glycan Shield of the Human Immunodeficiency Virus Envelope during Natural Infection and Implications for Exposure of the 2G12 Epitope. Journal of virology 78, 12625-12637.

Damond F., Worobey M., Campa P., Farfara I., Colin G., Matheron S., Brun-Vezinet F., Robertson D. L. and Simon F., 2004. Identification of a highly divergent HIV type 2 and proposal for a change in HIV type 2 classification. AIDS research and human retroviruses 20, 666-72.

David S. A., Smith M. S., Lopez G. J., Adany I., Mukherjee S., Buch S., Goodenow M. M. and Narayan O., 2001. Selective transmission of R5-tropic HIV type 1 from dendritic cells to resting CD4+ T cells. AIDS research and human retroviruses 17, 59-68.

de Parseval A., Chatterji U., Morris G., Sun P., Olson A. J. and Elder J. H., 2005. Structural mapping of CD134 residues critical for interaction with feline immunodeficiency virus. Nature structural & molecular biology 12, 60-6.

de Parseval A., Chatterji U., Sun P. and Elder J. H., 2004. Feline immunodeficiency virus targets activated CD4+ T cells by using CD134 as a binding receptor. Proceedings of the National Academy of Sciences of the United States of America 101, 13044-9.

de Parseval A. and Elder J. H., 1999. Demonstration that orf2 encodes the feline immunodeficiency virus transactivating (Tat) protein and characterization of a unique gene product with partial rev activity. Journal of virology 73, 608-17.

de Parseval A. and Elder J. H., 2001. Binding of recombinant feline immunodeficiency virus surface glycoprotein to feline cells: role of CXCR4, cell-surface heparans, and an unidentified non-CXCR4 receptor. Journal of virology 75, 4528-39.

de Parseval A., Grant C. K., Sastry K. J. and Elder J. H., 2006. Sequential CD134-CXCR4 interactions in feline immunodeficiency virus (FIV): soluble CD134 activates FIV Env for CXCR4-dependent entry and reveals a cryptic neutralization epitope. Journal of virology 80, 3088-91.

de Silva T. I., Aasa-Chapman M., Cotten M., Hue S., Robinson J., Bibollet-Ruche F., Sarge-Njie R., Berry N., Jaye A., Aaby P., Whittle H., Rowland-Jones S. and Weiss R., 2012. Potent autologous and heterologous neutralizing antibody responses occur in HIV-2 infection across a broad range of infection outcomes. Journal of virology 86, 930-46.

Dean G. A., LaVoy A. and Burkhard M. J., 2004. Peptide mapping of feline immunodeficiency virus by IFN-gamma ELISPOT. Veterinary immunology and immunopathology 100, 49-59.

Dean G. A., Reubel G. H., Moore P. F. and Pedersen N. C., 1996. Proviral burden and infection kinetics of feline immunodeficiency virus in lymphocyte subsets of blood and lymph node. Journal of virology 70, 5165-9.

Delon J. and Germain R. N., 2000. Information transfer at the immunological synapse. Current biology : CB 10, R923-33.

Delwart E. L., Mullins J. I., Gupta P., Learn G. H., Jr., Holodniy M., Katzenstein D., Walker B. D. and Singh M. K., 1998. Human immunodeficiency virus type 1 populations in blood and semen. Journal of virology 72, 617-23.

Delwart E. L., Pan H., Sheppard H. W., Wolpert D., Neumann A. U., Korber B. and Mullins J. I., 1997. Slower evolution of human immunodeficiency virus type 1 quasispecies during progression to AIDS. Journal of virology 71, 7498-7508.

Diehl L. J., Mathiason-Dubard C. K., O'Neil L. L., Obert L. A. and Hoover E. A., 1995. Induction of accelerated feline immunodeficiency virus disease by acute-phase virus passage. Journal of virology 69, 6149-57.

Dietrich I., 2013. Feline restriction factors to lentiviral replication, Vol. PhD Thesis, University of Glasgow.

Dietrich I., McMonagle E. L., Petit S. J., Vijayakrishnan S., Logan N., Chan C. N., Towers G. J., Hosie M. J. and Willett B. J., 2011. Feline tetherin efficiently restricts release of feline immunodeficiency virus but not spreading of infection. Journal of virology 85, 5840-52.

Domingo E. and Holland J. J., 1997. RNA virus mutations and fitness for survival. Annual review of microbiology 51, 151-78.

Donzella G. A., Schols D., Lin S. W., Este J. A., Nagashima K. A., Maddon P. J., Allaway G. P., Sakmar T. P., Henson G., De Clercq E. and Moore J. P., 1998. AMD3100, a small molecule inhibitor of HIV-1 entry via the CXCR4 co-receptor. Nature medicine 4, 72-7.

Dow S. W., Dreitz M. J. and Hoover E. A., 1992. Feline immunodeficiency virus neurotropism: evidence that astrocytes and microglia are the primary target cells. Veterinary immunology and immunopathology 35, 23-35.

Dow S. W., Mathiason C. K. and Hoover E. A., 1999. In vivo monocyte tropism of pathogenic feline immunodeficiency viruses. Journal of virology 73, 6852-61.

Dragic T., Litwin V., Allaway G. P., Martin S. R., Huang Y., Nagashima K. A., Cayanan C., Maddon P. J., Koup R. A., Moore J. P. and Paxton W. A., 1996. HIV-1 entry into CD4+ cells is mediated by the chemokine receptor CC-CKR-5. Nature 381, 667-73.

Driscoll C. A., Menotti-Raymond M., Roca A. L., Hupe K., Johnson W. E., Geffen E., Harley E. H., Delibes M., Pontier D., Kitchener A. C., Yamaguchi N., O'Brien S J. and Macdonald D. W., 2007. The Near Eastern origin of cat domestication. Science (New York, N.Y.) 317, 519-23.

Drummond A. J. and Rambaut A., 2007. BEAST: Bayesian evolutionary analysis by sampling trees. Bmc Evolutionary Biology 7.

Dunham S. P., Bruce J., Klein D., Flynn J. N., Golder M. C., MacDonald S., Jarrett O. and Neil J. C., 2006a. Prime-boost vaccination using DNA and whole inactivated virus vaccines provides limited protection against virulent feline immunodeficiency virus. Vaccine 24, 7095-108.

Dunham S. P., Bruce J., MacKay S., Golder M., Jarrett O. and Neil J. C., 2006b. Limited efficacy of an inactivated feline immunodeficiency virus vaccine. Veterinary Record 158, 561-562.

Eastman D., Piantadosi A., Wu X., Forthal D. N., Landucci G., Kimata J. T. and Overbaugh J., 2008. Heavily glycosylated, highly fit SIVMne variants continue to diversify and undergo selection after transmission to a new host and they elicit early antibody dependent cellular responses but delayed neutralizing antibody responses. Virology Journal 5.

Egberink H. F., De Clercq E., Van Vliet A. L., Balzarini J., Bridger G. J., Henson G., Horzinek M. C. and Schols D., 1999. Bicyclams, selective antagonists of the human chemokine receptor CXCR4, potently inhibit feline immunodeficiency virus replication. Journal of virology 73, 6346-52.

Eigen M., 1971. Selforganization of matter and the evolution of biological macromolecules. Die Naturwissenschaften 58, 465-523.

Elder J. H., Lin Y. C., Fink E. and Grant C. K., 2010. Feline immunodeficiency virus (FIV) as a model for study of lentivirus infections: parallels with HIV. Current HIV research 8, 73-80.

Elder J. H., Sundstrom M., de Rozieres S., de Parseval A., Grant C. K. and Lin Y. C., 2008. Molecular mechanisms of FIV infection. Veterinary immunology and immunopathology 123, 3-13.

Endres M. J., Clapham P. R., Marsh M., Ahuja M., Turner J. D., McKnight A., Thomas J. F., Stoebenau-Haggarty B., Choe S., Vance P. J., Wells T. N., Power C. A., Sutterwala S. S., Doms R. W., Landau N. R. and Hoxie J. A., 1996. CD4-independent infection by HIV-2 is mediated by fusin/CXCR4. Cell 87, 745-56.

English R. V., Johnson C. M., Gebhard D. H. and Tompkins M. B., 1993. In vivo lymphocyte tropism of feline immunodeficiency virus. Journal of virology 67, 5175-86.

Feng Y., Broder C. C., Kennedy P. E. and Berger E. A., 1996. HIV-1 entry cofactor: functional cDNA cloning of a seven-transmembrane, G protein-coupled receptor. Science (New York, N.Y.) 272, 872-7.

Ferrantelli F. and Ruprecht R. M., 2002. Neutralizing antibodies against HIV -- back in the major leagues? Current opinion in immunology 14, 495-502.

Fitzgibbon J. E., Mazar S. and Dubin D. T., 1993. A new type of G-->A hypermutation affecting human immunodeficiency virus. AIDS research and human retroviruses 9, 833-8.

Flynn J. N., Cannon C. A., Lawrence C. E. and Jarrett O., 1994. Polyclonal B-cell activation in cats infected with feline immunodeficiency virus. Immunology 81, 626-30.

Flynn J. N., Cannon C. A., Neil J. C. and Jarrett O., 1997. Vaccination with a feline immunodeficiency virus multiepitopic peptide induces cell-

mediated and humoral immune responses in cats, but does not confer protection. Journal of virology 71, 7586-92.

Flynn J. N., Dunham S., Mueller A., Cannon C. and Jarrett O., 2002. Involvement of cytolytic and non-cytolytic T cells in the control of feline immunodeficiency virus infection. Veterinary immunology and immunopathology 85, 159-70.

Fourati S., Malet I., Binka M., Boukobza S., Wirden M., Sayon S., Simon A., Katlama C., Simon V., Calvez V. and Marcelin A. G., 2010. Partially active HIV-1 Vif alleles facilitate viral escape from specific antiretrovirals. AIDS (London, England) 24, 2313-21.

Gabor L. J., Love D. N., Malik R. and Canfield P. J., 2001. Feline immunodeficiency virus status of Australian cats with lymphosarcoma. Australian veterinary journal 79, 540-5.

Gallo R. C., Salahuddin S. Z., Popovic M., Shearer G. M., Kaplan M., Haynes B. F., Palker T. J., Redfield R., Oleske J., Safai B. and et al., 1984. Frequent detection and isolation of cytopathic retroviruses (HTLV-III) from patients with AIDS and at risk for AIDS. Science (New York, N.Y.) 224, 500-3.

Gallo S. A., Puri A. and Blumenthal R., 2001. HIV-1 gp41 six-helix bundle formation occurs rapidly after the engagement of gp120 by CXCR4 in the HIV-1 Env-mediated fusion process. Biochemistry 40, 12231-6.

Gao F., Bailes E., Robertson D. L., Chen Y., Rodenburg C. M., Michael S. F., Cummins L. B., Arthur L. O., Peeters M., Shaw G. M., Sharp P. M. and Hahn B. H., 1999. Origin of HIV-1 in the chimpanzee Pan troglodytes troglodytes. Nature 397, 436-41.

Gaufin T., Ribeiro R. M., Gautam R., Dufour J., Mandell D., Apetrei C. and Pandrea I., 2010. Experimental depletion of CD8+ cells in acutely SIVagm-infected African Green Monkeys results in increased viral replication. Retrovirology 7, 42.

Gemeniano M. C., Sawai E. T., Leutenegger C. M. and Sparger E. E., 2003. Feline immunodeficiency virus ORF-Ais required for virus particle formation and virus infectivity. Journal of virology 77, 8819-30.

Gendelman H. E., Orenstein J. M., Martin M. A., Ferrua C., Mitra R., Phipps T., Wahl L. A., Lane H. C., Fauci A. S., Burke D. S. and et al., 1988. Efficient isolation and propagation of human immunodeficiency virus on recombinant colony-stimulating factor 1-treated monocytes. The Journal of experimental medicine 167, 1428-41.

Giannecchini S., Bonci F., Pistello M., Matteucci D., Sichi O., Rovero P. and Bendinelli M., 2004. The membrane-proximal tryptophan-rich region in the transmembrane glycoprotein ectodomain of feline immunodeficiency virus is important for cell entry. Virology 320, 156-66.

Giannecchini S., D'Ursi A. M., Esposito C., Scrima M., Zabogli E., Freer G., Rovero P. and Bendinelli M., 2007. Antibodies generated in cats by a lipopeptide reproducing the membrane-proximal external region of the feline immunodeficiency virus transmembrane enhance virus infectivity. Clinical and vaccine immunology : CVI 14, 944-51.

Giannecchini S., Di Fenza A., D'Ursi A. M., Matteucci D., Rovero P. and Bendinelli M., 2003. Antiviral activity and conformational features of an octapeptide derived from the membrane-proximal ectodomain of the feline immunodeficiency virus transmembrane glycoprotein. Journal of virology 77, 3724-33.

Giannecchini S., Matteucci D., Ferrari A., Pistello M. and Bendinelli M., 2001. Feline immunodeficiency virus-infected cat sera associated with the development of broad neutralization resistance in vivo drive similar reversions in vitro. Journal of virology 75, 8868-73.

Gillick K., Pollpeter D., Phalora P., Kim E. Y., Wolinsky S. M. and Malim M. H., 2013. Suppression of HIV-1 infection by APOBEC3 proteins in primary human CD4(+) T cells is associated with inhibition of processive reverse transcription as well as excessive cytidine deamination. Journal of virology 87, 1508-17.

Gnanakaran S., Bhattacharya T., Daniels M., Keele B. F., Hraber P. T., Lapedes A. S., Shen T., Gaschen B., Krishnamoorthy M., Li H., Decker J. M., Salazar-Gonzalez J. F., Wang S., Jiang C., Gao F., Swanstrom R., Anderson J. A., Ping L. H., Cohen M. S., Markowitz M., Goepfert P. A., Saag M. S., Eron J. J., Hicks C. B., Blattner W. A., Tomaras G. D., Asmal M., Letvin N. L., Gilbert P. B., Decamp A. C., Magaret C. A., Schief W. R., Ban Y. E., Zhang M., Soderberg K. A., Sodroski J. G., Haynes B. F., Shaw G. M., Hahn B. H. and Korber B., 2011. Recurrent signature patterns in HIV-1 B clade envelope glycoproteins associated with either early or chronic infections. PLoS pathogens 7, e1002209.

Gonzalez-Scarano F. and Martin-Garcia J., 2005. The neuropathogenesis of AIDS. Nature reviews. Immunology 5, 69-81.

Graham F. L., Smiley J., Russell W. C. and Nairn R., 1977. CHARACTERISTICS OF A HUMAN CELL LINE TRANSFORMED BY DNA FROM HUMAN ADENOVIRUS TYPE-5. Journal of General Virology 36, 59-72.

Gramaglia I., Weinberg A. D., Lemon M. and Croft M., 1998. Ox-40 ligand: a potent costimulatory molecule for sustaining primary CD4 T cell responses. Journal of immunology (Baltimore, Md. : 1950) 161, 6510-7.

Grant C. K., Fink E. A., Sundstrom M., Torbett B. E. and Elder J. H., 2009. Improved health and survival of FIV-infected cats is associated with the presence of autoantibodies to the primary receptor, CD134. Proceedings of the National Academy of Sciences of the United States of America 106, 19980-5.

Gray L., Sterjovski J., Churchill M., Ellery P., Nasr N., Lewin S. R., Crowe S. M., Wesselingh S. L., Cunningham A. L. and Gorry P. R., 2005. Uncoupling coreceptor usage of human immunodeficiency virus type 1 (HIV-1) from macrophage tropism reveals biological properties of CCR5-restricted HIV-1 isolates from patients with acquired immunodeficiency syndrome. Virology 337, 384-98.

Greene W. K., Meers J., del Fierro G., Carnegie P. R. and Robinson W. F., 1993. Extensive sequence variation of feline immunodeficiency virus env genes in isolates from naturally infected cats. Archives of virology 133, 51-62.

Grivel J. C., Shattock R. J. and Margolis L. B., 2011. Selective transmission of R5 HIV-1 variants: where is the gatekeeper? Journal of translational medicine 9 Suppl 1, S6.

Hallenberger S., Bosch V., Angliker H., Shaw E., Klenk H. D. and Garten W., 1992. Inhibition of furin-mediated cleavage activation of HIV-1 glycoprotein gp160. Nature 360, 358-61.

Harris R. S., Bishop K. N., Sheehy A. M., Craig H. M., Petersen-Mahrt S. K., Watt I. N., Neuberger M. S. and Malim M. H., 2003. DNA deamination mediates innate immunity to retroviral infection. Cell 113, 803-9.

Hartikka J., Sawdey M., CornefertJensen F., Margalith M., Barnhart K., Nolasco M., Vahlsing H. L., Meek J., Marquet M., Hobart P., Norman J. and Manthorpe M., 1996. An improved plasmid DNA expression vector for direct injection into skeletal muscle. Human Gene Therapy 7, 1205-1217.

Hasegawa M., Kishino H. and Yano T., 1985. Dating of the human-ape splitting by a molecular clock of mitochondrial DNA. Journal of molecular evolution 22, 160-74.

Hayward J. J. and Rodrigo A. G., 2008. Recombination in feline immunodeficiency virus from feral and companion domestic cats. Virology Journal 5, 76.

Hayward J. J. and Rodrigo A. G., 2010. Molecular epidemiology of feline immunodeficiency virus in the domestic cat (Felis catus). Veterinary immunology and immunopathology 134, 68-74.

Hein A., Schuh H., Thiel S., Martin J. P. and Dorries R., 2003. Ramified feline microglia selects for distinct variants of feline immunodeficiency virus during early central nervous system infection. Journal of neurovirology 9, 465-76.

Holmes C. B., Losina E., Walensky R. P., Yazdanpanah Y. and Freedberg K. A., 2003. Review of human immunodeficiency virus type 1-related opportunistic infections in sub-Saharan Africa. Clinical infectious diseases : an official publication of the Infectious Diseases Society of America 36, 652-62.

Holmes R. K., Koning F. A., Bishop K. N. and Malim M. H., 2007. APOBEC3F can inhibit the accumulation of HIV-1 reverse transcription products in the absence of hypermutation. Comparisons with APOBEC3G. The Journal of biological chemistry 282, 2587-95.

Hooks J. J. and Gibbs C. J., Jr., 1975. The foamy viruses. Bacteriological reviews 39, 169-85.

Hosie M. J. and Beatty J. A., 2007. Vaccine protection against feline immunodeficiency virus: setting the challenge. Australian veterinary journal 85, 5-12.

Hosie M. J., Broere N., Hesselgesser J., Turner J. D., Hoxie J. A., Neil J. C. and Willett B. J., 1998a. Modulation of feline immunodeficiency virus infection by stromal cell-derived factor. Journal of virology 72, 2097-104.

Hosie M. J., Dunsford T., Klein D., Willett B. J., Cannon C., Osborne R., Macdonald J., Spibey N., Mackay N., Jarrett O. and Neil J. C., 2000. Vaccination with inactivated virus but not viral DNA reduces virus load following challenge with a heterologous and virulent isolate of feline immunodeficiency virus. Journal of virology 74, 9403-11.

Hosie M. J. and Flynn J. N., 1996. Feline immunodeficiency virus vaccination: characterization of the immune correlates of protection. Journal of virology 70, 7561-8.

Hosie M. J., Flynn J. N., Rigby M. A., Cannon C., Dunsford T., Mackay N. A., Argyle D., Willett B. J., Miyazawa T., Onions D. E., Jarrett O. and Neil J. C., 1998b. DNA vaccination affords significant protection against feline immunodeficiency virus infection without inducing detectable antiviral antibodies. Journal of virology 72, 7310-9.

Hosie M. J., Osborne R., Yamamoto J. K., Neil J. C. and Jarrett O., 1995. Protection against homologous but not heterologous challenge induced by inactivated feline immunodeficiency virus vaccines. Journal of virology 69, 1253-5.

Hosie M. J., Pajek D., Samman A. and Willett B. J., 2011. Feline immunodeficiency virus (FIV) neutralization: a review. Viruses 3, 1870-90.

Hosie M. J., Robertson C. and Jarrett O., 1989. Prevalence of feline leukaemia virus and antibodies to feline immunodeficiency virus in cats in the United Kingdom. The Veterinary record 125, 293-7.

Hosie M. J., Willett B. J., Klein D., Dunsford T. H., Cannon C., Shimojima M., Neil J. C. and Jarrett O., 2002. Evolution of replication efficiency following infection with a molecularly cloned feline immunodeficiency virus of low virulence. Journal of virology 76, 6062-72.

Hu Q. Y., Fink E. and Elder J. H., 2012. Mapping of Receptor Binding Interactions with the FIV surface Glycoprotein (SU); Implications Regarding Immune surveillance and cellular Targets of Infection. Retrovirology 2012, 1-11.

Huang C., Conlee D., Loop J., Champ D., Gill M. and Chu H. J., 2004. Efficacy and safety of a feline immunodeficiency virus vaccine. Animal health research reviews / Conference of Research Workers in Animal Diseases 5, 295-300.

Huang X., Barchi J. J., Jr., Lung F. D., Roller P. P., Nara P. L., Muschik J. and Garrity R. R., 1997. Glycosylation affects both the three-dimensional structure and antibody binding properties of the HIV-1IIIB GP120 peptide RP135. Biochemistry 36, 10846-56.

Huisman W., Schrauwen E. J. A., Rimmelzwaan G. F. and Osterhaus A. D. M. E., 2008. Intrahost evolution of envelope glycoprotein and OrfA sequences after experimental infection of cats with a molecular clone and a biological isolate of feline immunodeficiency virus. Virus Research 137, 24-32.

Hutson C. A., Rideout B. A. and Pedersen N. C., 1991. Neoplasia associated with feline immunodeficiency virus infection in cats of southern California. Journal of the American Veterinary Medical Association 199, 1357-62.

Ikeda Y., Miyazawa T., Nishimura Y., Nakamura K., Tohya Y. and Mikami T., 2004. High genetic stability of TM1 and TM2 strains of subtype B feline immunodeficiency virus in long-term infection. Journal of Veterinary Medical Science 66, 287-289.

Ishida T., Taniguchi A., Matsumura S., Washizu T. and Tomoda I., 1992. Long-term clinical observations on feline immunodeficiency virus infected asymptomatic carriers. Veterinary immunology and immunopathology 35, 15-22.

Janini M., Rogers M., Birx D. R. and McCutchan F. E., 2001. Human immunodeficiency virus type 1 DNA sequences genetically damaged by hypermutation are often abundant in patient peripheral blood mononuclear cells and may be generated during near-simultaneous infection and activation of CD4(+) T cells. Journal of virology 75, 7973-86.

Jones P. L., Korte T. and Blumenthal R., 1998. Conformational changes in cell surface HIV-1 envelope glycoproteins are triggered by cooperation between cell surface CD4 and co-receptors. The Journal of biological chemistry 273, 404-9.

Kakinuma S., Motokawa K., Hohdatsu T., Yamamoto J. K., Koyama H. and Hashimoto H., 1995. Nucleotide sequence of feline immunodeficiency virus: Classification of Japanese isolates into two subtypes which are distinct from non-Japanese subtypes. Journal of virology 69, 3639-3646.

Kane M., Case L. K. and Golovkina T. V., 2011. Vital role for CD8+ cells in controlling retroviral infections. Journal of virology 85, 3415-23.

Kao S., Goila-Gaur R., Miyagi E., Khan M. A., Opi S., Takeuchi H. and Strebel K., 2007. Production of infectious virus and degradation of APOBEC3G are separable functional properties of human immunodeficiency virus type 1 Vif. Virology 369, 329-39.

Karlsson Hedestam G. B., Fouchier R. A., Phogat S., Burton D. R., Sodroski J. and Wyatt R. T., 2008. The challenges of eliciting neutralizing antibodies to HIV-1 and to influenza virus. Nature reviews. Microbiology 6, 143-55.

Keele B. F., Van Heuverswyn F., Li Y., Bailes E., Takehisa J., Santiago M. L., Bibollet-Ruche F., Chen Y., Wain L. V., Liegeois F., Loul S., Ngole E. M., Bienvenue Y., Delaporte E., Brookfield J. F., Sharp P. M., Shaw G. M., Peeters M. and Hahn B. H., 2006. Chimpanzee reservoirs of pandemic and nonpandemic HIV-1. Science (New York, N.Y.) 313, 523-6.

Kemal K. S., Foley B., Burger H., Anastos K., Minkoff H., Kitchen C., Philpott S. M., Gao W., Robison E., Holman S., Dehner C., Beck S., Meyer W. A., 3rd, Landay A., Kovacs A., Bremer J. and Weiser B., 2003. HIV-1 in genital tract and plasma of women: compartmentalization of viral sequences, coreceptor usage, and glycosylation. Proceedings of the National Academy of Sciences of the United States of America 100, 12972-7.

Kemler I., Barraza R. and Poeschla E. M., 2002. Mapping the encapsidation determinants of feline immunodeficiency virus. Journal of virology 76, 11889-903.

Kim E. Y., Bhattacharya T., Kunstman K., Swantek P., Koning F. A., Malim M. H. and Wolinsky S. M., 2010. Human APOBEC3G-mediated editing can promote HIV-1 sequence diversification and accelerate adaptation to selective pressure. Journal of virology 84, 10402-5.

Kimura M., 1980. A simple method for estimating evolutionary rates of base substitutions through comparative studies of nucleotide sequences. Journal of molecular evolution 16, 111-20.

Klein D., Bugl B., Gunzburg W. H. and Salmons B., 2000. Accurate estimation of transduction efficiency necessitates a multiplex real-time PCR. Gene therapy 7, 458-63.

Klein D., Leutenegger C. M., Bahula C., Gold P., Hofmann-Lehmann R., Salmons B., Lutz H. and Gunzburg W. H., 2001. Influence of preassay and sequence variations on viral load determination by a multiplex real-time reverse transcriptase-polymerase chain reaction for feline immunodeficiency virus. Journal of acquired immune deficiency syndromes (1999) 26, 8-20.

Kobayashi M., Takaori-Kondo A., Miyauchi Y., Iwai K. and Uchiyama T., 2005. Ubiquitination of APOBEC3G by an HIV-1 Vif-Cullin5-Elongin B-Elongin C

complex is essential for Vif function. The Journal of biological chemistry 280, 18573-8.

Kohl N. E., Emini E. A., Schleif W. A., Davis L. J., Heimbach J. C., Dixon R. A., Scolnick E. M. and Sigal I. S., 1988. Active human immunodeficiency virus protease is required for viral infectivity. Proceedings of the National Academy of Sciences of the United States of America 85, 4686-90.

Kong R., Li H., Bibollet-Ruche F., Decker J. M., Zheng N. N., Gottlieb G. S., Kiviat N. B., Sow P. S., Georgiev I., Hahn B. H., Kwong P. D., Robinson J. E. and Shaw G. M., 2012. Broad and potent neutralizing antibody responses elicited in natural HIV-2 infection. Journal of virology 86, 947-60.

Kopf M., Ruedl C., Schmitz N., Gallimore A., Lefrang K., Ecabert B., Odermatt B. and Bachmann M. F., 1999. OX40-deficient mice are defective in Th cell proliferation but are competent in generating B cell and CTL Responses after virus infection. Immunity 11, 699-708.

Koup R. A., Safrit J. T., Cao Y., Andrews C. A., McLeod G., Borkowsky W., Farthing C. and Ho D. D., 1994. Temporal association of cellular immune responses with the initial control of viremia in primary human immunodeficiency virus type 1 syndrome. Journal of virology 68, 4650-5.

Kourteva Y., De Pasquale M., Allos T., McMunn C. and D'Aquila R. T., 2012. APOBEC3G expression and hypermutation are inversely associated with human immunodeficiency virus type 1 (HIV-1) burden in vivo. Virology 430, 1-9.

Kraase M., Sloan R., Klein D., Logan N., McMonagle L., Biek R., Willett B. J. and Hosie M. J., 2010. Feline immunodeficiency virus env gene evolution in experimentally infected cats. Veterinary immunology and immunopathology 134, 96-106.

Labrijn A. F., Poignard P., Raja A., Zwick M. B., Delgado K., Franti M., Binley J., Vivona V., Grundner C., Huang C. C., Venturi M., Petropoulos C. J., Wrin T., Dimitrov D. S., Robinson J., Kwong P. D., Wyatt R. T., Sodroski J. and Burton D. R., 2003. Access of antibody molecules to the conserved coreceptor binding site on glycoprotein gp120 is sterically restricted on primary human immunodeficiency virus type 1. Journal of virology 77, 10557-65.

Lambotte O., Ferrari G., Moog C., Yates N. L., Liao H. X., Parks R. J., Hicks C. B., Owzar K., Tomaras G. D., Montefiori D. C., Haynes B. F. and Delfraissy J. F., 2009. Heterogeneous neutralizing antibody and antibody-dependent cell cytotoxicity responses in HIV-1 elite controllers. AIDS (London, England) 23, 897-906.

Latza U., Durkop H., Schnittger S., Ringeling J., Eitelbach F., Hummel M., Fonatsch C. and Stein H., 1994. The human OX40 homolog: cDNA

structure, expression and chromosomal assignment of the ACT35 antigen. European journal of immunology 24, 677-83.

Lawrence C. E., Callanan J. J., Willett B. J. and Jarrett O., 1995. Cytokine production by cats infected with feline immunodeficiency virus: a longitudinal study. Immunology 85, 568-74.

Leonard C. K., Spellman M. W., Riddle L., Harris R. J., Thomas J. N. and Gregory T. J., 1990. Assignment of intrachain disulfide bonds and characterization of potential glycosylation sites of the type 1 recombinant human immunodeficiency virus envelope glycoprotein (gp120) expressed in Chinese hamster ovary cells. The Journal of biological chemistry 265, 10373-82.

Lerner D. L., Wagaman P. C., Phillips T. R., Prospero-Garcia O., Henriksen S. J., Fox H. S., Bloom F. E. and Elder J. H., 1995. Increased mutation frequency of feline immunodeficiency virus lacking functional deoxyuridine-triphosphatase. Proceedings of the National Academy of Sciences of the United States of America 92, 7480-4.

Liang Y., Hudson L. C., Levy J. K., Ritchey J. W., Tompkins W. A. and Tompkins M. B., 2000. T cells overexpressing interferon-gamma and interleukin-10 are found in both the thymus and secondary lymphoid tissues of feline immunodeficiency virus-infected cats. The Journal of infectious diseases 181, 564-75.

Liddament M. T., Brown W. L., Schumacher A. J. and Harris R. S., 2004. APOBEC3F properties and hypermutation preferences indicate activity against HIV-1 in vivo. Current biology : CB 14, 1385-91.

Liu P., Hudson L. C., Tompkins M. B., Vahlenkamp T. W. and Meeker R. B., 2006. Compartmentalization and evolution of feline immunodeficiency virus between the central nervous system and periphery following intracerebroventricular or systemic inoculation. Journal of neurovirology 12, 307-21.

Luttge B. G. and Freed E. O., 2010. FIV Gag: virus assembly and host-cell interactions. Veterinary immunology and immunopathology 134, 3-13.

MacNeil A., Sarr A. D., Sankalé J. L., Meloni S. T., Mboup S. and Kanki P., 2007. Direct evidence of lower viral replication rates in vivo in human immunodeficiency virus type 2 (HIV-2) infection than in HIV-1 infection. Journal of virology 81, 5325-5330.

Malim M. H. and Bieniasz P. D., 2012. HIV Restriction Factors and Mechanisms of Evasion. Cold Spring Harbor perspectives in medicine 2, a006940.

Mangeat B., Turelli P., Caron G., Friedli M., Perrin L. and Trono D., 2003. Broad antiretroviral defence by human APOBEC3G through lethal editing of nascent reverse transcripts. Nature 424, 99-103.

Mansky L. M. and Temin H. M., 1995. Lower in vivo mutation rate of human immunodeficiency virus type 1 than that predicted from the fidelity of purified reverse transcriptase. Journal of virology 69, 5087-94.

Margolis L. and Shattock R., 2006. Selective transmission of CCR5-utilizing HIV-1: the 'gatekeeper' problem resolved? Nature reviews. Microbiology 4, 312-7.

Marozsan A. J., Moore D. M., Lobritz M. A., Fraundorf E., Abraha A., Reeves J. D. and Arts E. J., 2005. Differences in the fitness of two diverse wild-type human immunodeficiency virus type 1 isolates are related to the efficiency of cell binding and entry. Journal of virology 79, 7121-34.

Marshall R. D., 1974. The nature and metabolism of the carbohydrate-peptide linkages of glycoproteins. Biochemical Society symposium, 17-26.

McDonald D., Vodicka M. A., Lucero G., Svitkina T. M., Borisy G. G., Emerman M. and Hope T. J., 2002. Visualization of the intracellular behavior of HIV in living cells. The Journal of cell biology 159, 441-52.

McGrath K. M., Hoffman N. G., Resch W., Nelson J. A. E. and Swanstrom R., 2001. Using HIV-1 sequence variability to explore virus biology. Virus Research 76, 137-160.

McKnight A. and Clapham P. R., 1995. Immune escape and tropism of HIV. Trends Microbiol 3, 356-61.

Mehle A., Strack B., Ancuta P., Zhang C., McPike M. and Gabuzda D., 2004. Vif overcomes the innate antiviral activity of APOBEC3G by promoting its degradation in the ubiquitin-proteasome pathway. The Journal of biological chemistry 279, 7792-8.

Miyazawa T., Furuya T., Itagaki S., Tohya Y., Takahashi E. and Mikami T., 1989. ESTABLISHMENT OF A FELINE T-LYMPHOBLASTOID CELL-LINE HIGHLY SENSITIVE FOR REPLICATION OF FELINE IMMUNODEFICIENCY VIRUS. Archives of virology 108, 131-135.

Miyazawa T., Tomonaga K., Kawaguchi Y. and Mikami T., 1994. The genome of feline immunodeficiency virus. Archives of virology 134, 221-234.

Moog C., Fleury H. J., Pellegrin I., Kirn A. and Aubertin A. M., 1997. Autologous and heterologous neutralizing antibody responses following initial seroconversion in human immunodeficiency virus type 1-infected individuals. Journal of virology 71, 3734-41.

Motokawa K., Hohdatsu T., Imori A., Arai S. and Koyama H., 2005. Mutations in feline immunodeficiency (FIV) virus envelope gene V3-V5 regions in FIV-infected cats. Veterinary microbiology 106, 33-40.

Mulder L. C., Harari A. and Simon V., 2008. Cytidine deamination induced HIV-1 drug resistance. Proceedings of the National Academy of Sciences of the United States of America 105, 5501-6.

Munk C., Beck T., Zielonka J., Hotz-Wagenblatt A., Chareza S., Battenberg M., Thielebein J., Cichutek K., Bravo I. G., O'Brien S. J., Lochelt M. and Yuhki N., 2008. Functions, structure, and read-through alternative splicing of feline APOBEC3 genes. Genome biology 9, R48.

Munk C., Jensen B. E., Zielonka J., Haussinger D. and Kamp C., 2012. Running loose or getting lost: how HIV-1 counters and capitalizes on APOBEC3-induced mutagenesis through its Vif protein. Viruses 4, 3132-61.

Murakami T. and Freed E. O., 2000. Genetic evidence for an interaction between human immunodeficiency virus type 1 matrix and alpha-helix 2 of the gp41 cytoplasmic tail. Journal of virology 74, 3548-54.

Mussil B., Sauermann U., Motzkus D., Stahl-Hennig C. and Sopper S., 2011. Increased APOBEC3G and APOBEC3F expression is associated with low viral load and prolonged survival in simian immunodeficiency virus infected rhesus monkeys. Retrovirology 8, 77.

Nabatov A. A., Pollakis G., Linnemann T., Kliphius A., Chalaby M. I. M. and Paxton W. A., 2004. Intrapatient Alterations in the Human Immunodeficiency Virus Type 1 gp120 V1V2 and V3 Regions Differentially Modulate Coreceptor Usage, Virus Inhibition by CC/CXC Chemokines, Soluble CD4, and the b12 and 2G12 Monoclonal Antibodies. Journal of virology 78, 524-530.

Naganawa S., Yokoyama M., Shiino T., Suzuki T., Ishigatsubo Y., Ueda A., Shirai A., Takeno M., Hayakawa S., Sato S., Tochikubo O., Kiyoura S., Sawada K., Ikegami T., Kanda T., Kitamura K. and Sato H., 2008. Net positive charge of HIV-1 CRF01_AE V3 sequence regulates viral sensitivity to humoral immunity. PloS one 3, e3206.

Neher R. A. and Leitner T., 2010. Recombination rate and selection strength in HIV intra-patient evolution. PLoS computational biology 6, e1000660.

Neil S. J., Aasa-Chapman M. M., Clapham P. R., Nibbs R. J., McKnight A. and Weiss R. A., 2005. The promiscuous CC chemokine receptor D6 is a functional coreceptor for primary isolates of human immunodeficiency virus type 1 (HIV-1) and HIV-2 on astrocytes. Journal of virology 79, 9618-24.

Newman E. N., Holmes R. K., Craig H. M., Klein K. C., Lingappa J. R., Malim M. H. and Sheehy A. M., 2005. Antiviral function of APOBEC3G can be dissociated from cytidine deaminase activity. Current biology : CB 15, 166-70.

O'Neil L. L., Burkhard M. J., Diehl L. J. and Hoover E. A., 1995. Vertical transmission of feline immunodeficiency virus. AIDS research and human retroviruses 11, 171-82.

Oberlin E., Amara A., Bachelerie F., Bessia C., Virelizier J. L., Arenzana-Seisdedos F., Schwartz O., Heard J. M., Clark-Lewis I., Legler D. F., Loetscher M., Baggiolini M. and Moser B., 1996. The CXC chemokine SDF-1 is the ligand for LESTR/fusin and prevents infection by T-cell-line-adapted HIV-1. Nature 382, 833-5.

Ohagen A., Devitt A., Kunstman K. J., Gorry P. R., Rose P. P., Korber B., Taylor J., Levy R., Murphy R. L., Wolinsky S. M. and Gabuzda D., 2003. Genetic and functional analysis of full-length human immunodeficiency virus type 1 env genes derived from brain and blood of patients with AIDS. Journal of virology 77, 12336-45.

Okeoma C. M., Huegel A. L., Lingappa J., Feldman M. D. and Ross S. R., 2010. APOBEC3 proteins expressed in mammary epithelial cells are packaged into retroviruses and can restrict transmission of milk-borne virions. Cell host & microbe 8, 534-43.

Okeoma C. M., Lovsin N., Peterlin B. M. and Ross S. R., 2007. APOBEC3 inhibits mouse mammary tumour virus replication in vivo. Nature 445, 927-30.

Olmsted R. A., Hirsch V. M., Purcell R. H. and Johnson P. R., 1989. Nucleotide sequence analysis of feline immunodeficiency virus: Genome organization and relationship to other lentiviruses. Proceedings of the National Academy of Sciences of the United States of America 86, 8088-8092.

Opi S., Kao S., Goila-Gaur R., Khan M. A., Miyagi E., Takeuchi H. and Strebel K., 2007. Human immunodeficiency virus type 1 Vif inhibits packaging and antiviral activity of a degradation-resistant APOBEC3G variant. Journal of virology 81, 8236-46.

Osborne R., Rigby M., Siebelink K., Neil J. C. and Jarrett O., 1994. Virus neutralization reveals antigenic variation among feline immunodeficiency virus isolates. The Journal of general virology 75 ( Pt 12), 3641-5.

Paillot R., Richard S., Bloas F., Piras F., Poulet H., Brunet S., Andreoni C. and Juillard V., 2005. Toward a detailed characterization of feline immunodeficiency virus-specific T cell immune responses and mediated immune disorders. Veterinary immunology and immunopathology 106, 1-14.

Pancino G., Fossati I., Chappey C., Castelot S., Hurtrel B., Moraillon A., Klatzmann D. and Sonigo P., 1993. Structure and variations of feline immunodeficiency virus envelope glycoproteins. Virology 192, 659-62.

Pancino G. and Sonigo P., 1997. Retention of viral infectivity after extensive mutation of the highly conserved immunodominant domain of the feline immunodeficiency virus envelope. Journal of virology 71, 4339-46.

Pantaleo G., Demarest J. F., Soudeyns H., Graziosi C., Denis F., Adelsberger J. W., Borrow P., Saag M. S., Shaw G. M., Sekaly R. P. and et al., 1994. Major expansion of CD8+ T cells with a predominant V beta usage during the primary immune response to HIV. Nature 370, 463-7.

Pecon-Slattery J., Troyer J. L., Johnson W. E. and O'Brien S. J., 2008. Evolution of feline immunodeficiency virus in Felidae: implications for human health and wildlife ecology. Veterinary immunology and immunopathology 123, 32-44.

Pecoraro M. R., Tomonaga K., Miyazawa T., Kawaguchi Y., Sugita S., Tohya Y., Kai C., Etcheverrigaray M. E. and Mikami T., 1996. Genetic diversity of Argentine isolates of feline immunodeficiency virus. The Journal of general virology 77 ( Pt 9), 2031-5.

Pedersen N. C., Ho E. W., Brown M. L. and Yamamoto J. K., 1987. Isolation of a T-lymphotropic virus from domestic cats with an immunodeficiency-like syndrome. Science (New York, N.Y.) 235, 790-3.

Peng G., Lei K. J., Jin W., Greenwell-Wild T. and Wahl S. M., 2006. Induction of APOBEC3 family proteins, a defensive maneuver underlying interferon-induced anti-HIV-1 activity. The Journal of experimental medicine 203, 41-6.

Perelson A. S., Neumann A. U., Markowitz M., Leonard J. M. and Ho D. D., 1996. HIV-1 dynamics in vivo: virion clearance rate, infected cell life-span, and viral generation time. Science (New York, N.Y.) 271, 1582-6.

Peters P. J., Sullivan W. M., Duenas-Decamp M. J., Bhattacharya J., Ankghuambom C., Brown R., Luzuriaga K., Bell J., Simmonds P., Ball J. and Clapham P. R., 2006. Non-macrophage-tropic human immunodeficiency virus type 1 R5 envelopes predominate in blood, lymph nodes, and semen: implications for transmission and pathogenesis. Journal of virology 80, 6324-32.

Phillips T. R., Lamont C., Konings D. A., Shacklett B. L., Hamson C. A., Luciw P. A. and Elder J. H., 1992. Identification of the Rev transactivation and Rev-responsive elements of feline immunodeficiency virus. Journal of virology 66, 5464-71.

Philpott S., Burger H., Tsoukas C., Foley B., Anastos K., Kitchen C. and Weiser B., 2005. Human immunodeficiency virus type 1 genomic RNA sequences in the female genital tract and blood: compartmentalization and intrapatient recombination. Journal of virology 79, 353-63.

Pippig S. D., Pena-Rossi C., Long J., Godfrey W. R., Fowell D. J., Reiner S. L., Birkeland M. L., Locksley R. M., Barclay A. N. and Killeen N., 1999. Robust B cell immunity but impaired T cell proliferation in the absence of CD134 (OX40). Journal of immunology (Baltimore, Md. : 1950) 163, 6520-9.

Pistello M., Cammarota G., Nicoletti E., Matteucci D., Curcio M., Del Mauro D. and Bendinelli M., 1997. Analysis of the genetic diversity and phylogenetic relationship of Italian isolates of feline immunodeficiency virus indicates a high prevalence and heterogeneity of subtype B. Journal of General Virology 78, 2247-2257.

Pistello M., Matteucci D., Bonci F., Isola P., Mazzetti P., Zaccaro L., Merico A., Del Mauro D., Flynn N. and Bendinelli M., 2003. AIDS vaccination studies using an ex vivo feline immunodeficiency virus model: protection from an intraclade challenge administered systemically or mucosally by an attenuated vaccine. Journal of virology 77, 10740-50.

Poeschla E. M. and Looney D. J., 1998. CXCR4 is required by a nonprimate lentivirus: heterologous expression of feline immunodeficiency virus in human, rodent, and feline cells. Journal of virology 72, 6858-66.

Pond S. L. and Frost S. D., 2005a. Datamonkey: rapid detection of selective pressure on individual sites of codon alignments. Bioinformatics (Oxford, England) 21, 2531-3.

Pond S. L. K. and Frost S. D. W., 2005b. Not so different after all: A comparison of methods for detecting amino acid sites under selection. Molecular Biology and Evolution 22, 1208-1222.

Posada D. and Crandall K. A., 1998. MODELTEST: testing the model of DNA substitution. Bioinformatics (Oxford, England) 14, 817-8.

Rangel H. R., Weber J., Chakraborty B., Gutierrez A., Marotta M. L., Mirza M., Kiser P., Martinez M. A., Este J. A. and Quinones-Mateu M. E., 2003. Role of the human immunodeficiency virus type 1 envelope gene in viral fitness. Journal of virology 77, 9069-73.

Reeves J. D., Hibbitts S., Simmons G., McKnight A., Azevedo-Pereira J. M., Moniz-Pereira J. and Clapham P. R., 1999. Primary human immunodeficiency virus type 2 (HIV-2) isolates infect CD4-negative cells via CCR5 and CXCR4: comparison with HIV-1 and simian immunodeficiency virus and relevance to cell tropism in vivo. Journal of virology 73, 7795-804.

Reggeti F., Ackerley C. and Bienzle D., 2008. CD134 and CXCR4 expression corresponds to feline immunodeficiency virus infection of lymphocytes, macrophages and dendritic cells. The Journal of general virology 89, 277-87.

Reggeti F. and Bienzle D., 2004. Feline immunodeficiency virus subtypes A, B and C and intersubtype recombinants in Ontario, Canada. The Journal of general virology 85, 1843-52.

Rerks-Ngarm S., Pitisuttithum P., Nitayaphan S., Kaewkungwal J., Chiu J., Paris R., Premsri N., Namwat C., de Souza M., Adams E., Benenson M., Gurunathan S., Tartaglia J., McNeil J. G., Francis D. P., Stablein D., Birx D. L., Chunsuttiwat S., Khamboonruang C., Thongcharoen P., Robb M. L., Michael N. L., Kunasol P. and Kim J. H., 2009. Vaccination with ALVAC and AIDSVAX to prevent HIV-1 infection in Thailand. The New England journal of medicine 361, 2209-20.

Richardson J., Pancino G., Merat R., Leste-Lasserre T., Moraillon A., Schneider-Mergener J., Alizon M., Sonigo P. and Heveker N., 1999. Shared Usage of the Chemokine Receptor CXCR4 by Primary and Laboratory-Adapted Strains of Feline Immunodeficiency Virus. Journal of virology 73, 3661-3671.

Richman D. D., Wrin T., Little S. J. and Petropoulos C. J., 2003. Rapid evolution of the neutralizing antibody response to HIV type 1 infection. Proceedings of the National Academy of Sciences of the United States of America 100, 4144-9.

Rideout B. A., Lowensteine L. J., Hutson C. A., Moore P. F. and Pedersen N. C., 1992. Characterization of morphologic changes and lymphocyte subset distribution in lymph nodes from cats with naturally acquired feline immunodeficiency virus infection. Veterinary pathology 29, 391-9.

Roberts J. D., Bebenek K. and Kunkel T. A., 1988. The accuracy of reverse transcriptase from HIV-1. Science (New York, N.Y.) 242, 1171-3.

Rodrigo A. G., Goracke P. C., Rowhanian K. and Mullins J. I., 1997. Quantitation of target molecules from polymerase chain reaction-based limiting dilution assays. AIDS research and human retroviruses 13, 737-42.

Rose P. P. and Korber B. T., 2000. Detecting hypermutations in viral sequences with an emphasis on G --> A hypermutation. Bioinformatics (Oxford, England) 16, 400-1.

Rossio J. L., Esser M. T., Suryanarayana K., Schneider D. K., Bess J. W., Jr., Vasquez G. M., Wiltrout T. A., Chertova E., Grimes M. K., Sattentau Q., Arthur L. O., Henderson L. E. and Lifson J. D., 1998. Inactivation of human immunodeficiency virus type 1 infectivity with preservation of conformational and functional integrity of virion surface proteins. Journal of virology 72, 7992-8001.

Ryan G., Klein D., Knapp E., Hosie M. J., Grimes T., Mabruk M. J., Jarrett O. and Callanan J. J., 2003. Dynamics of viral and proviral loads of feline immunodeficiency virus within the feline central nervous system during

the acute phase following intravenous infection. Journal of virology 77, 7477-85.

Sagar M., Lavreys L., Baeten J. M., Richardson B. A., Mandaliya K., Chohan B. H., Kreiss J. K. and Overbaugh J., 2003. Infection with multiple human immunodeficiency virus type 1 variants is associated with faster disease progression. Journal of virology 77, 12921-6.

Salazar-Gonzalez J. F., Salazar M. G., Keele B. F., Learn G. H., Giorgi E. E., Li H., Decker J. M., Wang S., Baalwa J., Kraus M. H., Parrish N. F., Shaw K. S., Guffey M. B., Bar K. J., Davis K. L., Ochsenbauer-Jambor C., Kappes J. C., Saag M. S., Cohen M. S., Mulenga J., Derdeyn C. A., Allen S., Hunter E., Markowitz M., Hraber P., Perelson A. S., Bhattacharya T., Haynes B. F., Korber B. T., Hahn B. H. and Shaw G. M., 2009. Genetic identity, biological phenotype, and evolutionary pathways of transmitted/founder viruses in acute and early HIV-1 infection. The Journal of experimental medicine 206, 1273-89.

Samman A., Logan N., McMonagle E. L., Ishida T., Mochizuki M., Willett B. J. and Hosie M. J., 2010. Neutralization of feline immunodeficiency virus by antibodies targeting the V5 loop of Env. The Journal of general virology 91, 242-9.

Sanjuan R., Moya A. and Elena S. F., 2004. The distribution of fitness effects caused by single-nucleotide substitutions in an RNA virus. Proceedings of the National Academy of Sciences of the United States of America 101, 8396-401.

Santiago M. L., Montano M., Benitez R., Messer R. J., Yonemoto W., Chesebro B., Hasenkrug K. J. and Greene W. C., 2008. Apobec3 encodes Rfv3, a gene influencing neutralizing antibody control of retrovirus infection. Science (New York, N.Y.) 321, 1343-6.

Schaller T., Ocwieja K. E., Rasaiyaah J., Price A. J., Brady T. L., Roth S. L., Hue S., Fletcher A. J., Lee K., KewalRamani V. N., Noursadeghi M., Jenner R. G., James L. C., Bushman F. D. and Towers G. J., 2011. HIV-1 capsid-cyclophilin interactions determine nuclear import pathway, integration targeting and replication efficiency. PLoS pathogens 7, e1002439.

Seidel A., Ye Y., de Armas L. R., Soto M., Yarosh W., Marcsisin R. A., Tran D., Selsted M. E. and Camerini D., 2010. Cyclic and acyclic defensins inhibit human immunodeficiency virus type-1 replication by different mechanisms. PloS one 5, e9737.

Shankarappa R., Margolick J. B., Gange S. J., Rodrigo A. G., Upchurch D., Farzadegan H., Gupta P., Rinaldo C. R., Learn G. H., He X., Huang X. L. and Mullins J. I., 1999. Consistent viral evolutionary changes associated with the progression of human immunodeficiency virus type 1 infection. Journal of virology 73, 10489-10502.

Shapiro B., Rambaut A. and Drummond A. J., 2006. Choosing appropriate substitution models for the phylogenetic analysis of protein-coding sequences. Molecular Biology and Evolution 23, 7-9.

Sheehy A. M., Gaddis N. C., Choi J. D. and Malim M. H., 2002. Isolation of a human gene that inhibits HIV-1 infection and is suppressed by the viral Vif protein. Nature 418, 646-50.

Shimojima M., Miyazawa T., Ikeda Y., McMonagle E. L., Haining H., Akashi H., Takeuchi Y., Hosie M. J. and Willett B. J., 2004. Use of CD134 as a primary receptor by the feline immunodeficiency virus. Science (New York, N.Y.) 303, 1192-5.

Shiver J. W., Fu T. M., Chen L., Casimiro D. R., Davies M. E., Evans R. K., Zhang Z. Q., Simon A. J., Trigona W. L., Dubey S. A., Huang L., Harris V. A., Long R. S., Liang X., Handt L., Schleif W. A., Zhu L., Freed D. C., Persaud N. V., Guan L., Punt K. S., Tang A., Chen M., Wilson K. A., Collins K. B., Heidecker G. J., Fernandez V. R., Perry H. C., Joyce J. G., Grimm K. M., Cook J. C., Keller P. M., Kresock D. S., Mach H., Troutman R. D., Isopi L. A., Williams D. M., Xu Z., Bohannon K. E., Volkin D. B., Montefiori D. C., Miura A., Krivulka G. R., Lifton M. A., Kuroda M. J., Schmitz J. E., Letvin N. L., Caulfield M. J., Bett A. J., Youil R., Kaslow D. C. and Emini E. A., 2002. Replication-incompetent adenoviral vaccine vector elicits effective anti-immunodeficiency-virus immunity. Nature 415, 331-5.

Siebelink K. H., Huisman W., Karlas J. A., Rimmelzwaan G. F., Bosch M. L. and Osterhaus A. D., 1995. Neutralization of feline immunodeficiency virus by polyclonal feline antibody: simultaneous involvement of hypervariable regions 4 and 5 of the surface glycoprotein. Journal of virology 69, 5124-7.

Simmons G., Reeves J. D., McKnight A., Dejucq N., Hibbitts S., Power C. A., Aarons E., Schols D., De Clercq E., Proudfoot A. E. and Clapham P. R., 1998. CXCR4 as a functional coreceptor for human immunodeficiency virus type 1 infection of primary macrophages. Journal of virology 72, 8453-7.

Sodora D. L., Shpaer E. G., Kitchell B. E., Dow S. W., Hoover E. A. and Mullins J. I., 1994. Identification of three feline immunodeficiency virus (FIV) env gene subtypes and comparison of the FIV and human immunodeficiency virus type 1 evolutionary patterns. Journal of virology 68, 2230-8.

Sodroski J. G., 1999. HIV-1 entry inhibitors in the side pocket. Cell 99, 243-6.

Sparger E. E., Luciw P. A., Elder J. H., Yamamoto J. K., Lowenstine L. J. and Pedersen N. C., 1989. Feline immunodeficiency virus is a lentivirus associated with an AIDS-like disease in cats. AIDS (London, England) 3 Suppl 1, S43-9.

Spenlehauer C., Kirn A., Aubertin A. M. and Moog C., 2001. Antibody-mediated neutralization of primary human immunodeficiency virus type 1 isolates:

investigation of the mechanism of inhibition. Journal of virology 75, 2235-45.

Spijkerman I. J., Koot M., Prins M., Keet I. P., van den Hoek A. J., Miedema F. and Coutinho R. A., 1995. Lower prevalence and incidence of HIV-1 syncytium-inducing phenotype among injecting drug users compared with homosexual men. AIDS (London, England) 9, 1085-92.

Starcich B. R., Hahn B. H., Shaw G. M., McNeely P. D., Modrow S., Wolf H., Parks E. S., Parks W. P., Josephs S. F., Gallo R. C. and et al., 1986. Identification and characterization of conserved and variable regions in the envelope gene of HTLV-III/LAV, the retrovirus of AIDS. Cell 45, 637-48.

Steagall W. K., Robek M. D., Perry S. T., Fuller F. J. and Payne S. L., 1995. Incorporation of uracil into viral DNA correlates with reduced replication of EIAV in macrophages. Virology 210, 302-13.

Steinrigl A. and Klein D., 2003. Phylogenetic analysis of feline immunodeficiency virus in Central Europe: a prerequisite for vaccination and molecular diagnostics. The Journal of general virology 84, 1301-7.

Stern M. A., Hu C., Saenz D. T., Fadel H. J., Sims O., Peretz M. and Poeschla E. M., 2010. Productive replication of Vif-chimeric HIV-1 in feline cells. Journal of virology 84, 7378-95.

Sundstrom M., Chatterji U., Schaffer L., de Rozieres S. and Elder J. H., 2008. Feline immunodeficiency virus OrfA alters gene expression of splicing factors and proteasome-ubiquitination proteins. Virology 371, 394-404.

Takeda E., Tsuji-Kawahara S., Sakamoto M., Langlois M. A., Neuberger M. S., Rada C. and Miyazawa M., 2008. Mouse APOBEC3 restricts friend leukemia virus infection and pathogenesis in vivo. Journal of virology 82, 10998-1008.

Talbott R. L., Sparger E. E., Lovelace K. M., Fitch W. M., Pedersen N. C., Luciw P. A. and Elder J. H., 1989. Nucleotide sequence and genomic organization of feline immunodeficiency virus. Proceedings of the National Academy of Sciences of the United States of America 86, 5743-7.

Tamura K., Peterson D., Peterson N., Stecher G., Nei M. and Kumar S., 2011. MEGA5: Molecular Evolutionary Genetics Analysis Using Maximum Likelihood, Evolutionary Distance, and Maximum Parsimony Methods. Molecular Biology and Evolution 28, 2731-2739.

Tanabe T. and Yamamoto J. K., 2001. Phenotypic and functional characteristics of FIV infection in the bone marrow stroma. Virology 282, 113-22.

Taswell C., 1981. Limiting dilution assays for the determination of immunocompetent cell frequencies. I. Data analysis. Journal of immunology (Baltimore, Md. : 1950) 126, 1614-9.

Temin H. M. and Mizutani S., 1970. RNA-dependent DNA polymerase in virions of Rous sarcoma virus. Nature 226, 1211-3.

Thomas E. R., Dunfee R. L., Stanton J., Bogdan D., Taylor J., Kunstman K., Bell J. E., Wolinsky S. M. and Gabuzda D., 2007. Macrophage entry mediated by HIV Envs from brain and lymphoid tissues is determined by the capacity to use low CD4 levels and overall efficiency of fusion. Virology 360, 105-19.

Thomas M. J., Platas A. A. and Hawley D. K., 1998. Transcriptional fidelity and proofreading by RNA polymerase II. Cell 93, 627-37.

Thompson J. D., Higgins D. G. and Gibson T. J., 1994. CLUSTAL W: improving the sensitivity of progressive multiple sequence alignment through sequence weighting, position-specific gap penalties and weight matrix choice. Nucleic acids research 22, 4673-80.

Tokunaga K., Greenberg M. L., Morse M. A., Cumming R. I., Lyerly H. K. and Cullen B. R., 2001. Molecular basis for cell tropism of CXCR4-dependent human immunodeficiency virus type 1 isolates. Journal of virology 75, 6776-85.

Troth S. P., Dean A. D. and Hoover E. A., 2008. In vivo CXCR4 expression, lymphoid cell phenotype, and feline immunodeficiency virus infection. Veterinary immunology and immunopathology 123, 97-105.

Troyer J. L., Vandewoude S., Pecon-Slattery J., McIntosh C., Franklin S., Antunes A., Johnson W. and O'Brien S. J., 2008. FIV cross-species transmission: an evolutionary prospective. Veterinary immunology and immunopathology 123, 159-66.

Troyer R., Zheng X., Miller C., MacMillan M., Sprague W., Wood B. and VandeWoude S., 2012. Expression of APOBEC3 lentiviral restriction factors in felines, Vol. Poster presentation.

Troyer R. M., Thompson J., Elder J. H. and VandeWoude S., 2013. Accessory genes confer a high replication rate to virulent feline immunodeficiency virus. Journal of virology 87, 7940-51.

Uhl E. W., Martin M., Coleman J. K. and Yamamoto J. K., 2008. Advances in FIV vaccine technology. Veterinary immunology and immunopathology 123, 65-80.

Vahlenkamp T. W., Verschoor E. J., Schuurman N. N., van Vliet A. L., Horzinek M. C., Egberink H. F. and de Ronde A., 1997. A single amino acid substitution in the transmembrane envelope glycoprotein of feline

immunodeficiency virus alters cellular tropism. Journal of virology 71, 7132-5.

van Marle G., Gill M. J., Kolodka D., McManus L., Grant T. and Church D. L., 2007. Compartmentalization of the gut viral reservoir in HIV-1 infected patients. Retrovirology 4, 87.

VandeWoude S. and Apetrei C., 2006. Going wild: lessons from naturally occurring T-lymphotropic lentiviruses. Clinical microbiology reviews 19, 728-62.

Verschoor E. J., Boven L. A., Blaak H., van Vliet A. L., Horzinek M. C. and de Ronde A., 1995. A single mutation within the V3 envelope neutralization domain of feline immunodeficiency virus determines its tropism for CRFK cells. Journal of virology 69, 4752-7.

Vestheim H. and Jarman S. N., 2008. Blocking primers to enhance PCR amplification of rare sequences in mixed samples - a case study on prey DNA in Antarctic krill stomachs. Frontiers in zoology 5, 12.

Vigne J. D., Guilaine J., Debue K., Haye L. and Gerard P., 2004. Early taming of the cat in Cyprus. Science (New York, N.Y.) 304, 259.

Vila-Coro A. J., Rodriguez-Frade J. M., Martin De Ana A., Moreno-Ortiz M. C., Martinez A. C. and Mellado M., 1999. The chemokine SDF-1alpha triggers CXCR4 receptor dimerization and activates the JAK/STAT pathway. FASEB journal : official publication of the Federation of American Societies for Experimental Biology 13, 1699-710.

Wang J., Zhang W., Lv M., Zuo T., Kong W. and Yu X., 2011. Identification of a Cullin5-ElonginB-ElonginC E3 complex in degradation of feline immunodeficiency virus Vif-mediated feline APOBEC3 proteins. Journal of virology 85, 12482-91.

Wang Q., Barr I., Guo F. and Lee C., 2008. Evidence of a novel RNA secondary structure in the coding region of HIV-1 pol gene. RNA (New York, N.Y.) 14, 2478-88.

Wei X., Decker J. M., Wang S., Hui H., Kappes J. C., Wu X., Salazar-Gonzalez J. F., Salazar M. G., Kilby J. M., Saag M. S., Komarova N. L., Nowak M. A., Hahn B. H., Kwong P. D. and Shaw G. M., 2003. Antibody neutralization and escape by HIV-1. Nature 422, 307-12.

Weissenhorn W., Dessen A., Harrison S. C., Skehel J. J. and Wiley D. C., 1997. Atomic structure of the ectodomain from HIV-1 gp41. Nature 387, 426-30.

Wiegand H. L., Doehle B. P., Bogerd H. P. and Cullen B. R., 2004. A second human antiretroviral factor, APOBEC3F, is suppressed by the HIV-1 and HIV-2 Vif proteins. The EMBO journal 23, 2451-8.

Wilgenbusch J. C. and Swofford D., 2003. Inferring evolutionary trees with PAUP*. Current protocols in bioinformatics / editoral board, Andreas D. Baxevanis ... [et al.] Chapter 6, Unit 6 4.

Willett B. J., Cannon C. A. and Hosie M. J., 2003. Expression of CXCR4 on feline peripheral blood mononuclear cells: effect of feline immunodeficiency virus infection. Journal of virology 77, 709-12.

Willett B. J., Flynn J. N. and Hosie M. J., 1997a. FIV infection of the domestic cat: an animal model for AIDS. Immunology today 18, 182-9.

Willett B. J. and Hosie M. J., 2008. Chemokine receptors and co-stimulatory molecules: Unravelling feline immunodeficiency virus infection. Veterinary immunology and immunopathology 123, 56-64.

Willett B. J., Hosie M. J., Callanan J. J., Neil J. C. and Jarrett O., 1993. Infection with feline immunodeficiency virus is followed by the rapid expansion of a CD8+ lymphocyte subset. Immunology 78, 1-6.

Willett B. J., Hosie M. J., Dunsford T. H., Neil J. C. and Jarrett O., 1991. Productive infection of T-helper lymphocytes with feline immunodeficiency virus is accompanied by reduced expression of CD4. AIDS (London, England) 5, 1469-75.

Willett B. J., Hosie M. J., Neil J. C., Turner J. D. and Hoxie J. A., 1997b. Common mechanism of infection by lentiviruses. Nature 385, 587-587.

Willett B. J., Kraase M., Logan N., McMonagle E., Varela M. and Hosie M. J., 2013. Selective expansion of viral variants following experimental transmission of a reconstituted feline immunodeficiency virus quasispecies. PloS one 8, e54871.

Willett B. J., Kraase M., Logan N., McMonagle E. L., Samman A. and Hosie M. J., 2010. Modulation of the virus-receptor interaction by mutations in the V5 loop of feline immunodeficiency virus (FIV) following in vivo escape from neutralising antibody. Retrovirology 7, 38.

Willett B. J., McMonagle E. L., Bonci F., Pistello M. and Hosie M. J., 2006a. Mapping the domains of CD134 as a functional receptor for feline immunodeficiency virus. Journal of virology 80, 7744-7747.

Willett B. J., McMonagle E. L., Logan N., Samman A. and Hosie M. J., 2008. A single site for N-linked glycosylation in the envelope glycoprotein of feline immunodeficiency virus modulates the virus-receptor interaction. Retrovirology 5, 77.

Willett B. J., McMonagle E. L., Logan N., Schneider P. and Hosie M. J., 2009. Enforced covalent trimerisation of soluble feline CD134 (OX40)-ligand generates a functional antagonist of feline immunodeficiency virus. Molecular immunology 46, 1020-1030.

Willett B. J., McMonagle E. L., Logan N., Spiller O. B., Schneider P. and Hosie M. J., 2007. Probing the interaction between feline immunodeficiency virus and CD134 by using the novel monoclonal antibody 7D6 and the CD134 (Ox40) ligand. Journal of virology 81, 9665-79.

Willett B. J., McMonagle E. L., Ridha S. and Hosie M. J., 2006b. Differential utilization of CD134 as a functional receptor by diverse strains of feline immunodeficiency virus. Journal of virology 80, 3386-3394.

Wilson J. D., Ogg G. S., Allen R. L., Davis C., Shaunak S., Downie J., Dyer W., Workman C., Sullivan S., McMichael A. J. and Rowland-Jones S. L., 2000. Direct visualization of HIV-1-specific cytotoxic T lymphocytes during primary infection. AIDS (London, England) 14, 225-33.

Wyatt R. and Sodroski J., 1998. The HIV-1 envelope glycoproteins: fusogens, antigens, and immunogens. Science (New York, N.Y.) 280, 1884-8.

Yamamoto J. K., Hansen H., Ho E. W., Morishita T. Y., Okuda T., Sawa T. R., Nakamura R. M. and Pedersen N. C., 1989. Epidemiologic and clinical aspects of feline immunodeficiency virus infection in cats from the continental United States and Canada and possible mode of transmission. Journal of the American Veterinary Medical Association 194, 213-20.

Yamamoto J. K., Sparger E., Ho E. W., Andersen P. R., O'Connor T. P., Mandell C. P., Lowenstine L., Munn R. and Pedersen N. C., 1988. Pathogenesis of experimentally induced feline immunodeficiency virus infection in cats. American journal of veterinary research 49, 1246-58.

Yu Q., Konig R., Pillai S., Chiles K., Kearney M., Palmer S., Richman D., Coffin J. M. and Landau N. R., 2004. Single-strand specificity of APOBEC3G accounts for minus-strand deamination of the HIV genome. Nature structural & molecular biology 11, 435-42.

Yu X., Yu Y., Liu B., Luo K., Kong W., Mao P. and Yu X. F., 2003. Induction of APOBEC3G ubiquitination and degradation by an HIV-1 Vif-Cul5-SCF complex. Science (New York, N.Y.) 302, 1056-60.

Zhang H., Yang B., Pomerantz R. J., Zhang C., Arunachalam S. C. and Gao L., 2003. The cytidine deaminase CEM15 induces hypermutation in newly synthesized HIV-1 DNA. Nature 424, 94-8.

Zhang L., He T., Huang Y., Chen Z., Guo Y., Wu S., Kunstman K. J., Brown R. C., Phair J. P., Neumann A. U., Ho D. D. and Wolinsky S. M., 1998. Chemokine coreceptor usage by diverse primary isolates of human immunodeficiency virus type 1. Journal of virology 72, 9307-12.

Zheng Y. H. and Peterlin B. M., 2005. Intracellular immunity to HIV-1: newly defined retroviral battles inside infected cells. Retrovirology 2, 25.

Zhu T., Mo H., Wang N., Nam D. S., Cao Y., Koup R. A. and Ho D. D., 1993. Genotypic and phenotypic characterization of HIV-1 patients with primary infection. Science (New York, N.Y.) 261, 1179-81.

Zhu T., Wang N., Carr A., Nam D. S., Moor-Jankowski R., Cooper D. A. and Ho D. D., 1996. Genetic characterization of human immunodeficiency virus type 1 in blood and genital secretions: evidence for viral compartmentalization and selection during sexual transmission. Journal of virology 70, 3098-107.

Zhuang J., Jetzt A. E., Sun G., Yu H., Klarmann G., Ron Y., Preston B. D. and Dougherty J. P., 2002. Human Immunodeficiency Virus Type 1 Recombination: Rate, Fidelity, and Putative Hot Spots. Journal of virology 76, 11273-11282.

Zielonka J., Marino D., Hofmann H., Yuhki N., Lochelt M. and Munk C., 2010a. Vif of feline immunodeficiency virus from domestic cats protects against APOBEC3 restriction factors from many felids. Journal of virology 84, 7312-24.

Zielonka J., Marino D., Hofmann H., Yuhki N., Lochelt M. and Munk C., 2010b. Vif of feline immunodeficiency virus from domestic cats protects against APOBEC3 restriction factors from many felids. Journal of virology 84, 7312-24.

Zuo T., Liu D., Lv W., Wang X., Wang J., Lv M., Huang W., Wu J., Zhang H., Jin H., Zhang L., Kong W. and Yu X., 2012. Small-molecule inhibition of human immunodeficiency virus type 1 replication by targeting the interaction between Vif and ElonginC. Journal of virology 86, 5497-507.

Zwick M. B., Jensen R., Church S., Wang M., Stiegler G., Kunert R., Katinger H. and Burton D. R., 2005. Anti-human immunodeficiency virus type 1 (HIV-1) antibodies 2F5 and 4E10 require surprisingly few crucial residues in the membrane-proximal external region of glycoprotein gp41 to neutralize HIV-1. Journal of virology 79, 1252-61.

# 11. Authors declaration

I declare that this thesis is the result of my own work, unless specifically referenced and has not been submitted for any other degree at the Free University of Berlin or any other institution.

Martin Kraase

October 2013